AD_____
(Leave blank)

Award Number: W81XWH-05-1-0272

TITLE: Biological Function of Plasma Kallikrein in Mammary Gland Stromal Development and Tumor Metastasis

PRINCIPAL INVESTIGATOR: Jennifer N. Lilla

CONTRACTING ORGANIZATION: University of California, San Francisco
San Francisco, CA 94143

REPORT DATE: March 2008

TYPE OF REPORT: annual summary (final)

PREPARED FOR: U.S. Army Medical Research and Materiel Command
Fort Detrick, Maryland 21702-5012

DISTRIBUTION STATEMENT:

x Approved for public release; distribution unlimited

☐ Distribution limited to U.S. Government agencies only; report contains proprietary information

REPORT DOCUMENTATION PAGE

Form Approved
OMB No. 0704-0188

1. REPORT DATE *(DD-MM-YYYY)*	**2. REPORT TYPE**	**3. DATES COVERED** *(From - To)*
03-04-2008	Final Summary	15 Feb 2005 – 14 Feb 2008

4. TITLE AND SUBTITLE
Biological Function of Plasma Kallikrein in Mammary Gland Stromal Development and Tumor Metastasis

5a. CONTRACT NUMBER
W81XWH-05-1-0272

5b. GRANT NUMBER

5c. PROGRAM ELEMENT NUMBER

6. AUTHOR(S)
Jennifer N. Lilla

5d. PROJECT NUMBER

5e. TASK NUMBER

5f. WORK UNIT NUMBER

7. PERFORMING ORGANIZATION NAME(S) AND ADDRESS(ES)
University of California, San Francisco
513 Parnassus Avenue, Box 0452
San Francisco, CA 94143-0452

Email: jennifer.lilla@ucsf.edu

8. PERFORMING ORGANIZATION REPORT NUMBER

9. SPONSORING / MONITORING AGENCY NAME(S) AND ADDRESS(ES)
U.S. Army Medical Research and Materiel Command
Fort Detrick, MD 21702-5012

10. SPONSOR/MONITOR'S ACRONYM(S)

11. SPONSOR/MONITOR'S REPORT NUMBER(S)

12. DISTRIBUTION / AVAILABILITY STATEMENT

Approved for public release; distribution unlimited

13. SUPPLEMENTARY NOTES

14. ABSTRACT

The plasminogen cascade of serine proteases has been affiliated in the mammary gland with both development and tumorigenesis. We have found that the dominant plasminogen activator during mammary gland stromal involution is plasma kallikrein (PKal), and that active PKal appears in connective tissue-type mast cells in the mammary stroma during different phases of development. Examination of the extrahepatic expression of PKal has shown that PKal message is present in the mammary gland, and that increased expression levels correlate to periods of stromal remodeling. Additionally, an inhibitor of PKal that has been demonstrated to diminish mammary gland involution may be used to characterize PKal expression in the mammary gland as well as to identify targets of PKal activity during involution. Furthermore, mast cells are required for normal mammary duct branching morphogenesis during puberty. Lastly, attempts to produce a PKal knockout mouse were unsuccessful.

15. SUBJECT TERMS
mammary gland, serine protease, plasma kallikrein, mast cell, mouse model, involution, adipocyte, extracellular matrix, plasminogen

16. SECURITY CLASSIFICATION OF:			**17. LIMITATION OF ABSTRACT**	**18. NUMBER OF PAGES**	**19a. NAME OF RESPONSIBLE PERSON**
a. REPORT	**b. ABSTRACT**	**c. THIS PAGE**			Jennifer N. Lilla
U	U	U	UU	84	**19b. TELEPHONE NUMBER** *(include area code)* (415) 476-4758

Standard Form 298 (Rev. 8-98)
Prescribed by ANSI Std. Z39.18

TABLE OF CONTENTS

INTRODUCTION

The plasminogen cascade of serine proteases has been affiliated in the mammary gland with both development and tumorigenesis. The ultimate effector in this cascade, plasminogen (active form: plasmin), is managed by an intricate cascade of plasminogen activators and protease inhibitors. Plasminogen activators and inhibitors are strongly associated with poor prognosis in a variety of human tumors, including breast cancer (Stephens et al., 1998). Furthermore, plasminogen-deficient mice yield significantly fewer metastases in a viral oncogene-induced model of breast cancer (Bugge et al., 1997; Bugge et al., 1998) and exhibit significant defects in lactational competence and post-lactational mammary gland involution (Lund et al., 2000). This study focuses on the role of a plasminogen activator in murine mammary stromal development and metastasis. This lab has demonstrated that the dominant plasminogen activator for mammary stromal involution is plasma kallikrein (PKal)(Selvarajan et al., 2001) and that active PKal appears in connective tissue-type mast cells in the stroma and surrounding the blood vessels of the murine mammary gland. This project aims to study the plausible relationship between mast cell activation, PKal release, and plasmin conversion in the mammary gland by examining the role of PKal in mammary gland development, involution and metastasis. Additionally, this project has established a novel role for mast cells in mammary gland development. This report details the work accomplished during the three years of my predoctoral traineeship award.

FINAL REPORT

Task 1. The generation of a prekallikrein-deficient mouse is the crucial first step towards determining the effects of the loss of PKal on mammary gland development and tumorigenesis. Prekallikrein consists of two domains: a binding domain, and a trypsin-like serine protease domain (supporting data Figure 1). Its binding domain, consisting of four apple (PAN) domains, is thought to mediate interactions between prekallikrein and plasma-borne PKal activators such as Factor XII (McMullen et al., 1991; Rojkjaer and Schmaier, 1999). PKal's serine protease domain is highly conserved amongst other proteases in the plasminogen cascade as well as other members of the large trypsin-like protease family. At the time of the beginning of this award, a knockout construct was half-completed that would insert the gene encoding green fluorescent protein (GFP) behind the endogenous start codon for prekallikrein. Due to difficulties during the cloning process, the original strategy was modified: firstly, one of the homology arms was difficult to amplify by polymerase chain reaction (PCR); secondly, the drug resistance cassette that was originally used (Puromycin resistance) had to be exchanged for another selection cassette (Hygromycin resistance) to avoid recombination events between too-similar polyA sequences at the end of the GFP cassette and the Puromycin resistance cassette (supporting data Figure 2). The final knockout construct was completed in month 6 of the award.

Task 1a. As previously reported, cloning difficulties led to a delay in the generation of the PKal (allele name: *Klkb1*) knockout construct, and then screening of E14 (SV129/Ola) embryonic stem (ES) cell colonies for correct targeting by Southern blot hybridization also proved challenging. Eight different probes were generated against regions 5' and 3' to the homology arms of the knockout construct, and all yielded inconsistent or weak signals with significant background, making screening of the candidate cell lines inconclusive. An alternate

strategy using an internal probe consisting of the majority of the Hygromycin resistance coding sequence resulted in clean Southern blots with strong signal, so correct targeting had to be determined using multiple independent restriction digestions of candidate DNA. In month 2 of the second year of this award, three ES cell lines confirmed to be correctly targeted were analyzed by karyotype, and two were found to be sufficiently normal (>90% of cells typed had normal chromosome number) to be suitable for blastocyst injection. The *Klkb1* targeting strategy is depicted in supplemental data Figure 2.

The Statement of Work for this award did not allow for difficulties in the final cloning steps for the knockout construct, nor for in the ES cell screening, therefore the timeline for *Task 1* was significantly delayed. The locus for the plasma kallikrein gene proved to be a difficult template for many standard molecular biology techniques such as PCR, cloning, and Southern hybridization. In fact, the annotation for the gene was removed from the Ensembl database (www.ensembl.org/mus_musculus) for three assemblies of the mouse genome, and was only recently reposted with many changes to the 5' region of the locus. Communication with the Ensembl consortium had revealed that the PKal annotation (Klkb1) had been "temporarily" removed due to multiple sequencing difficulties in the locus. Comparison of the sequence used to create the PKal knockout construct employed in this project with other published sequence (NCBI and published bacterial artificial chromosome (BAC)) data for the prekallikrein locus confirmed that use of the construct we generated should not have failed to produce a prekallikrein-deficient mouse.

Task 1b. Blastocyst injections of two clones, D10 and E8, were performed in months 3 and 4 of year two of this award by the UCSF Comprehensive Cancer Center Transgenic/Targeted Mutagenesis Core. Three male chimeras from the E8 line were obtained from the first round of injections, and two male chimeras from the D10 line resulted from the second round.

Task 1c. Upon reaching sexual maturity, chimeras were mated with C57Bl/6 females to generate heterozygous offspring. The first F1 generations were born in month 7 of year two of this award. Two of the three E8 chimeras yielded consistent offspring and demonstrated germline transmission of the *Klkb1*^{tm1} allele. The third E8 chimera only yielded two female offspring and never successfully mated thereafter. The two D10 chimeras completely failed to generate offspring; it is likely that they were phenotypic males, without functional gametes, as is common in chimeras obtained through blastocyst injection (Iannaccone et al., 1985). Regardless, sufficient numbers of F1 progeny from the functional E8 chimeras were determined by Southern blotting and by polymerase chain reaction (PCR) to be heterozygous to confirm germline transmission and therefore set up heterozygous mating pairs. Assessment of heterozygous animals for GFP expression showed that GFP expression by immunofluorescence was consistent with that of plasma kallikrein by *in situ* hybridization (supplemental data Figure 3). Therefore, GFP was to be used as a reporter of PKal expression; though endogenous GFP fluorescence appeared weak even in the liver, where PKal is largely expressed, visualization via immunofluorescence worked well.

Task 1d. Heterozygous F1 *Klkb1*$^{+/tm1}$ mice did not exhibit any overt phenotype and proved to be fertile and lactationally competent. F2 progeny, representing offspring from heterozygous breeding couples, were first generated in month 10 of the second year of this award period. Nineteen F2 litters were generated, and no live homozygous mutant animals were identified. Wild-type and heterozygous mice appeared in nearly all litters, and of 134 progeny from these nineteen litters, 39 were wild-type and 95 were heterozygous, in a ratio of approximately 2.4:1. The likelihood of this result as non-Mendelian (expected 1 wildtype: 2 heterozygotes: 1

homozygote mutant) was $p = 0.97x10^{-12}$ as determined by a χ^2 test for goodness-of-fit. As this was strongly suggestive of an embryonic lethal homozygous phenotype, work was begun in the last six weeks of the second year of this award period to identify homozygous mutants *in utero*. F2 litters from heterozygous crosses were analyzed at embryonic day (E) 12, 10.5, 9.5, 8, and 7.5. At E12, 10.5, and 9.5, no homozygous mutants were genotyped. At E8 and E7.5, sufficient genomic DNA has not been recovered to perform genotyping by PCR; however, abnormal embryos were observed at these timepoints (supplemental data Figure 4). At the beginning of year three of this award, it had not been determined whether these abnormal embryos were due to loss of PKal or the result of natural attrition.

Further analysis of the *Klkb1*-targeted mice failed to account for the lack of homozygous mutants. Subsequent attempts to sequence the *Klkb1* locus in these targeted mice were also unsuccessful, so we turned to a Southern hybridization strategy to determine whether the mice were correctly targeted or not, as Western blotting also yielded inconsistent results (data not shown). Using ES clone DNA or genomic DNA from the F1 or F2 generations, PCR amplification of the recombination site was inconsistent; oligos internal to the targeting vector insert were used to amplify various regions spanning the site of recombination, however, while some PCRs produced bands of appropriate size, others failed altogether. Sequencing results of the PCR products were either inconclusive or the sequencing reactions failed. Reevaluation of the initial Southern blots screens suggested further screening using other probes or restriction enzymes was required.

A second round of Southern blotting on F1 or F2 genomic DNA, using *Eco*RI, *Hind*III, *Hpa*I, and *Spe*I for digestion and a probe spanning the majority of the EGFP coding sequence gave clean blots suitable for analysis. Only the *Spe*I-digested band showed bands of appropriate size, while the other digests either showed no bands or bands of inappropriate size. Thus, in light of the PCR genotyping and sequencing difficulties discussed above, this result led us to conclude that the generated *Klkb1*^{tm1ZW} allele did not properly target the *Klkb1* locus and would therefore be unsuitable for further study. Therefore, we were unable to complete *Tasks 1d* and *1e* as described in the Statement of Work.

<u>*Task 2.*</u> Analysis of plasma kallikrein expression in the mouse mammary gland was necessary to confirm preliminary data suggesting extrahepatic expression of PKal in the mammary gland stroma and/or in connective tissue-type mast cells. These data are presented in Appendix 1, which details our analysis of plasma kallikrein expression in the mouse mammary gland. These data are currently being prepared for publication. Appendix 2 is a publication in which the primary investigator of this award participated to demonstrate PKal expression in skin wound healing, using techniques developed while supported by this predoctoral award.

If plasma kallikrein is produced outside of the liver in tissues that require its activity and is activated non-canonically apart from the contact activation system in blood vessels, then this would represent a novel pathway for the plasminogen cascade of protease activity. It has recently been shown that plasminogen is expressed by a wide range of tissues (Zhang et al., 2002) therefore, it is not unreasonable to hypothesize that tissues in which plasmin activity is required would also have locally expressed plasminogen activators to better control the activation cascade.

Task 2a. Plasma kallikrein expression in the mouse mammary gland at different developmental time points is described in Appendix 1.

Task 2b. Identification of mammary gland binding factors for ecotin PKal, a macromolecular inhibitor for PKal, is described in Appendix 1.

Task 2c. As inhibition of PKal retards adipocyte replenishment and stromal remodeling during mammary gland involution, it is important to determine whether this inhibition is due to impaired plasminogen activation by PKal, or if there are other downstream targets of PKal during involution. Plans to address this question were once again impaired by the delay in obtaining prekallikrein-deficient mice, which would have served as an essential control for this analysis. Alternative methods were considered, but were able to be attempted during the period of this award.

Task 2d. It has been demonstrated previously that inflammatory cells play an important role in both mammary gland development (Gouron-Evans et al., 2000; Stein et al., 2004) and mammary tumor progression (Coussens and Werb, 2002; Jussi-Pekka Kankkunen, 1997; Michael Samoszuk, 2003; Wiseman and Werb, 2002). However, no previous work has attempted to elucidate the specific role of mast cells in mammary gland development. In the last 15 months of the award period, mammary development has been analyzed in the W-*sash* ($Kit^{W\text{-}sh/W\text{-}sh}$) mouse on the C57Bl/6 background, which is deficient in connective tissue-type mast cells (Duttlinger et al., 1993; Grimbaldeston et al., 2005).

This analysis of the role of mast cells in pubertal mammary gland branching morphogenesis is described in detail in Appendix 3, which represents a manuscript in preparation for publication. Again, without the prekallikrein-deficient mouse model proposed in *Task 1* of this award, further examination of the connections between mast cells and PKal expression in the mammary gland was not possible. However, this work presents a novel role for mast cells in mammary gland development that bears further scrutiny, especially in light of recent reports such as that mast cells play an important role in regulating angiogenesis of pancreatic tumors (Soucek et al., 2007).

KEY RESEARCH ACCOMPLISHMENTS

- Prekallikrein mRNA is present in the mammary gland, and increased levels correlate to phases of stromal remodeling.
- Ecotin PKal, a macromolecular inhibitor of plasma kallikrein, can be used to "pull-down" PKal from mammary tissue lysates and localize active PKal to mast cells in the mammary gland.
- Mast cells are necessary for mammary ductal morphogenesis during puberty.

REPORTABLE OUTCOMES

Abstracts/presentations: The investigator presented data from Task 2 of this award in a poster entitled: "Biological function for plasma kallikrein in mammary gland involution" at the Gordon Research Conference on Plasminogen Activation and Extracellular Proteolysis, February 2008. This poster received an American Heart Association 2008 Poster Award. The abstract is included in this report as Appendix 4.

Manuscripts:
Appendix 1 will be part of this manuscript: **Lilla JN**, Stoop AA, Craik CS, Werb Z. Mammary gland involution requires plasma kallikrein. 2008 *in preparation*

Appendix 2: Lund LR, Green KA, Stoop AA, Ploug M, Almholt K, **Lilla J**, Nielsen BS, Christensen IJ, Craik CS, Werb Z, Dano K, Romer J. Plasminogen activation independent of uPA and tPA maintains wound healing in gene-deficient mice. EMBO J. 2006 Jun 21;25(12):2686-97.

Appendix 3: **Lilla JN**, Werb Z. Mast cells are required for postnatal mammary development. 2008 *in preparation*

Degrees obtained: This award period represents the last three years of the investigator's dissertation period. The dissertation has been accepted and is currently undergoing minor revision, and a Ph.D. will be granted to the investigator in March 2008.

Employment opportunities: The investigator is currently seeking postdoctoral positions and has to date been offered two positions, one at the Collège de France, Paris, and another at Stanford University. Work supported by this predoctoral award directly contributed to these employment opportunities.

Personnel receiving pay from this award: Jennifer N. Lilla, Ph.D. candidate

CONCLUSIONS

The work presented in this report establishes plasma kallikrein (PKal) expression in the mammary gland during development and involution (Appendix 1) as well as identifies a role for mast cells in mammary gland development (Appendix 3). The intriguing colocalization of PKal with mast cell granules in the mammary gland (Chapter 1) heightens the mystery, as observations made during the course of this award period suggest that mast cells, though present, are not required for mammary gland involution (data not shown). If this is the case, then there may be no functional link between mast cells and PKal activation, despite their colocalization. Even so, as this colocalization does change depending on the activity of the mast cells (Appendix 1), it begs the question as to how mast cells might be playing a role, redundant or not, in directing PKal activation and activity.

Several tools need to be developed and several technical obstacles need to be overcome in order to answer this question. The first and most obvious tool would be a plasma kallikrein knockout mouse, which I attempted as described for *Task 1* of this report. Unforeseeable complications to the generation of the PKal knockout mouse obviously hindered planned experiments that depended on kallikrein-deficient tissues for analysis of mammary development, and ultimately, the effect of PKal on breast cancer development. In the last year of this award, our collaborator Leif Lund, Finsen Laboratories, Denmark obtained *Klkb1*-targeted mouse produced by Deltagen though my preliminary analysis has shown that the mouse might not

represent a functional knockout, and furthermore does not have a developmental defect. Further efforts by the Lund laboratory hopefully will determine definitively whether the mouse indeed is a functional knockout before more experiments are attempted. As Fletcher Factor-deficient humans are reportedly healthy other than a very subtle bleeding defect (Hathaway et al., 1976), we would only expect PKal-deficient animals to have a mammary involution phenotype, which based on our experiments with Ecotin PKal during mammary gland involution (data not shown in this report). If the Deltagen *Klkb1*-targeted mouse is not a functional null, then pending the arrival of another group's knockout efforts, one might attempt knockdown experiments in both the mammary gland and in liver using siRNAs against *Klkb1* expression, though siRNA design would have to take into account any recent changes in the reported sequence of the *Klkb1* locus. Fortunately, no microRNAs are predicted in the *Klkb1* locus (T. Cuellar, UCSF, personal communication) that might confound efforts to knockdown KLKB1 expression in the liver or mammary gland.

The generation of a knockout or knockdown model for PKal would also have enabled independent confirmation of the specificity of ecotin PKal. Ecotin PKal was developed to not bind and inhibit PKal's nearest related serine proteases, including Factors XIa and XIIa, uPA, tPA, and plasmin (Stoop and Craik, 2003), yet the *in vivo* specificity has not been fully characterized to date. Efforts are under way in the Craik laboratory to assess the specificity of ecotin PKal in mouse plasma, and once the PKal knockout is available, parallel studies could be conducted *in vivo*. In particular, the large host of serine proteases found in mast cell granules, some of which have likely not been fully identified, could contain a different ecotin PKal-binding protease. Though this possibility has been somewhat negated by the use of a polyclonal antibody against PKal to stain mast cells in the mammary gland (Appendix 1), further studies should rule out any doubts as to ecotin PKal's *in vivo* specificity.

Plasma kallikrein activity appears to be associated with the function of two major stromal cell types of the mammary gland: mast cells and adipocytes. This research has aimed to elucidate the role of PKal in mammary gland involution and metastasis. As many models of breast cancer highly implicate stromal signals as effectors or inhibitors of breast cancer progression, it is imperative to acquire a better understanding of the normal functioning of this protease to prepare for its possible characterization as a breast cancer indicator like other members of the plasminogen protease cascade, or as a target for drug therapies. And as many breast cancers are strongly associated with mast cell infiltration (in addition to other leukocytes), it is important to understand their normal physiological role in breast development, perhaps as mediators of protease activity (including PKal) and as attractors to other inflammatory cells.

The complexity of mast cell protease content itself confounds further efforts to characterize the localization of PKal to mast cell granules. The context-specificity of mast cell products requires us to examine mast cells *in situ* in the tissues of interest, yet their delicate integrity makes it difficult to extract them from their tissues of residence, such as by flow cytometry. Peritoneal mast cells can be extracted from lavage fluid, and bone marrow and ES cells may be differentiated into mast cells, yet their granule contents will not resemble that found in other tissues, such as in the mammary gland. Only when situated in their tissues of residence will mast cells acquire their context-specific phenotype. Until these technical difficulties can be overcome, such as by single-cell laser capture or more context-specific *in vitro* differentiation techniques, further exploration of the colocalization of PKal and mast cell granules will rely on the development of more genetic models.

The work described in this report has addressed interesting questions as to the function and importance of previously little-regarded participants in mammary gland biology, plasma kallikrein and mast cells. It is the hope of this investigator that further research into the physiological role of PKal in normal mammary gland biology and mammary cancer development will be stimulated by the research undertaken during the course of this award. Furthermore, the intriguing role of mast cells in normal mammary development should lead to further research into the possible function of mast cells in the promotion of breast tumors and metastasis. As mast cell function and inhibition has been extensively studied in the context of allergy and infectious responses, it is possible that clinical applications for mast cell biology in mammary tumor treatment could be easily investigated.

This research has required the investigator to master a wide-reaching and comprehensive set of experimental techniques, from molecular biology to biochemistry to tissue biology and to animal husbandry. This wide range of skills should prove indispensable to a future career as a breast cancer researcher. In addition, this course of study has required contact with related disciplines, such as research in wound healing, skin cancer, and prostate cancer, all of which are important as parallels in those fields are often made to breast cancer, to the benefit of all. The support offered by this predoctoral award has made it possible for this investigator to be well-prepared to pursue many more avenues of fruitful investigation of breast cancer, for which she is very grateful.

REFERENCES

Albrecht, U., G. Eichele, J.A. Helms, and H. Lu. 1997. Visualization of gene expression patterns by *in situ* hybridization. *In* Molecular and Cellular Methods in Developmental Toxicology. G.P. Daston, editor. CRC Press, Boca Raton. 23-48.

Blair, R.J., H. Meng, M.J. Marchese, S. Ren, L.B. Schwartz, M.G. Tonnesen, and B.L. Gruber. 1997. Human mast cells stimulate vascular tube formation. Tryptase is a novel, potent angiogenic factor. *The Journal of clinical investigation*. 99:2691-700.

Bugge, T.H., K.W. Kombrinck, Q. Xiao, K. Holmback, C.C. Daugherty, D.P. Witte, and J.L. Degen. 1997. Growth and dissemination of Lewis lung carcinoma in plasminogen-deficient mice. *Blood*. 90:4522-31.

Bugge, T.H., L.R. Lund, K.K. Kombrinck, B.S. Nielsen, K. Holmback, A.F. Drew, M.J. Flick, D.P. Witte, K. Dano, and J.L. Degen. 1998. Reduced metastasis of Polyoma virus middle T antigen-induced mammary cancer in plasminogen-deficient mice. *Oncogene*. 16:3097-104.

Cerf, M.E., and D.M. Raidoo. 2000. Immunolocalization of plasma kallikrein in human brain. *Metabolic brain disease*. 15:315-23.

Ciechanowicz, A., M. Bader, J. Wagner, and D. Ganten. 1993. Extra-hepatic transcription of plasma prekallikrein gene in human and rat tissues. *Biochemical and biophysical research communications*. 197:1370-6.

Coussens, L.M., W.W. Raymond, G. Bergers, M. Laig-Webster, O. Behrendtsen, Z. Werb, G.H. Caughey, and D. Hanahan. 1999. Inflammatory mast cells up-regulate angiogenesis during squamous epithelial carcinogenesis. *Genes Dev*. 13:1382-97.

Coussens, L.M., and Z. Werb. 2002. Inflammation and cancer. *Nature*. 420:860-7.

Cunha, G.R., and Y.K. Hom. 1996. Role of mesenchymal-epithelial interactions in mammary gland development. *Journal of mammary gland biology and neoplasia*. 1:21-35.

Cunha, G.R., J.F. Wiesen, Z. Werb, P. Young, Y.K. Hom, P.S. Cooke, and D.B. Lubahn. 2000. Paracrine mechanisms of mouse mammary ductal growth. *Advances in experimental medicine and biology*. 480:93-7.

Duttlinger, R., K. Manova, T.Y. Chu, C. Gyssler, A.D. Zelenetz, R.F. Bachvarova, and P. Besmer. 1993. W-sash affects positive and negative elements controlling c-kit expression: ectopic c-kit expression at sites of kit-ligand expression affects melanogenesis. *Development*. 118:705-17.

Gaboury, J.P., B. Johnston, X.F. Niu, and P. Kubes. 1995. Mechanisms underlying acute mast cell-induced leukocyte rolling and adhesion in vivo. *Journal of immunology (Baltimore, Md*. 154:804-13.

Galli, S.J. 2000. Mast cells and basophils. *Curr Opin Hematol*. 7:32-9.

Galli, S.J., J. Kalesnikoff, M.A. Grimbaldeston, A.M. Piliponsky, C.M. Williams, and M. Tsai. 2005. Mast cells as "tunable" effector and immunoregulatory cells: recent advances. *Annu Rev Immunol*. 23:749-86.

Galli, S.J., and M. Tsai. 2008. Mast cells: Versatile regulators of inflammation, tissue remodeling, host defense and homeostasis. *Journal of dermatological science*. 49:7-19.

Gouon-Evans, V., E.Y. Lin, and J.W. Pollard. 2002. Requirement of macrophages and eosinophils and their cytokines/chemokines for mammary gland development. *Breast cancer research*. 4:155-64.

Gouon-Evans, V., M.E. Rothenberg, and J.W. Pollard. 2000. Postnatal mammary gland development requires macrophages and eosinophils. *Development (Cambridge, England)*. 127:2269-82.

Gouron-Evans, V., M.E. Rothenberg, and J.W. Pollard. 2000. Postnatal mammary gland development requires macrophages and eosinophils. *Development*. 127:2269-82.

Grimbaldeston, M.A., C.-C. Chen, A.M. Piliponsky, M. Tsai, S.-Y. Tam, and S.J. Galli. 2005. Mast Cell-Deficient W-sash c-kit Mutant KitW-sh/W-sh Mice as a Model for Investigating Mast Cell Biology in Vivo. *Am J Pathol*. 167:835-848.

Hathaway, W.E., K.D. Wuepper, W.L. Weston, J.R. Humbert, R.P. Rivers, E. Genton, C.S. August, R.R. Montgomery, and M.F. Mass. 1976. Clinical and physiologic studies of two siblings with prekallikrein (Fletcher factor) deficiency. *Am J Med*. 60:654-64.

Hendzel, M.J., Y. Wei, M.A. Mancini, A. Van Hooser, T. Ranalli, B.R. Brinkley, D.P. Bazett-Jones, and C.D. Allis. 1997. Mitosis-specific phosphorylation of histone H3 initiates primarily within pericentromeric heterochromatin during G2 and spreads in an ordered fashion coincident with mitotic chromosome condensation. *Chromosoma*. 106:348-60.

Howlin, J., J. McBryan, and F. Martin. 2006. Pubertal mammary gland development: insights from mouse models. *Journal of mammary gland biology and neoplasia*. 11:283-97.

Iannaccone, P.M., E.P. Evans, and M.D. Burtenshaw. 1985. Chromosomal sex and distribution of functional germ cells in a series of chimeric mice. *Exp Cell Res*. 156:471-7.

Ingman, W.V., J. Wyckoff, V. Gouon-Evans, J. Condeelis, and J.W. Pollard. 2006. Macrophages promote collagen fibrillogenesis around terminal end buds of the developing mammary gland. *Developmental dynamics*. 235:3222-9.

Jamieson, T., D.N. Cook, R.J. Nibbs, A. Rot, C. Nixon, P. McLean, A. Alcami, S.A. Lira, M. Wiekowski, and G.J. Graham. 2005. The chemokine receptor D6 limits the inflammatory response in vivo. *Nature immunology*. 6:403-11.

Johnson, J.L., C.L. Jackson, G.D. Angelini, and S.J. George. 1998. Activation of matrix-degrading metalloproteinases by mast cell proteases in atherosclerotic plaques. *Arteriosclerosis, thrombosis, and vascular biology*. 18:1707-15.

Jussi-Pekka Kankkunen, I.T.H., Anita Naukkarinen,. 1997. Quantitative analysis of tryptase and chymase containing mast cells in benign and malignant breast lesions. *International Journal of Cancer*. 72:385-388.

Kitamura, Y. 1989. Heterogeneity of mast cells and phenotypic change between subpopulations. *Annu Rev Immunol*. 7:59-76.

Kubes, P., and S. Kanwar. 1994. Histamine induces leukocyte rolling in post-capillary venules. A P-selectin-mediated event. *Journal of immunology (Baltimore, Md.* 152:3570-7.

Lund, L.R., S.F. Bjorn, M.D. Sternlicht, B.S. Nielsen, H. Solberg, P.A. Usher, R. Osterby, I.J. Christensen, R.W. Stephens, T.H. Bugge, K. Dano, and Z. Werb. 2000. Lactational competence and involution of the mouse mammary gland require plasminogen. *Development*. 127:4481-92.

Lund, L.R., K.A. Green, A.A. Stoop, M. Ploug, K. Almholt, J. Lilla, B.S. Nielsen, I.J. Christensen, C.S. Craik, Z. Werb, K. Dano, and J. Romer. 2006. Plasminogen activation independent of uPA and tPA maintains wound healing in gene-deficient mice. *The EMBO journal*. 25:2686-97.

Malorny, U., E. Michels, and C. Sorg. 1986. A monoclonal antibody against an antigen present on mouse macrophages and absent from monocytes. *Cell and tissue research*. 243:421-8.

Maslinski, C., D. Kierska, W.A. Fogel, A. Kinnunen, and P. Panula. 1993. Histamine: its metabolism and localization in mammary gland. *Comparative biochemistry and physiology*. 105:269-73.

McIntyre, J.A., E.D. Neerunjun, W.P. Faulk, and M. Papamichail. 1981. Inhibition of in vitro allogeneic reactions with disodium cromoglycate. *International archives of allergy and applied immunology*. 66:244-50.

McMullen, B.A., K. Fujikawa, and E.W. Davie. 1991. Location of the disulfide bonds in human plasma prekallikrein: the presence of four novel apple domains in the amino-terminal portion of the molecule. *Biochemistry*. 30:2050-6.

Metcalfe, D.D., D. Baram, and Y.A. Mekori. 1997. Mast cells. *Physiol Rev*. 77:1033-79.

Metz, M., M.A. Grimbaldeston, S. Nakae, A.M. Piliponsky, M. Tsai, and S.J. Galli. 2007. Mast cells in the promotion and limitation of chronic inflammation. *Immunological reviews*. 217:304-28.

Michael Samoszuk, M.A.C. 2003. Mast cell inhibitor cromolyn increases blood clotting and hypoxia in murine breast cancer. *International Journal of Cancer*. 107:159-163.

Miles, L.A., J.S. Greengard, and J.H. Griffin. 1983. A comparison of the abilities of plasma kallikrein, beta-Factor XIIa, Factor XIa and urokinase to activate plasminogen. *Thromb Res*. 29:407-17.

Moloney, W.C., K. McPherson, and L. Fliegelman. 1960. Esterase activity in leukocytes demonstrated by the use of naphthol AS-D chloroacetate substrate. *The journal of histochemistry and cytochemistry*. 8:200-7.

Motta, G., R. Rojkjaer, A.A. Hasan, D.B. Cines, and A.H. Schmaier. 1998. High molecular weight kininogen regulates prekallikrein assembly and activation on endothelial cells: a novel mechanism for contact activation. *Blood*. 91:516-28.

Nagle, D.L., C.A. Kozak, H. Mano, V.M. Chapman, and M. Bucan. 1995. Physical mapping of the Tec and Gabrb1 loci reveals that the Wsh mutation on mouse chromosome 5 is associated with an inversion. *Human molecular genetics*. 4:2073-9.

Neth, P., M. Arnhold, H. Nitschko, and E. Fink. 2001. The mRNAs of prekallikrein, factors XI and XII, and kininogen, components of the contact phase cascade are differentially expressed in multiple non-hepatic human tissues. *Thrombosis and haemostasis*. 85:1043-7.

Neth, P., M. Arnhold, V. Sidarovich, K.D. Bhoola, and E. Fink. 2005. Expression of the plasma prekallikrein gene: utilization of multiple transcription start sites and alternative promoter regions. *Biological chemistry*. 386:101-9.

Ohtsu, H., S. Tanaka, T. Terui, Y. Hori, Y. Makabe-Kobayashi, G. Pejler, E. Tchougounova, L. Hellman, M. Gertsenstein, N. Hirasawa, E. Sakurai, E. Buzas, P. Kovacs, G. Csaba, A. Kittel, M. Okada, M. Hara, L. Mar, K. Numayama-Tsuruta, S. Ishigaki-Suzuki, K. Ohuchi, A. Ichikawa, A. Falus, T. Watanabe, and A. Nagy. 2001. Mice lacking histidine decarboxylase exhibit abnormal mast cells. *FEBS letters*. 502:53-6.

Pham, C.T., and T.J. Ley. 1999. Dipeptidyl peptidase I is required for the processing and activation of granzymes A and B in vivo. *Proceedings of the National Academy of Sciences of the United States of America*. 96:8627-32.

Razin, E., J.N. Ihle, D. Seldin, J.M. Mencia-Huerta, H.R. Katz, P.A. LeBlanc, A. Hein, J.P. Caulfield, K.F. Austen, and R.L. Stevens. 1984. Interleukin 3: A differentiation and growth factor for the mouse mast cell that contains chondroitin sulfate E proteoglycan. *Journal of immunology (Baltimore, Md*. 132:1479-86.

Richert, M.M., K.L. Schwertfeger, J.W. Ryder, and S.M. Anderson. 2000. An atlas of mouse mammary gland development. *J Mammary Gland Biol Neoplasia*. 5:227-41.

Rojkjaer, R., and A.H. Schmaier. 1999. Activation of the plasma kallikrein/kinin system on endothelial cell membranes. *Immunopharmacology*. 43:109-14.

Rugh, R. 1968. The mouse; its reproduction and development. Burgess Pub. Co., Minneapolis,. iv, 430 pp.

Schmaier, A.H., R. Rojkjaer, and Z. Shariat-Madar. 1999. Activation of the plasma kallikrein/kinin system on cells: a revised hypothesis. *Thromb Haemost*. 82:226-33.

Selvarajan, S., L.R. Lund, T. Takeuchi, C.S. Craik, and Z. Werb. 2001. A plasma kallikrein-dependent plasminogen cascade required for adipocyte differentiation. *Nat Cell Biol*. 3:267-75.

Sferruzzi-Perri, A.N., S.A. Robertson, and L.A. Dent. 2003. Interleukin-5 transgene expression and eosinophilia are associated with retarded mammary gland development in mice. *Biology of reproduction*. 69:224-33.

Silberstein, G.B., K.C. Flanders, A.B. Roberts, and C.W. Daniel. 1992. Regulation of mammary morphogenesis: evidence for extracellular matrix-mediated inhibition of ductal budding by transforming growth factor-beta 1. *Developmental biology*. 152:354-62.

Soucek, L., E.R. Lawlor, D. Soto, K. Shchors, L.B. Swigart, and G.I. Evan. 2007. Mast cells are required for angiogenesis and macroscopic expansion of Myc-induced pancreatic islet tumors. *Nature medicine*. 13:1211-8.

Stein, T., J. Morris, C. Davies, S. Weber-Hall, M.-A. Duffy, V. Heath, A. Bell, R. Ferrier, G. Sandilands, and B. Gusterson. 2004. Involution of the mouse mammary gland is associated with an immune cascade and an acute-phase response, involving LBP, CD14 and STAT3. *Breast Cancer Res*. 6:R75 - R91.

Stephens, R.W., N. Brunner, F. Janicke, and M. Schmitt. 1998. The urokinase plasminogen activator system as a target for prognostic studies in breast cancer. *Breast Cancer Res Treat*. 52:99-111.

Stoop, A.A., and C.S. Craik. 2003. Engineering of a macromolecular scaffold to develop specific protease inhibitors. *Nat Biotechnol*. 21:1063-8.

Topper, Y.J., and C.S. Freeman. 1980. Multiple hormone interactions in the developmental biology of the mammary gland. *Physiological reviews*. 60:1049-106.

Tordai, H., L. Banyai, and L. Patthy. 1999. The PAN module: the N-terminal domains of plasminogen and hepatocyte growth factor are homologous with the apple domains of the prekallikrein family and with a novel domain found in numerous nematode proteins. *FEBS letters*. 461:63-7.

Vartio, T., H. Seppa, and A. Vaheri. 1981. Susceptibility of soluble and matrix fibronectins to degradation by tissue proteinases, mast cell chymase and cathepsin G. *The Journal of biological chemistry*. 256:471-7.

Wagner, W., A. Ichikawa, S. Tanaka, P. Panula, and W.A. Fogel. 2003. Mouse mammary epithelial histamine system. *Journal of physiology and pharmacology*. 54:211-23.

Walsh, L.J., G. Trinchieri, H.A. Waldorf, D. Whitaker, and G.F. Murphy. 1991. Human dermal mast cells contain and release tumor necrosis factor alpha, which induces endothelial

leukocyte adhesion molecule 1. *Proceedings of the National Academy of Sciences of the United States of America*. 88:4220-4.

Wiseman, B.S., and Z. Werb. 2002. Stromal effects on mammary gland development and breast cancer. *Science*. 296:1046-9.

Wolters, P.J., M. Laig-Webster, and G.H. Caughey. 2000. Dipeptidyl peptidase I cleaves matrix-associated proteins and is expressed mainly by mast cells in normal dog airways. *American journal of respiratory cell and molecular biology*. 22:183-90.

Wolters, P.J., C.T. Pham, D.J. Muilenburg, T.J. Ley, and G.H. Caughey. 2001. Dipeptidyl peptidase I is essential for activation of mast cell chymases, but not tryptases, in mice. *The Journal of biological chemistry*. 276:18551-6.

Yee, L.D., Y. Guo, J. Bradbury, S. Suster, S.K. Clinton, and V.L. Seewaldt. 2003. The antiproliferative effects of PPARgamma ligands in normal human mammary epithelial cells. *Breast cancer research and treatment*. 78:179-92.

Zhang, L., D. Seiffert, B.J. Fowler, G.R. Jenkins, T.C. Thinnes, D.J. Loskutoff, R.J. Parmer, and L.A. Miles. 2002. Plasminogen has a broad extrahepatic distribution. *Thromb Haemost*. 87:493-501.

SUPPORTING DATA

Figure 1. Domains of Plasma Kallikrein
Prekallikrein (active form: Plasma Kallikrein) consists of 4 apple (PAN) domains and a trypsin-like serine protease domain (catalytic residues H-D-S). Activation of the protease requires cleavage between the heavy and light chains by Factor XII.

Figure 2. Gene targeting strategy for *Klkb1*^{tm1}. EGFP was inserted immediately after the endogenous Klkb1 ATG. Recombinants were screened by Southern blot for presence of the hygromycin resistance gene using five different restriction enzymes outside of the sites of homologous recombination: *Bgl*II, *Spe*I, *Eco*RV, *Pvu*II, and *Stu*I.

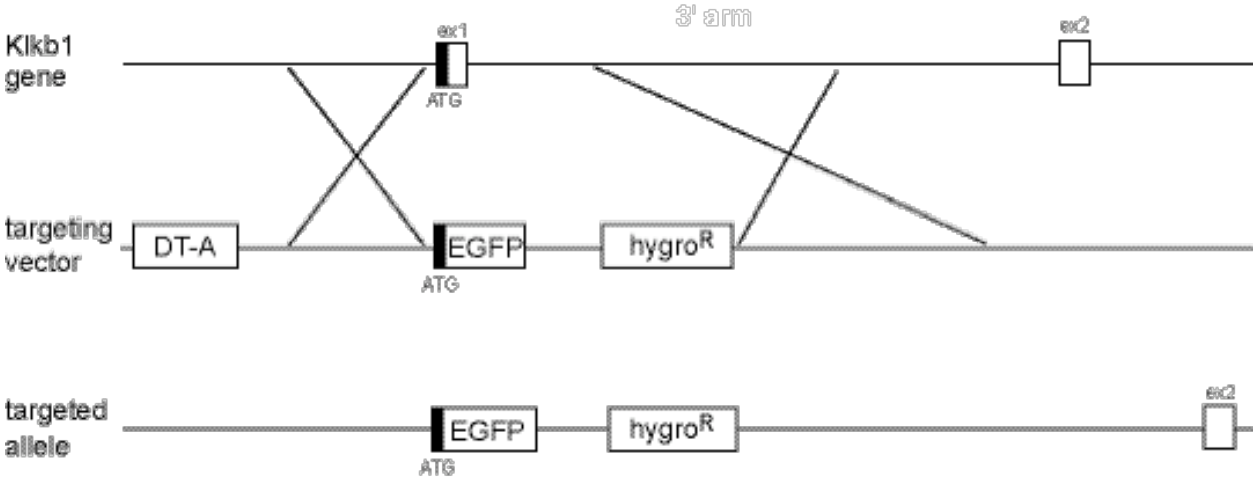

Figure 3. Expression of GFP in a *Klkb1*$^{+/tm1}$ mouse appears identical to localization of prekallikrein message in the liver. A) *In situ* hybridization for prekallikrein in a wild-type mouse liver, 100x. B) Immunofluorescence using anti-GFP antibody on *Klkb1*$^{+/+}$ and *Klkb1*$^{+/tm1ZW}$ littermate liver, 200x.

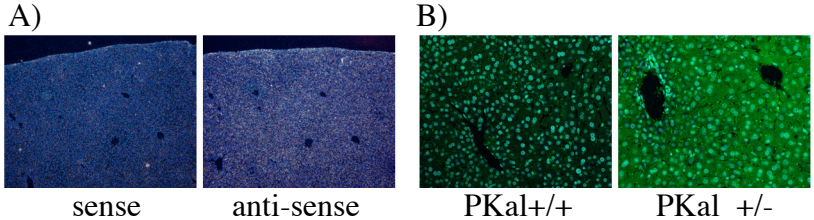

Figure 4. F2 Embryos at embryonic day 7.5 recovered from a *Klkb1* heterozygous cross. At left, abnormal embryos appear much smaller, and lack distinct embryonic-extraembryonic boundaries. The ectoplacental cone is also significantly diminished.

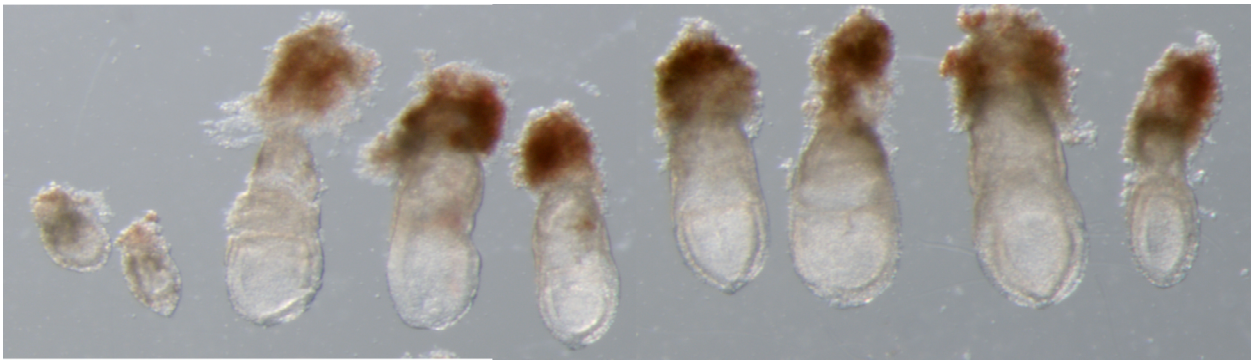

This page contains unpublished data which should be protected.

APPENDIX 1: Expression of Plasma Kallikrein in the Mammary Gland

PLEASE NOTE: This appendix represents unpublished data that are being prepared for publication and therefore should be protected.

INTRODUCTION

In the mammary gland, the plasminogen cascade of serine proteases has been associated with both development and tumorigenesis. The ultimate effector in this cascade, plasminogen (active form: plasmin), is managed by an intricate cascade of plasminogen activators and protease inhibitors. Plasminogen activators and inhibitors are strongly associated with poor prognosis in a variety of human tumors, including breast cancer (Stephens et al., 1998). Furthermore, plasminogen-deficient mice yield significantly fewer metastases in a viral oncogene-induced model of breast cancer (Bugge et al., 1997; Bugge et al., 1998) and exhibit significant defects in lactational competence and post-lactational mammary gland involution (Lund et al., 2000). Our laboratory has demonstrated that the dominant plasminogen activator for mammary involution, the normal physiological process by which a lactating gland returns to a less differentiated, prepregnant state, is plasma kallikrein (PKal) ((Selvarajan et al., 2001) and J. Lilla, Chapter 3).

As many models of breast cancer highly implicate stromal signals and proteases such as plasminogen as effectors (or inhibitors) of breast cancer progression, it is imperative to acquire a better understanding of the normal expression of all plasminogen activators. We and others have shown PKal to be an *in vivo* plasminogen activator important to normal physiological processes such as in mammary involution. It is also possible that PKal contributes to breast cancer like other members of the plasminogen protease cascade, and thus it potentially is a target for drug therapies.

Both plasminogen and PKal are synthesized in the liver and circulate as zymogens through blood plasma presumably to all vascularized tissues of the body, where they may be proteolytically activated. As this expression and circulation are constant, to avoid rampant tissue proteolysis, activation of the plasminogen cascade must be controlled locally; this control could be at the level of activation of upstream factors, and/or by local expression of upstream factors. In the case of PKal, it is unclear under what conditions PKal is activated to in turn convert plasminogen into plasmin. In the canonical contact activation kallikrein/kinin system, Factor XII, another serine protease in the contact activation cascade, converts the zymogen prekallikrein into active PKal. This is thought to happen while prekallikrein and Factor XIIa are in complex with high molecular weight kininogen (HMWK) on cell surfaces, allowing PKal to in turn rapidly digest HMWK to release the proinflammatory, vasoactive peptide bradykinin. PKal is best known for its role in this kallikrein/kinin system as the generator of bradykinin, which then goes on to stimulate clot dissolution (Motta et al., 1998; Rojkjaer and Schmaier, 1999; Schmaier et al., 1999). PKal's participation in the plasminogen activation cascade is likely mediated by shared binding domains: prodomains of both plasminogen and PKal contain apple/PAN domains (one or four, respectively) which facilitate binding to targets (Tordai et al., 1999).

Plasminogen activation by PKal has been demonstrated both *in vitro* and *in vivo* (Lund et al., 2006; Miles et al., 1983; Selvarajan et al., 2001). However, the mechanisms by which this activation may be controlled in specific tissues under appropriate circumstances have not been elucidated. It has recently been shown that plasminogen is expressed by a wide range of tissues (Zhang et al., 2002) therefore, it is not unreasonable to hypothesize that tissues in which plasmin activity is required would also have locally expressed plasminogen activators to better control the activation cascade. This is likely the case for PKal, whose extrahepatic expression has been documented in tissues as diverse as brain, spleen, and kidney (Cerf and Raidoo, 2000; Ciechanowicz et al., 1993; Neth et al., 2001). Here, we report that prekallikrein is expressed in the mammary gland, and that prekallikrein expression is upregulated during periods when the mammary gland is undergoing significant stromal remodeling. We confirmed this by Western blot analysis of mammary gland lysates, as well as by pull-down of PKal from mammary lysates using ecotin PKal, a macromolecular inhibitor of active PKal (Stoop and Craik, 2003). Furthermore, when we use immunohistochemistry or inhibitor-localization methods to visualize PKal, we see PKal localized to mast cells in the mammary gland, as well as mast cells in other tissues. Intriguingly, the specific localization of PKal to mast cells is dependent on the activity of these cells.

METHODS

Experimental animals

Care of animals and animal experiments were performed in accordance with protocols approved by the UCSF Institutional Animal Use and Care Committee (IACUC). Wild-type FVB and CD1 mice were obtained from Charles River Laboratories (Wilmington, MA). C57BL/6J-*Kit*$^{W\text{-}sh/W\text{-}sh}$ mice were obtained from the Jackson Laboratory and C57BL/6 mice were obtained from Charles River Laboratories. DPPI -/- mice (Pham and Ley, 1999) were provided by L. Coussens (UCSF). For all mouse mammary models, thoracic mammary glands 2 and 3 were removed for RNA or protein collection, and/or mammary glands 4 were removed for microscopic analysis. To inhibit mast cell degranulation, CD1 (Charles River Laboratories) female mice were intraperitoneally injected as previously described (Jamieson et al., 2005) with 50 mg/kg body weight sodium cromoglycate (Sigma, St. Louis, MO, USA) dissolved in saline, then two hours later mammary glands were removed for analysis.

Real-time quantitative polymerase chain reaction

Total RNA was isolated from thoracic mammary glands cleared for muscle and lymph tissue at 3 weeks, 5 weeks, 15 days pregnant, 10 days lactating, and 4 days involuted CD1 mice. Liver tissue was used as a positive control. RNA isolation was performed using the RNA-Bee (Tel-Test, Inc., Friendswood, TX) phenol/quanidine thiocynate/chloroform method for RNA isolation and concentration of RNA was measured spectrophotometrically. Five μg of total RNA was used to perform reverse transcriptase polymerase chain reaction using Superscript II reverse transcriptase

oligo(dT) reagents (Invitrogen). cDNA products were electrophoresed in 1% agarose/TAE gels to check thoroughness of the reverse transcriptase reaction.

Real-time quantitative polymerase chain reaction (RT-qPCR) was performed by the Biomolecular Resource Center at the University of California, San Francisco. *Klkb1* gene expression was normalized against expression of hypoxanthine phosphoribosyltransferase (HPRT), and reported as a RQ score relative to *Klkb1* expression in 5 week-old mammary glands. Oligonucleotide primers and TaqMan probe used were as follows:

Klkb1 (1272) forward primer: 5'-TGGTCGCCAATGGGTACTG-3'
Klkb1 (1342) reverse primer: 5'-ATATACGCCACACATCTGGATAGG-3'
Klkb1 probe: 5'-(FAM)-CAGCTGCCCATTGCTTTGATGGAATT-(BHQ1)-3'

PCR was conducted in triplicate with 20 μl reaction volumes of TaqMan Universal PCR Master Mix (Applied Biosystems, Foster City, CA), 0.9 mM of each primer, 250 nM probe, and 5 μl cDNA. PCR reaction was performed under the following conditions: 95ºC, 10 minutes, 1 cycle; 95ºC, 15 seconds then 60ºC, 2 minutes, 40 cycles. Analysis was carried out using the sequence detection software (SDS 2.1) supplied with TaqMan 7900HT (Applied Biosystems).

Western blotting and pull-down assays

Mammary glands were lysed in pH 8 RIPA buffer [50 mM TrisHCl (pH 7.5), 150 mM NaCl, 1% Nonidet P-40, 0.5% deoxycholate (DOC), and 0.1% sodium dodecyl sulfate (SDS)] plus complete protease inhibitors, homogenized, then centrifuged at 14,000 rpm at 4ºC to collect supernatant. Ecotin PKal (Stoop and Craik, 2003) biotinylated with Sulfo-NHS-LC-LC biotin (EZ-Link, Pierce, Rockford, IL) was used to generate pull-down columns using immobilized streptavidin beads (Pierce). Mammary lysates (1 mg) were added to the columns and incubated for 2 hours at 4ºC. PKal was detected by Western blotting of mammary lysates or ecotin PKal column eluates. Samples were separated by electrophoresis under reducing, denaturing conditions on 4-12% Bis-Tris acrylamide gels (Invitrogen, Carlsbad, CA) and then blotted onto PVDF membranes (Amersham). Membranes were blocked with 5% nonfat milk and 0.1% Tween in PBS and incubated overnight with a polyclonal antibody raised against recombinant mouse KLKB1 (1:1000, R&D Systems, Minneapolis, MN) in blocking solution. Membranes were washed and incubated with donkey anti-goat IgG (1:2000, Amersham) before detection with ECL chemiluminescent reagent (Amersham).

Inhibitor-localization, immunohistochemistry, enzyme histochemistry, and histology

Abdominal mammary glands were removed and either immediately embedded in OCT (Sakura) medium on dry ice or fixed overnight at 4ºC in 4% paraformaldehyde for paraffin processing. 5 μm frozen or paraffin sections were cut for use in inhibitor-localization, histology, enzyme histochemistry, and immunohistochemistry. To visualize mast cells, frozen sections were air-dried for ≥30 minutes, post-fixed in ice-cold acetone for 10 minutes, rinsed in PBS, and then stained in either Toluidine blue [a metachromatic dye for mast cells, made up as 0.1% Toluidine blue O (Sigma) in 1% sodium chloride, pH 2.3], Alcian blue/Safranin O [an amine/heparin stain for mast cells, made up as 0.36% Alcian blue (Sigma), 0.018% Safranin O (Sigma) in acetate buffer,

pH 1.42], or by using an enzymatic reaction with naphthol AS-D chloroacetate esterase (Sigma) to detect chymase activity (Moloney et al., 1960) then counterstained with Gill's hematoxylin or DAPI. For inhibitor-localization, frozen sections were prepared as above, then incubated overnight with 50 nM ecotin PKal (Stoop and Craik, 2003) biotinylated with Sulfo-NHS-LC-LC biotin (EZ-Link, Pierce, Rockford, IL), followed by an hour incubation with Alexa 488-conjugated streptavidin (Molecular Probes, Invitrogen). Plasma kallikrein immunohistochemistry was performed on paraffin sections following sodium citrate antigen retrieval using a polyclonal antibody against recombinant mouse KLKB1 (R&D Systems, Minneapolis, MN) 1:50 overnight at 4ºC followed by a 30 minute incubation with biotinylated anti-goat secondary (Amersham) visualized using Vectastain ABC (Vector Laboratories, Burlingame, CA) and 3, 3' diaminobenzidine (Fast DAB, Sigma). Histological and immunochemical images were acquired at 100x or 200x using a Leica DMR microscope and Leica FireCam with accompanying software. Images were then imported into Adobe Photoshop software for analysis.

In situ hybridization

Paraffin sections were placed on TESPA-treated slides and prepared for *in situ* hybridization as described (Albrecht et al., 1997). A *Klkb1* probe representing a fragment of *Klkb1* cDNA from nucleotides 915-1414 was generated by PCR amplification from mammary cDNA by PCR and then used as a template for transcription of sense or antisense ^{35}S-labeled riboprobes. Probes were stored at –20ºC before use. Slides were washed at a final stringency of 65ºC in 23x sodium chloride-sodium citrate buffer (SSC), dipped in emulsion, and exposed for approximately 2 weeks. DNA was counterstained with Hoechst 33342.

RESULTS

Mouse plasma kallikrein is differentially expressed in the developing mammary gland

Plasma kallikrein expression has been demonstrated in a variety of mouse and human tissues outside of the liver (Cerf and Raidoo, 2000; Ciechanowicz et al., 1993; Neth et al., 2001). Accordingly, we wished to test the hypothesis that PKal is expressed in the mammary gland, and that expression is altered during different phases of mammary gland development, when careful regulation of plasminogen activation is required.

The process of pubertal mammary gland development begins around 3 weeks of age and continues until the advancing ductal epithelium reaches the end of the fat pad, around 8-10 weeks of age. We examined *Klkb1* (the gene encoding prekallikrein) gene expression in the mouse mammary gland at different postnatal development time points (3 weeks, 5 weeks, 15 days pregnant, 10 days lactating, and 4 days involuting) by real-time quantitative polymerase chain reaction (RT-PCR). Prekallikrein mRNA was abundant during pubertal development, when the mammary gland is undergoing active remodeling as the ductal epithelium expands and advances through the stromal fat pad (Figure 1).

During pregnancy and lactation, when the stroma has largely been replaced by secretory alveoli and extensive ductal structures, prekallikrein mRNA is markedly reduced. Prekallikrein mRNA increased significantly during the program of mammary gland involution, when the secretory lactation epithelial structures apoptose and the mammary stromal compartment is replenished. These findings indicate that not only is PKal produced in the mammary gland, but that increased expression levels correlate with periods of stromal remodeling.

Ecotin PKal binds mammary gland plasma kallikrein

Using ecotin PKal, a macromolecular inhibitor of active PKal (Stoop and Craik, 2003), we have shown that inhibition of PKal during mammary gland involution significantly inhibits secretory epithelial apoptosis, adipocyte replenishment and stromal remodeling (J. Lilla, Chapter 3). To demonstrate that the target of this inhibitor *in vivo* is PKal, we collected mammary gland lysates from 5 week and 4 days involuting mammary glands, when PKal is highly expressed in these tissues, to determine whether ecotin PKal can bind PKal from mammary tissue lysates. Using biotinylated ecotin PKal–bound streptavidin beads, we pulled down PKal from virgin 5 week-old mouse mammary gland lysates (Figure 2). The bands indicated on the blot represent the full-length protein (approximately 80 kDa), and its heavy (~42 kDa) and light (~28 kDa) chains, which respectively have one and two identified N-glycosylated Asn residues according to the SwissProt Protein Database (http://www.expasy.org/uniprot/P26262). Similar results were obtained from 4 day involuted mammary gland lysates (data not shown). These data confirm that Ecotin PKal binds PKal found in the mammary gland.

Biotinylated ecotin PKal localizes active plasma kallikrein to mast cells

Our data indicate that PKal is expressed in the mammary gland, in addition to circulating prekallikrein from the liver, and that *in vivo* PKal inhibition with ecotin PKal inhibits mammary gland involution (Chapter 3). We next wished to identify what cells in the mammary gland are the site of PKal expression and/or activity. We used the biotinylated form of ecotin PKal to localize the active protease in 5 day-involuting mammary gland tissue sections, taking advantage of ecotin PKal's picomolar affinity (K_i^* = 11 pM, (Stoop and Craik, 2003)) for the active form of PKal. With this method, we observed that active PKal localized to specific cells in the mammary gland (Figure 3A) and that this staining was absent in 1000-fold excess of non-biotinylated ecotin PKal (Figure 3B). Furthermore, as wild-type ecotin does weakly bind prekallikrein, wild-type biotinylated ecotin staining could only be seen in mast cells after applying a 10,000-fold increase of the inhibitor (data not shown). The ecotin PKal-positive cells appeared clustered near blood vessels, ducts, and scattered throughout the fatty stroma and the loose connective tissue surrounding the mammary fat pad (Figure 3C). We identified these $PKal^+$ cells as mast cells, as first shown by serial section alcian blue staining (Figure 3D). We confirmed that plasma kallikrein localizes to mammary gland mast cells by immunohistochemistry using a polyclonal antibody against mouse KLKB1, counterstained with Toluidine blue, another mast cell-specific stain (Figure 3E-F). These data represent a novel connection between plasma kallikrein and mast cells.

Mast cells in both mice and humans can be subdivided into two general classes according to staining properties, proteoglycan and protease content, and histamine

concentration: connective tissue and mucosal (Metcalfe et al., 1997). Connective tissue-type mast cells are predominantly found in skin and the peritoneal cavity, while mucosal-type mast cells are found in the lamina propria of the small intestine and in the lung. Because PKal localization to mast cells has not previously been demonstrated, we tested the ability of ecotin PKal to localize the protease to different mast cell types in other tissues. We found that ecotin PKal stained connective tissue-type mast cells of the skin and tongue (Figure 4A and B), but not the mucosal-type mast cells of the intestine (Figure 4D). Importantly, we also did not see ecotin PKal staining in the liver (Figure 4C), where prekallikrein is produced for circulation in the plasma, demonstrating the specificity of the inhibitor for the active form of the protease.

Plasma kallikrein specifically localizes to mast cell granules

To determine the subcellular localization of Ecotin PKal, we co-stained with naphthol chloroacetate esterase, a marker of mast cell granule chymase that appears red in both light and fluorescent microscopy (Moloney et al., 1960). We observed that PKal localized to the cytoplasmic granules of mast cells (Figure 5A). Ecotin PKal staining was absent in mammary glands of the mast cell-deficient *Kit* mutant W-*sash* mouse line (Duttlinger et al., 1993), supporting the observation that active PKal is only seen in mammary mast cells (Figure 5B). We examined ecotin $PKal^{+}$ mast cells by confocal microscopy to pinpoint the subcellular localization of active PKal to mast cell granules (Figure 5C), and observed that not all granules stained positively for ecotin PKal within a specific mast cell, and not all mammary mast cells were positive for active PKal (data not shown). These observations suggest that PKal-mast cell interactions are context-specific, though the mechanisms for this interaction still need to be identified.

We then asked whether the localization of PKal to mast cell granules depended on the activation state of the mast cell by inhibiting mast cell degranulation or by using mutant mice that have a defect in activating their mast cell serine proteases. To inhibit mast cell degranulation, we used cromolyn sodium treatment to inhibit the calcium ion influx that is required to trigger mast cell degranulation (McIntyre et al., 1981). Dipeptidyl peptidase I (DPP I, or cathepsin C) deficient mice have mast cells that can degranulate, yet their mast cell proteases are either inactive or downregulated (Wolters et al., 2001). We compared ecotin PKal/chloroacetate esterase staining in mammary gland mast cells between wild-type, mast cell degranulation-inhibited, and mast cell protease-inactivated mice. In normal, wild-type adult virgin mice, ecotin PKal localizes specifically to mast cell granules (Figure 5D). In mice treated with cromolyn sodium, we observed active PKal localization change to appear as a “halo” surrounding the mast cells in the majority of cells observed (Figure 5E). Mammary mast cells from DPP I-deficient mice stained with ecotin PKal/chloroacetate esterase did not stain positively for active PKal (Figure 5F), suggesting that DPP I activity is upstream of PKal activation. These changes in active PKal location relative to mast cell activity and mast cell protease activation indicate a curious interaction between plasma kallikrein and mammary gland mast cells.

DISCUSSION

This study elucidates a new pattern of expression and activation for plasma kallikrein, which is best known as a liver-synthesized, plasma-borne activator of bradykinin. Our previous work has determined that plasma kallikrein is an essential

activator of plasminogen in the process of mammary gland involution, with effects on both the epithelial and stromal compartments of the gland (Chapter 3). An outstanding question is the mechanism of PKal itself during mammary gland involution; if prekallikrein constantly circulates in plasma at high concentration (about 40 μg/ml), how could PKal be activated specifically to participate as a plasminogen activator in mammary gland involution?

We detected *Klkb1* mRNA in the mammary gland, and determined that it is upregulated in the gland during pubertal development and postlactational involution. Recent work examining the human prekallikrein promoter suggests that the promoter region has both repression and enhancer regions, as well as multiple alternative transcription initiation sites (Neth et al., 2005), providing multiple means for tissue-specific control of PKal at the level of transcription. It is interesting to speculate as to why PKal would be locally produced in tissues that would already potentially have a large reservoir of prekallikrein available through their vasculature. One hypothesis is that the source of PKal determines its substrate(s), either by bioavailability or by method of activation. Further studies to determine the tissue-specific regulation of PKal transcription would be very helpful in future analysis of its participation in different physiological processes, such as whether systemic or local expression of this plasminogen activator is more important to the function of plasma kallikrein during processes such as mammary gland involution.

We took advantage of the development of a macromolecular inhibitor highly specific to active PKal, ecotin PKal (Stoop and Craik, 2003), to pinpoint the site of PKal function in the mammary gland. We found that ecotin PKal could be used to pull down PKal from mammary gland lysates and as a specific marker for PKal in mammary tissue sections. Surprisingly, using biotinylated ecotin PKal as a probe for the active protease, we localized PKal to mammary gland mast cells. We confirmed this result by immunohistochemistry. We also used ecotin PKal to localize PKal specifically to mast cell granules in tissues that contain connective tissue-type mast cells. While this result is intriguing, it poses a significant experimental difficulty in that connective tissue-type mast cells are not easily isolated from tissues, and differentiation of primary bone marrow cells into mast cells with interleukin-3 results in mast cells of the mucosal phenotype (Razin et al., 1984), which were not positive for ecotin PKal. Therefore, though our immunohistochemistry data and ecotin PKal results associate PKal with mast cells, an important confirmation that ecotin PKal is specifically binding PKal in mast cell granules will be available only when the prekallikrein knockout mouse is developed. We also attempted to pinpoint the sites of PKal expression in the mammary gland by *in situ* hybridization. Whether due to high background or low expression levels, we have not been able to identify convincingly which cells in the mammary gland might be expressing PKal (data not shown).

In the meantime, our staining for active PKal demonstrates that localization of PKal to mast cell granules is dependent on the activation state of the mast cells. Treatment with cromolyn sodium, which is used to inhibit mast cell degranulation by blocking calcium influx (McIntyre et al., 1981), changed the localization of PKal so that mast cell granules were no longer PKal-positive, but instead active PKal was pericellular. One potential explanation for this observation is that cromolyn sodium may block endocytic pathways that would allow uptake of active PKal into mast cells, which

may serve to sequester PKal from the extracellular environment. Alternatively, if mast cells are a source of prekallikrein production in the mammary gland, they may be able to activate and/or release PKal through exocytotic pathways independent of mast cell granules. However, these hypotheses are complicated by our observation that active PKal was not detected in mammary gland mast cells from mice deficient for DPP I, the lysosomal cysteine protease required for the activation and/or normal expression of granule-associated proteases (Pham and Ley, 1999; Wolters et al., 2001). This observation suggests that mast cell protease activity is required for PKal activation and/or sequestration to mast cell granules. In either case, these results signify a new pathway for plasma kallikrein activity and activation, which has never before been associated with mast cell granules.

Furthermore, in conjunction with our observations that PKal is the predominant plasminogen activator in the mammary gland during involution, this study establishes a plausible relationship between mast cells, PKal, and plasmin conversion in the mammary gland that represents a novel pathway for the plasminogen activation cascade. Further study into the different roles of systemically-circulated and locally-produced PKal and its activation is clearly necessary.

REFERENCES

Albrecht, U., G. Eichele, J.A. Helms, and H. Lu. 1997. Visualization of gene expression patterns by *in situ* hybridization. *In* Molecular and Cellular Methods in Developmental Toxicology. G.P. Daston, editor. CRC Press, Boca Raton. 23-48.

Bugge, T.H., K.W. Kombrinck, Q. Xiao, K. Holmback, C.C. Daugherty, D.P. Witte, and J.L. Degen. 1997. Growth and dissemination of Lewis lung carcinoma in plasminogen-deficient mice. *Blood*. 90:4522-31.

Bugge, T.H., L.R. Lund, K.K. Kombrinck, B.S. Nielsen, K. Holmback, A.F. Drew, M.J. Flick, D.P. Witte, K. Dano, and J.L. Degen. 1998. Reduced metastasis of Polyoma virus middle T antigen-induced mammary cancer in plasminogen-deficient mice. *Oncogene*. 16:3097-104.

Cerf, M.E., and D.M. Raidoo. 2000. Immunolocalization of plasma kallikrein in human brain. *Metabolic brain disease*. 15:315-23.

Ciechanowicz, A., M. Bader, J. Wagner, and D. Ganten. 1993. Extra-hepatic transcription of plasma prekallikrein gene in human and rat tissues. *Biochemical and biophysical research communications*. 197:1370-6.

Duttlinger, R., K. Manova, T.Y. Chu, C. Gyssler, A.D. Zelenetz, R.F. Bachvarova, and P. Besmer. 1993. W-sash affects positive and negative elements controlling c-kit expression: ectopic c-kit expression at sites of kit-ligand expression affects melanogenesis. *Development*. 118:705-17.

Jamieson, T., D.N. Cook, R.J. Nibbs, A. Rot, C. Nixon, P. McLean, A. Alcami, S.A. Lira, M. Wiekowski, and G.J. Graham. 2005. The chemokine receptor D6 limits the inflammatory response in vivo. *Nature immunology*. 6:403-11.

Lund, L.R., S.F. Bjorn, M.D. Sternlicht, B.S. Nielsen, H. Solberg, P.A. Usher, R. Osterby, I.J. Christensen, R.W. Stephens, T.H. Bugge, K. Dano, and Z. Werb. 2000. Lactational competence and involution of the mouse mammary gland require plasminogen. *Development*. 127:4481-92.

Lund, L.R., K.A. Green, A.A. Stoop, M. Ploug, K. Almholt, J. Lilla, B.S. Nielsen, I.J. Christensen, C.S. Craik, Z. Werb, K. Dano, and J. Romer. 2006. Plasminogen activation independent of uPA and tPA maintains wound healing in gene-deficient mice. *The EMBO journal*. 25:2686-97.

McIntyre, J.A., E.D. Neerunjun, W.P. Faulk, and M. Papamichail. 1981. Inhibition of in vitro allogeneic reactions with disodium cromoglycate. *International archives of allergy and applied immunology*. 66:244-50.

Metcalfe, D.D., D. Baram, and Y.A. Mekori. 1997. Mast cells. *Physiol Rev*. 77:1033-79.

Miles, L.A., J.S. Greengard, and J.H. Griffin. 1983. A comparison of the abilities of plasma kallikrein, beta-Factor XIIa, Factor XIa and urokinase to activate plasminogen. *Thromb Res*. 29:407-17.

Moloney, W.C., K. McPherson, and L. Fliegelman. 1960. Esterase activity in leukocytes demonstrated by the use of naphthol AS-D chloroacetate substrate. *The journal of histochemistry and cytochemistry*. 8:200-7.

Motta, G., R. Rojkjaer, A.A. Hasan, D.B. Cines, and A.H. Schmaier. 1998. High molecular weight kininogen regulates prekallikrein assembly and activation on endothelial cells: a novel mechanism for contact activation. *Blood*. 91:516-28.

Neth, P., M. Arnhold, H. Nitschko, and E. Fink. 2001. The mRNAs of prekallikrein, factors XI and XII, and kininogen, components of the contact phase cascade are differentially expressed in multiple non-hepatic human tissues. *Thrombosis and haemostasis*. 85:1043-7.

Neth, P., M. Arnhold, V. Sidarovich, K.D. Bhoola, and E. Fink. 2005. Expression of the plasma prekallikrein gene: utilization of multiple transcription start sites and alternative promoter regions. *Biological chemistry*. 386:101-9.

Pham, C.T., and T.J. Ley. 1999. Dipeptidyl peptidase I is required for the processing and activation of granzymes A and B in vivo. *Proceedings of the National Academy of Sciences of the United States of America*. 96:8627-32.

Razin, E., J.N. Ihle, D. Seldin, J.M. Mencia-Huerta, H.R. Katz, P.A. LeBlanc, A. Hein, J.P. Caulfield, K.F. Austen, and R.L. Stevens. 1984. Interleukin 3: A differentiation and growth factor for the mouse mast cell that contains chondroitin sulfate E proteoglycan. *Journal of immunology (Baltimore, Md.* 132:1479-86.

Rojkjaer, R., and A.H. Schmaier. 1999. Activation of the plasma kallikrein/kinin system on endothelial cell membranes. *Immunopharmacology*. 43:109-14.

Schmaier, A.H., R. Rojkjaer, and Z. Shariat-Madar. 1999. Activation of the plasma kallikrein/kinin system on cells: a revised hypothesis. *Thromb Haemost*. 82:226-33.

Selvarajan, S., L.R. Lund, T. Takeuchi, C.S. Craik, and Z. Werb. 2001. A plasma kallikrein-dependent plasminogen cascade required for adipocyte differentiation. *Nat Cell Biol*. 3:267-75.

Stephens, R.W., N. Brunner, F. Janicke, and M. Schmitt. 1998. The urokinase plasminogen activator system as a target for prognostic studies in breast cancer. *Breast Cancer Res Treat*. 52:99-111.

Stoop, A.A., and C.S. Craik. 2003. Engineering of a macromolecular scaffold to develop specific protease inhibitors. *Nat Biotechnol*. 21:1063-8.

Tordai, H., L. Banyai, and L. Patthy. 1999. The PAN module: the N-terminal domains of plasminogen and hepatocyte growth factor are homologous with the apple domains of the prekallikrein family and with a novel domain found in numerous nematode proteins. *FEBS letters*. 461:63-7.

Wolters, P.J., C.T. Pham, D.J. Muilenburg, T.J. Ley, and G.H. Caughey. 2001. Dipeptidyl peptidase I is essential for activation of mast cell chymases, but not tryptases, in mice. *The Journal of biological chemistry*. 276:18551-6.

Zhang, L., D. Seiffert, B.J. Fowler, G.R. Jenkins, T.C. Thinnes, D.J. Loskutoff, R.J. Parmer, and L.A. Miles. 2002. Plasminogen has a broad extrahepatic distribution. *Thromb Haemost*. 87:493-501.

FIGURES

Figure 1. Real-time PCR analysis of *Klkb1* expression in mammary gland RNA shows that *Klkb1* is differentially expressed throughout postnatal mammary gland development. Real-time qPCR performed in triplicate for *Klkb1* expression normalized against HPRT and reported as a RQ score relative to *Klkb1* expression in 5 week old mammary glands from CD1 mice. Increased expression correlates to periods of active stromal remodeling during mammary development.

This page contains unpublished data which should be protected.

Figure 1

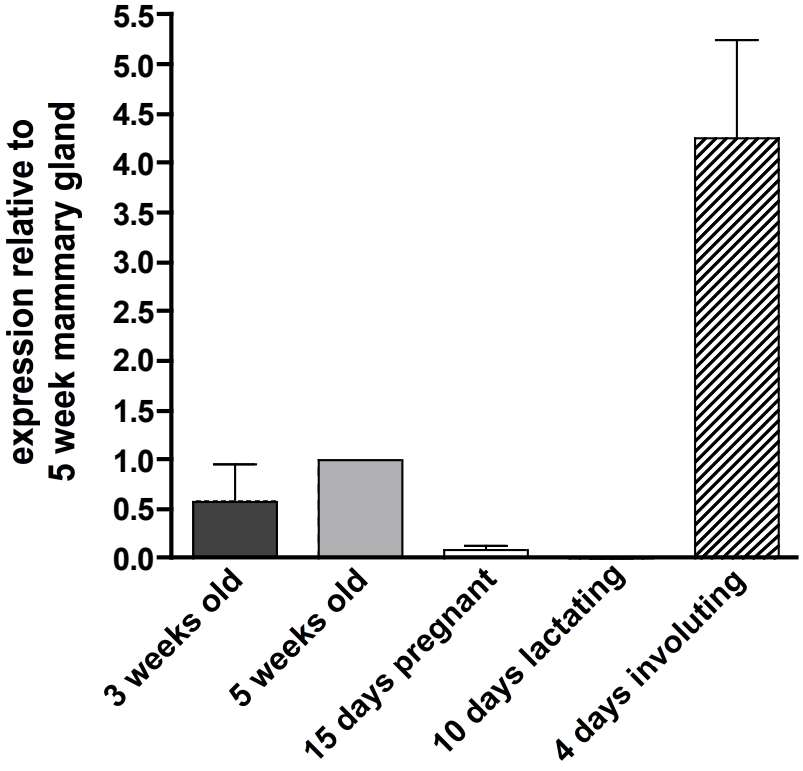

Figure 2. Ecotin PKal binds plasma kallikrein isolated from mammary gland lysates. Protein lysates from five week old virgin mammary glands were run over either streptavidin beads or beads bound with biotinylated EcoPK ("pull-down") and subjected to electrophoresis and Western blotting using an antibody against mouse prekallikrein (α-mouse KLKB1, R&D Systems). The bands likely represent full-length PKal (appx. 80 kDa), its heavy chain (42 kDa unglycosylated), and its light chain (28 kDa, unglycosylated). mPKal = mouse prekallikrein peptide R&D Systems, Minneapolis, MN), against which the antibody was raised.

Figure 2

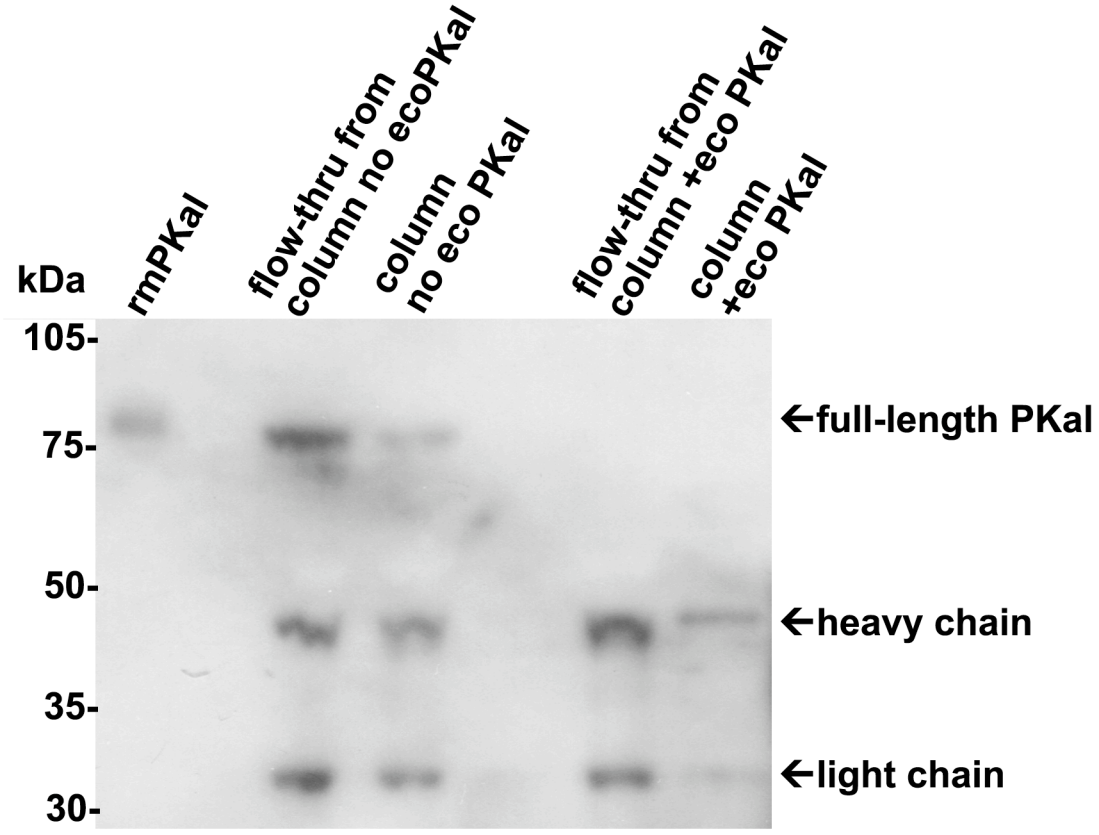

Figure 3. Biotinylated ecotin PKal may be used to localize active protease in the mammary gland to resident mast cells. A) Frozen section of 5 day involuting mammary gland using Alexa 488-conjugated streptavidin (green) to visualize 50 nM bound biotinylated ecotin PKal; DAPI counterstain, 100x. B) Staining is absent in presence of excess (50μM) non-biotinylated ecotin PKal. Scale bar for A-D = 100 μm. C) Mast cells clustered around a large mammary blood vessel stain positively for active PKal when visualized using biotinylated ecotin PKal. Frozen sections of 5 day involuting mammary gland stained with biotinylated ecotin PKal as above. D) Serial section of C stained for mast cells with Alcian Blue/Safranin O shows that cells labeled by ecotin PKal staining are mast cells. E) Paraffin section of 5 week old mammary gland shows mast cells in the mammary stroma stained with Toluidine blue, which stains mast cell granules purple. Sections were treated as a negative control for staining shown in F. F) Serial section of E immunostained with KLKB1 antibody followed by DAB shows that mammary gland mast cells stain positively for plasma kallikrein using conventional immunhohistochemistry. Scale bar for E-F = 100 μm.

Figure 3

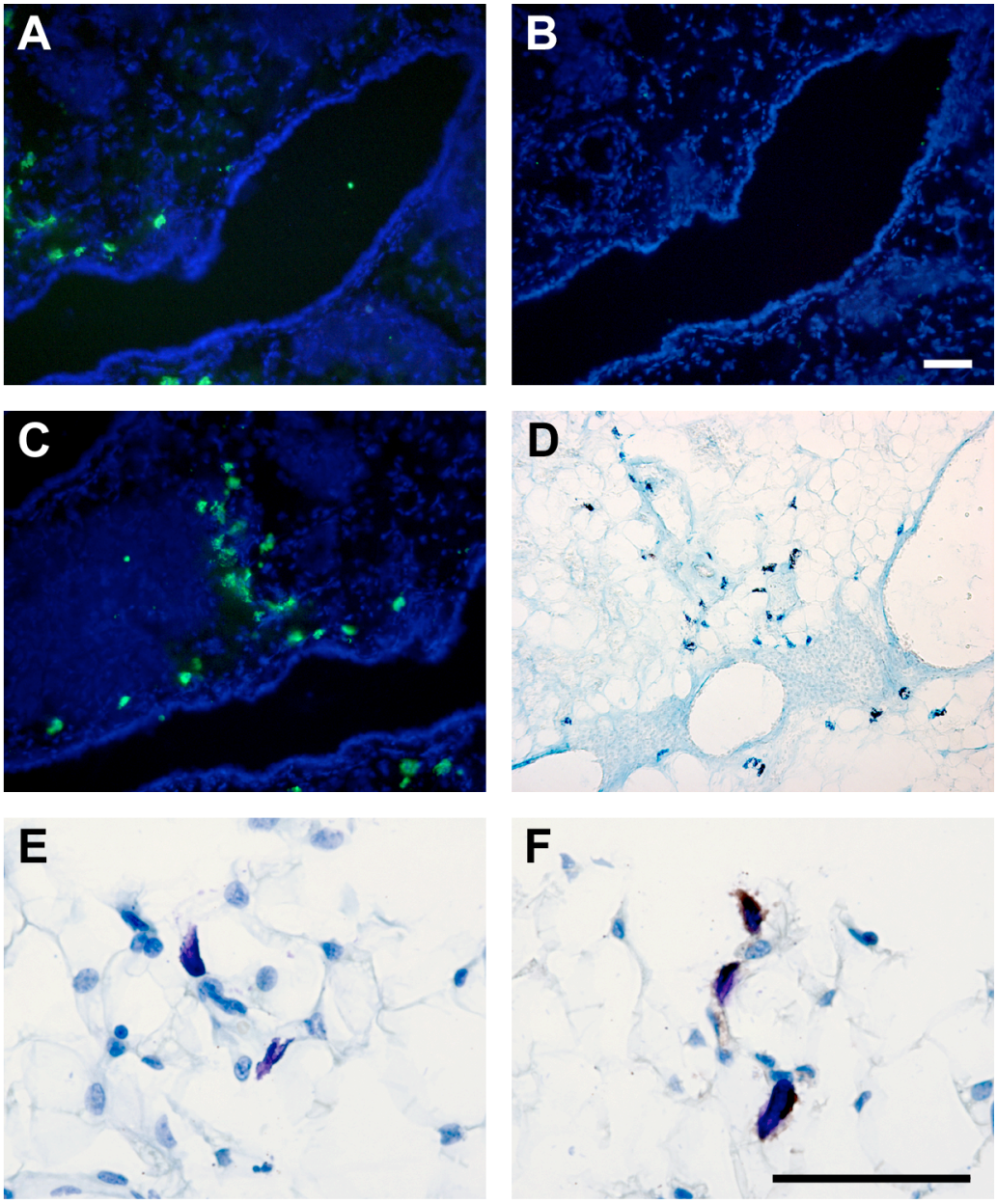

Figure 4. Biotinylated ecotin PKal stains tissues with connective tissue-type mast cells but not liver. Frozen sections using 50 nM ecotin PKal plus Alexa 488-conjugated streptavidin, DAPI counterstain. Scale bar for A-D = 100 μm. Active PKal is seen in mast cells of the skin (A) and tongue (B), but not in liver (C) or intestine (D). Active PKal cannot be seen in liver, where prekallikrein is synthesized but not activated, and therefore is not bound by ecotin PKal. Active PKal is not seen in the small intestine, where mast cells are of the mucosal sub-type.

Figure 4

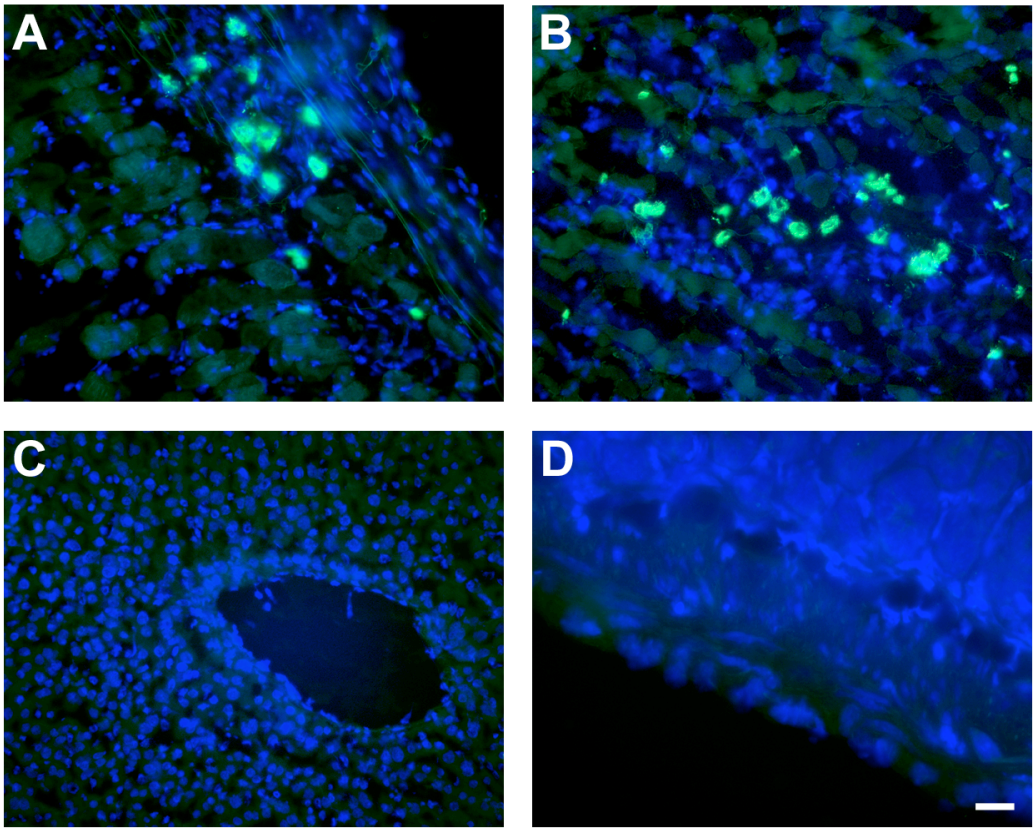

Figure 5. Ecotin PKal stains mast cell granules, and colocalization is dependent on the activation of mammary mast cells. A) Biotinylated ecotin PKal colocalizes specifically with mast cell granules. Frozen section of 5 week old mammary gland using 50 nM biotinylated ecotin PKal plus Alexa 488-conjugated streptavidin (green) and naphthol chloroacetate esterase (CAE), a marker of mast cell granule chymase (red). B) Frozen section of 5 week old W-*sash* mouse mammary gland, which are deficient for mast cells, stained with biotinylated ecotin PKal and CAE as above. Scale bar for A-B = 100 μm. C) Confocal image of a single mast cell from a 5 week old mouse mammary gland stained with biotinylated ecotin PKal and CAE as described above. Not all granules are ecotin PKal positive, and not all mammary mast cells are stained by ecotin PKal (data not shown). Scale bar = 10 μm. D-F) Adult virgin mammary gland frozen sections stained with 50 nM biotinylated ecotin PKal and CAE. D) Wild-type, saline controls show PKal localized to mast cell granules. E) PKal stains as a “halo” around mast cells in wild-type mice treated with cromolyn sodium, which inhibits Ca^{2+} influx and prevents mast cell degranulation. F) Mammary glands from mice deficient for cathepsin C (DPP I), the activator of most mast cell granule proteases, do not stain positively for PKal. Scale bar for D-F = 100 μm.

Figure 5

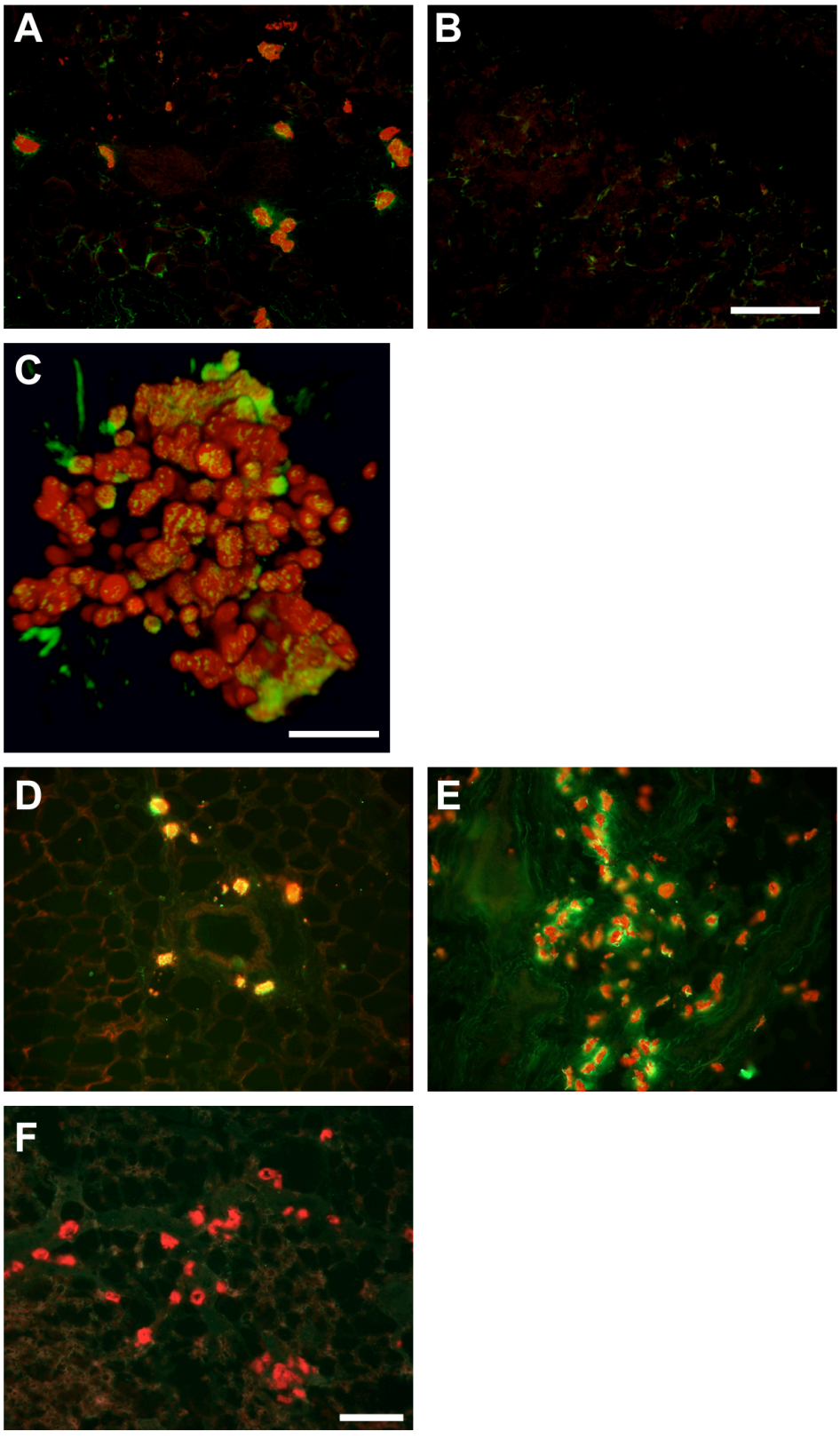

The EMBO Journal (2006) 25, 2686–2697 | © 2006 European Molecular Biology Organization | All Rights Reserved 0261-4189/06
www.embojournal.org

THE EMBO JOURNAL

Plasminogen activation independent of uPA and tPA maintains wound healing in gene-deficient mice

Leif R Lund[1,*], Kirsty A Green[1], Allart A Stoop[2], Michael Ploug[1], Kasper Almholt[1], Jennifer Lilla[3], Boye S Nielsen[1], Ib J Christensen[1,4], Charles S Craik[2], Zena Werb[3], Keld Danø[1] and John Rømer[1]

[1]Finsen Laboratory, Rigshospitalet, Strandboulevarden 49, Copenhagen, Denmark, [2]Department of Pharmaceutical Chemistry, University of California, San Francisco, CA, USA and [3]Department of Anatomy, University of California, San Francisco, CA, USA

Simultaneous ablation of the two known activators of plasminogen (Plg), urokinase-type (uPA) and the tissue-type (tPA), results in a substantial delay in skin wound healing. However, wound closure and epidermal re-epithelialization are significantly less impaired in *uPA;tPA* double-deficient mice than in *Plg*-deficient mice. Skin wounds in *uPA;tPA*-deficient mice treated with the broad-spectrum matrix metalloproteinase (MMP) inhibitor galardin (*N*-[(2*R*)-2-(hydroxamido-carbonylmethyl)-4-methylpentanoyl]-L-tryptophan methylamide) eventually heal, whereas skin wounds in galardin-treated *Plg*-deficient mice do not heal. Furthermore, plasmin is biochemically detectable in wound extracts from *uPA;tPA* double-deficient mice. *In vivo* administration of a plasma kallikrein (pKal)-selective form of the serine protease inhibitor ecotin exacerbates the healing impairment of *uPA;tPA* double-deficient wounds to a degree indistinguishable from that observed in *Plg*-deficient mice, and completely blocks the activity of pKal, but not uPA and tPA in wound extracts. These findings demonstrate that an additional plasminogen activator provides sufficient plasmin activity to sustain the healing process albeit at decreased speed in the absence of uPA, tPA and galardin-sensitive MMPs and suggest that pKal plays a role in plasmin generation.

The EMBO Journal (2006) **25,** 2686–2697. doi:10.1038/sj.emboj.7601173; Published online 8 June 2006
Subject Categories: molecular biology of disease
Keywords: fibrinolysis; plasma kallikrein; plasmin; *uPA*-, *tPA*- and *plasminogen*-deficient mice; wound healing

Introduction

Confined proteolytic degradation of the extracellular matrix by the concerted action of the serine protease plasmin and members of the matrix metalloprotease (MMP) family is considered to play a key role in a variety of physiological and pathological processes involving tissue remodeling and cell migration, including cancer invasion (Danø *et al*, 2005; Egeblad and Werb, 2002). A role for the plasmin precursor plasminogen (Plg) in tissue remodeling processes has been conclusively demonstrated by studies of skin wound healing (Rømer *et al*, 1996), cancer metastasis (Bugge *et al*, 1998), post-lactational mammary gland involution (Lund *et al*, 2000) and placental development (Solberg *et al*, 2003) in mice with a disrupted Plg gene. Plasmin is formed from Plg by cleavage catalyzed by Plg activators. Two physiologically active mammalian Plg activators are known, the urokinase-type (uPA) and the tissue-type (tPA) (Danø *et al*, 1985; Collen and Lijnen, 2005). uPA is secreted as an inactive precursor, pro-uPA, which can bind to the uPA receptor (uPAR), a glycolipid-anchored membrane protein with three-fold finger domains (Llinas *et al*, 2005). Pro-uPA is activated to uPA by plasmin while bound to uPAR, and receptor-bound uPA can activate Plg (Ploug, 2003). Concomitant binding of pro-uPA and Plg to cell surfaces strongly accelerates plasmin generation owing to an increased efficiency of the reciprocal activation of the two proenzymes (Ellis *et al*, 1991). tPA-directed plasminogen activation is accelerated by concomitant binding of tPA and Plg to fibrin (Carmeliet *et al*, 1994; Collen and Lijnen, 2005). Preferential sites for the uPA and tPA pathways of Plg activation are therefore surfaces of uPAR-expressing cells and fibrin deposits, respectively. In accordance, the primary established functions of uPA are within tissue remodeling processes (Danø *et al*, 1999), whereas those of tPA are within vascular thrombolysis (Collen and Lijnen, 2005). Despite this divergence in their basic biological functions, uPA and tPA can to some extent serve as mutual, functional substitutes, as has been observed in gene-deficient mice (Carmeliet *et al*, 1994; Bugge *et al*, 1996a). In addition to uPA and tPA, a few other serine proteases such as the blood coagulation factors XI and XII and plasma kallikrein are capable of activating plasminogen in test tubes (Danø *et al*, 1985). However, the physiological impact of such activators has not been thoroughly demonstrated *in vivo* during, for example, skin wound healing. In mammary gland involution, it was suggested that plasma kallikrein (pKal) is a Plg activator during adipocyte differentiation (Selvarajan *et al*, 2001).

During healing of skin wounds, the migrating leading-edge keratinocytes express uPA and uPAR. tPA is more scarcely expressed but has been detected in a few keratinocytes late in the re-epithelialization of human wounds (Rømer, 2003). In *Plg*-deficient mice there is a pronounced delay in wound healing characterized by a decreased rate of migration of keratinocytes from the wound edges and an accumulation of fibrin in front of the leading-edge keratinocytes, suggesting that the delay is owing to a diminished ability of these cells to proteolytically dissect their way through the extracellular

*Corresponding author. Finsen Laboratory, Copenhagen University Hospital, Strandboulevarden 49, 2100 Copenhagen, Denmark. Tel.: 45 35455907; Fax: 45 35385450; E-mail: lund@inet.uni2.dk
[4]Present address: Department of Surgical Gastroenterology, Hvidovre Hospital, DK-2650 Hvidovre, Denmark

Received: 13 September 2005; accepted: 8 May 2006; published online: 8 June 2006

matrix (Rømer *et al*, 1996). This interpretation is supported by the observation that skin wound healing is restored in mice deficient in both *plasminogen* and *fibrin* (Bugge *et al*, 1996b). Although delayed, complete wound healing is eventually achieved in all *Plg*-deficient mice. Several MMPs, including MMP3, MMP9 and MMP13, are expressed in murine leading-edge keratinocytes (Madlener *et al*, 1998; Lund *et al*, 1999), and wound healing is severely impaired in transgenic mice with human collagenase-1-resistant collagen I (Beare *et al*, 2003). Treatment of wild-type mice with a broad-spectrum MMP inhibitor, galardin (*N*-[(2*R*)-2-(hydroxamido-carbonylmethyl)-4-methylpentanoyl]-L-tryptophan methylamide), causes a delay in wound healing time, but all wounds do eventually heal. However, when Plg-deficient mice are treated with galardin, healing is completely arrested, demonstrating that protease activity is essential for wound healing and that there is a functional overlap between the two classes of matrix-degrading proteases in this process (Lund *et al*, 1999).

In order to study the relative contribution of the individual plasminogen activators during wound healing, we have examined the impact on skin repair of single deficiencies in *uPA*, *tPA* and *Plg* as well as double deficiency in *uPA* and *tPA*. We now provide *in vivo* biochemical and genetic evidence to demonstrate first a functional overlap between uPA and tPA, and second the existence of at least one additional Plg activator contributing to wound healing. Further experimental evidence points to plasma kallikrein as the possible third plasminogen activator with *in vivo* activity during skin wound healing.

Results

Functional overlap between uPA and tPA in wound healing

We first examined the effect on wound healing of single deficiencies in *uPA* and *tPA* and double deficiency in both activators. Standardized 20 mm long, full thickness, incisional wounds were generated in wild-type mice ($n=30$), *uPA*-deficient mice ($n=13$), *tPA*-deficient mice ($n=17$) and mice double-deficient for *uPA* and *tPA* ($n=13$). All mice were F2-generation siblings derived from backcrossing single-deficient mice into the C57Bl/6J strain for 16 generations. The wounds were examined grossly by visual inspection, and the wound lengths measured three times a week. Immediately after surgery, the wounds were spindle-shaped with well-separated incision edges and the underlying muscle fascia was exposed. By the second day post-wounding, the wounds were covered by a dehydrated wound crust, which was gradually lost as healing progressed. Lesions were scored as fully healed when there was a complete loss of the wound crust and closure of the incision interface with restoration of the epidermal covering. Immediately after the wounds were scored as healed by gross inspection, the wounded skin was removed for histological examination. Healing was in all cases verified by the presence of an intact multilayered epidermis (see Figure 3).

The mean times to complete healing for mice with single deficiencies in either *uPA* or *tPA* was 18.2 ± 2.7 and 17.6 ± 2.8 days, respectively, which were similar to the healing time of 16.9 ± 3.2 days in wild-type mice (Table I; Figure 1A). In mice double-deficient for *uPA* and *tPA*, the mean healing time increased to 31.2 ± 11.3 days, a significant delay in skin wound healing compared to the wild-type mice ($P=0.0006$) and also to the *uPA* ($P=0.0008$) or *tPA* ($P=0.0007$) single-deficient mice (Table I; Figure 1A). The combined ablation of *uPA* and *tPA* thus results in a pronounced impairment of wound healing, whereas there is virtually no effect on wound healing of deficiency in either of the two genes alone. We conclude that the presence of either uPA or tPA is required to maintain full wound healing capacity and that there is a functional overlap between the two.

Skin wound healing is less impaired in mice double deficient for uPA and tPA compared to Plg-deficient mice

We next compared the efficiency of the skin wound healing in the *uPA;tPA* double-deficient mice with that in *Plg*-deficient

Table I Effect of uPA, tPA and Plg single deficiencies, uPA;tPA double-deficiency and galardin treatment on wound healing time

Group	Genotype	Number of backcrossings	Treatment	Number of mice	Mean healing time (days)	s.d.	*P*-value
1	Wild-type	16	None	30	16.9	3.2	
2	*uPA−/−; tPA+/+*	16	None	13	18.2	2.7	2 versus 1 NS[a]
3	*uPA+/+; tPA−/−*	16	None	17	17.6	2.8	3 versus 1 NS[a]
4	*uPA−/−; tPA−/−*	16	None	13	31.2	11.3	4 versus 1 0.0006
5	Wild-type	21	None	24	16.8	2.2	
6	*Plg−/−*	21	None	20	42.9	15.6	6 versus 5 0.0001; 6 versus 4 0.03
7	Wild-type	16	Mock	16	17.0	3.7	
8	Wild-type	16	Galardin[b]	10	22.3	5.5	8 versus 7 0.008
9	*uPA−/−; tPA−/−*	16	Mock	13	30.2	10.0	9 versus 7 0.0004
10	*uPA−/−; tPA−/−*	16	Galardin[b]	7	45.9	6.9	10 versus 9 0.002
11	Wild-type	21	Mock	15	19.0	2.9	
12	Wild-type	21	Galardin[b]	15	24.9	3.8	12 versus 11 0.0001
13	*Plg−/−*	21	Mock	14	50.9	19.3	13 versus 11 0.0001; 13 versus 9 0.002
14	*Plg−/−*	21	Galardin[b]	12	>70 days[c]		14 versus 13 0.0001; 14 versus 10 0.0001

[a]Not significant ($P>0.05$).
[b]100 mg/kg daily.
[c]No wounds healed at end of galardin treatment.
Abbreviations: Plg, plasminogen; tPA, tissue-type plasminogen activator; uPA, urokinase-type plasminogen activator.

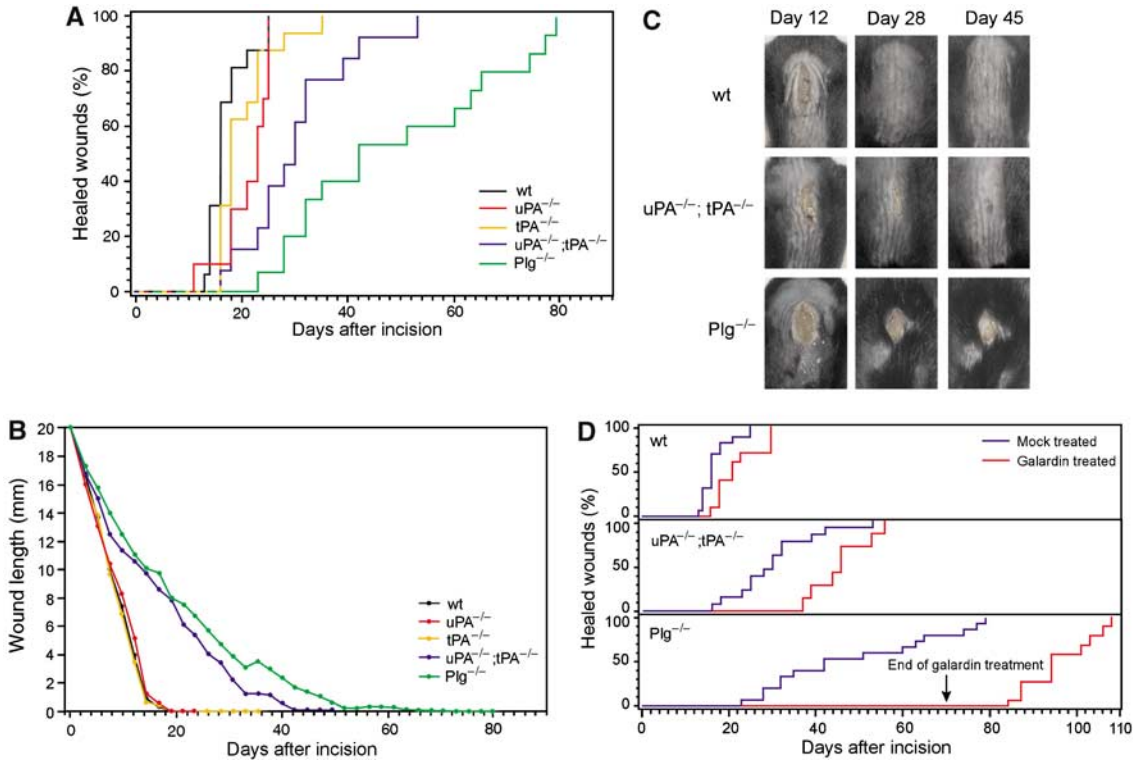

Figure 1 Time course for healing of full-thickness skin wounds in wild-type, *tPA*-deficient, *uPA*-deficient, *uPA;tPA* double-deficient and *Plg*-deficient mice. (**A**) The percentage fraction of mice with complete gross healing is plotted versus time after the incision. A modest and nonsignificant delay was observed in *tPA* single-deficient and *uPA* single-deficient mice compared to wild-type mice, whereas a significant delay was observed in *uPA;tPA* double-deficient mice. In *Plg*-deficient mice, there was an even more pronounced delay and the healing occurred significantly later than in the *uPA;tPA* double-deficient mice. (**B**) The average wound length is plotted versus time after incision. The average wound length of wild-type, *uPA*-deficient and *tPA*-deficient mice was indistinguishable until re-epithelialization. In contrast, the wound length of *uPA;tPA* double-deficient mice was significantly increased compared to either wild-type or *uPA*- or *tPA* single-deficient mice. The average wound length of *Plg*-deficient mice was significantly increased compared to *uPA;tPA* double-deficient mice. (**C**) Examples of the progress of wound repair in wild-type, *uPA;tPA* double-deficient and *Plg*-deficient mice. (**D**) Galardin or mock treatment of wild-type, *uPA;tPA* double-deficient and *Plg*-deficient mice. The percentage fraction of wounds healed is plotted versus time after the incision. The wild-type and *uPA;tPA* double-deficient mice treated with galardin exhibited a delay in healing compared to mock-treated mice but all wounds eventually healed. In contrast, galardin treatment of *Plg*-deficient mice completely blocked healing. However, this arrest was reversible as cessation of galardin treatment in these mice at day 70 resulted in completion of healing, so that the wounds were completely healed within 28 days.

mice. For this purpose, we used *Plg* gene-targeted mice backcrossed into the C57Bl/6J strain for 21 generations. These heterozygous *Plg* gene-deficient mice were interbred, resulting in an F1 generation of mice, of which the homozygous Plg-deficient mice ($n=20$) and their wild-type siblings ($n=24$) were used in the experiment.

The mean wound healing time in the *Plg*-deficient mice was 42.9 ± 15.6 days, whereas the mean healing time in the control group of wild-type mice was 16.8 ± 2.2 days (Table I; Figure 1A) in accordance with previous studies (Rømer *et al*, 1996). The mean healing time in the *Plg*-deficient mice was also significantly longer ($P=0.03$) than the 31.2 ± 11.3 days observed in the *uPA;tPA* double-deficient mice as shown in Figure 1A. Importantly, the healing time in the two control groups of wild-type siblings corresponding to the *uPA;tPA* double-deficient and the *Plg*-deficient mice, respectively, were indistinguishable (16.9 ± 3.2 and 16.8 ± 2.2 days). In a separate experimental setup, wild-type mice obtained by breeding of *MMP-9;Plg* and *MMP3;Plg* double-heterozygous mice exhibited similar healing times (17.0 ± 3.2 and 17.8 ± 3.6 days). Notably, these were indistinguishable from the healing times in the background strain C57Bl/6J (16.3 ± 2.8 days). This emphasize that the observed difference between the *uPA;tPA* double-deficient and *Plg*-deficient mice is not caused by random genetic differences between the various lines of gene-targeted mice, but is clearly ascribed to a role of Plg in wound healing that is not entirely dependent on the presence of the cognate activators uPA and tPA.

Following wounding, the average wound lengths of wild-type, *uPA* single-deficient and *tPA* single-deficient mice were indistinguishable until completion of re-epithelialization (Figure 1B). As opposed to this, the average wound length in *uPA;tPA* double-deficient mice was significantly increased compared to either wild-type or *uPA*- or *tPA* single-deficient mice ($P<0.001$). Furthermore, the average wound length of *Plg*-deficient mice was significantly increased compared to *uPA;tPA* double-deficient mice ($P<0.02$) (Figure 1B).

In the presence of galardin, wound healing is delayed in uPA and tPA double-deficient mice but arrested in Plg-deficient mice

We have previously demonstrated that the MMP inhibitor galardin delays wound healing in wild-type mice and that healing in *Plg*-deficient mice is completely blocked by galardin treatment (Lund *et al*, 1999). We now compared the effect of galardin on skin wound healing in *uPA;tPA*

double-deficient mice and *Plg*-deficient mice. For each of the genotypes, we used mock-treated wild-type mice that were siblings to the gene-deficient mice as controls. By daily administration of galardin at a dose of 100 mg/kg, healing was further delayed in the *uPA;tPA* double-deficient mice (from 30.2±10.0 days in mock-treated mice to 45.9±6.9 days in galardin-treated mice). However, all the galardin-treated *uPA;tPA* double-deficient mice did eventually heal. In contrast, there was a complete arrest of the healing in the galardin-treated *Plg*-deficient mice for the treatment period of 70 days (Table I and Figure 1D). Notably, there was no difference in the wound healing times between the two mock-treated wild-type control groups or between the two galardin-treated wild-type controls (Table I). These findings indicate that the higher wound healing capability in *uPA;tPA* double-deficient mice in comparison with *Plg*-deficient mice is not dependent on a galardin-sensitive protease.

Interestingly, the *Plg*-deficient mice that had been treated with galardin for 70 days were still capable of healing following discontinuation of galardin treatment, and the tissue repair processes were completed within 28 days (see Figure 1D), indicating that the effect of galardin is due to a transient inhibition, and not to permanent defects in the wound-healing program independent of direct protease inhibition.

Pronounced histological differences between skin wounds in uPA;tPA double-deficient and Plg-deficient mice

We next analyzed histological sections of wound sites from mice of the various genotypes at day 10 after incision (Figure 2), at the time point when the wounds were grossly scored as healed, and 1 month after healing (Figure 3). Wounds in wild-type mice obtained from the breeding of both heterozygous $Plg^{+/-}$ mice and heterozygous $uPA^{+/-}$; $tPA^{+/-}$ mice were indistinguishable with respect to gross healing as well as histology at all time points post-wounding (data not shown).

At 10 days after wounding, the newly formed epidermal layer underneath the wound crust had completely covered the wound gap in the majority of wild-type and *tPA*-deficient mice (Figure 2A; panels a–d). The wound crust was still retained, which explains why these wounds were not yet scored as healed by gross inspection. The epidermal layer had not covered the wound field in most of the *uPA*-deficient mice, but complete epidermal closure was occasionally observed at this time point (Figure 2A; panels e and f). In contrast, none of the wounds in *uPA;tPA* double-deficient or *Plg*-deficient mice were covered by a new epidermal layer at day 10 post-wounding. (Figure 2A; panels g–j). The provisional matrix was almost completely degraded and replaced by newly formed granulation tissue in wild-type and *tPA*-deficient mice at day 10 (Figure 2A; panels a–d). The formation of granulation tissue was less pronounced in the *uPA*-deficient mice and almost completely absent in the area beneath the epidermal outgrowths in the *uPA;tPA* double-deficient and *Plg*-deficient mice (Figure 2A; panels h and j). All *Plg*-deficient mice and most of the mice single deficient in uPA or double deficient in *uPA* and *tPA* showed keratinocyte outgrowths that were markedly blunt-ended (Figure 2A; panels f, h and j). In the *Plg*-deficient mice, the keratinocyte outgrowth was covered by a dense layer of provisional matrix (Figure 2A; panels i and j), with an accumulation of fibrin(ogen) in front of the keratinocytes that was not seen to the same extent in the other genotypes, although considerable amounts of fibrin(ogen) accumulates beneath the epidermal outgrowth in *uPA;tPA* double-deficient mice (Figure 2B; panels a–c).

At the time of gross healing, which occurred from 12 to 80 days after incision dependent on the genotype of the mice, the newly formed epidermal layer covering the wound was thickened and multilayered both in wild-type mice and in the various protease-deficient mice (Figure 3A, C and E and data not shown). However, at the time of healing, the overall morphology of the provisional matrix and granulation tissue in the dermis differed between the genotypes. In wild-type, *uPA* single-deficient and *tPA* single-deficient mice, the entire provisional matrix was replaced by a well-organized granulation tissue (Figure 3A and B and data not shown). In contrast, in both *uPA;tPA* double-deficient and *Plg*-deficient mice, large areas of nondegraded provisional matrix were interspersed with foci of apparently normal vessel- and collagen-rich granulation tissue (Figure 3C and E).

At 1 month after completion of re-epithelialization, the area with regenerated tissue could not be distinguished from the adjacent noninjured epidermis in wild-type, *uPA*-deficient, *tPA*-deficient and *uPA;tPA* double-deficient mice (Figure 3B and D, and data not shown), whereas *Plg*-deficient mice still revealed clusters of nondegraded provisional matrix interspersed in areas of granulation tissue (Figure 3F).

Attenuated defect in keratinocyte re-epithelialization in uPA;tPA double-deficient versus Plg-deficient mice

To assess the impact of *uPA*-deficiency, *tPA*-deficiency, *uPA;tPA* double deficiency and *Plg*-deficiency on re-epithelialization by morphometric analysis, we calculated the percentage fraction of the wound width covered by keratinocytes from both sides of the wound. At 10 days after wounding, the re-epithelialization was lower in the mice with single deficiency for uPA (55±7%), double-deficiency for *uPA* and *tPA* (53±4%) and deficiency for *Plg* (45±7%), than in both wild-type mice (88±4%) and *tPA*-deficient mice (92±5%) (Figure 4A). At day 21 after incision, the fraction of the wound width covered by keratinocytes was significantly lower in *Plg*-deficient mice (76±8%) than in *uPA;tPA*-deficient mice (93±4%; *t*-test $P=0.001$) (Figure 4B). In all other genotypes, the wounds were completely re-epithelialized at this time point.

Wound extracts contain a fibrinolytic activity corresponding to pKal

Because previous studies have suggested a role for plasma kallikrein (pKal) in plasminogen activation during adipocyte differentiation (Selvarajan *et al*, 2001), we next analyzed purified pKal and wound extracts for fibrinolytic activities by fibrin/Plg overlay zymography. As shown in Figure 5A, there was a concentration-dependent degradation of fibrin by purified human pKal. The fibrinolytic activity of 0.5 μg pKal is comparable to that of 0.5 ng of purified murine uPA. pKal showed lower fibrinolytic activity in the absence of Plg, which indicates that pKal has some Plg-activator activity (Figure 5A).

In wound extracts from wild-type mice, fibrinolytic activities with electrophoretic mobilities corresponding to purified

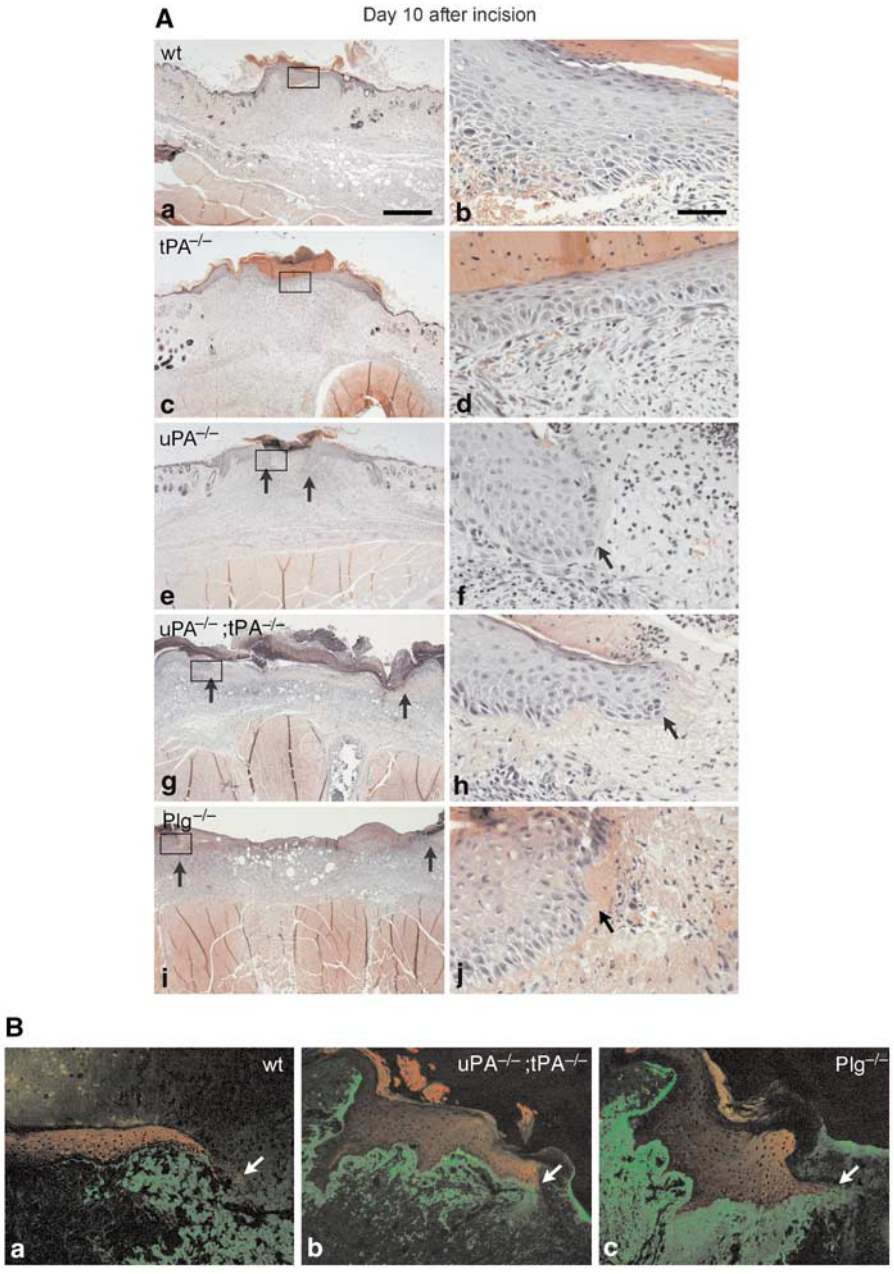

Figure 2 Analysis of skin wounds in wild-type, *tPA*-deficient, *uPA*-deficient, *uPA;tPA* double-deficient and *Plg*-deficient mice at day 10 after incision. (**A**) H&E-stained sections of wounds from wild-type (a, b), *tPA*-deficient (c, d), *uPA*-deficient (e, f), *uPA;tPA* double-deficient (g, h) and *Plg*-deficient mice (i, j). The boxes in a, c, e, g and i are shown in higher magnification in b, d, f, h, and j. Sections of wild-type (a, b) and *tPA*-deficient mouse wounds (c, d) show a complete multilayered epidermal barrier underneath the wound crust and a newly formed granulation tissue with a small isolated Islets of provisional matrix remaining. A section from a *uPA*-deficient mouse (e, f) reveals the leading-edge keratinocytes underneath the wound crust (f). A section of a *uPA;tPA* double-deficient mouse (g, h) reveals migrating keratinocytes surrounded by provisional matrix. Accumulation of amorphous material is observed both in front of, and underneath, the keratinocytes. Similar, but more pronounced accumulations are seen in the sections from *Plg*-deficient mice (i and j). The straight black arrows in (e, g, i, f, h and j) point to the tip of the leading-edge keratinocytes. (**B**) Tissue sections of day 7 wounds from wild-type (a) *uPA;tPA* double-deficient (b) and *Plg*-deficient (c) mice were stained by double immunofluorescence for cytokeratin 8 (red) and fibrin(ogen) (green). Accumulation of immunoreactivity for fibrinogen was observed underneath the keratinocytes in wild-type (a) and *uPA;tPA* double-deficient mice (b). In *Plg*-deficient mice, similar but more pronounced accumulations are seen underneath as well as in front of the keratinocytes (c). The straight white arrows point to the tip of the leading-edge keratinocytes. Bar: Aa, c, e, g and i ~140 μm; Ab, d, f, h and j ~35 μm.

uPA and pKal were detected after prolonged development of the fibrin/Plg zymograms (Figure 5B). After standard development of the zymograms, uPA activity was found in extracts from *tPA*-deficient and *Plg*-deficient mice, whereas virtually no uPA was visible in the wild-type wounds, suggesting an upregulation of uPA in *tPA*- and *Plg*-deficient wounds (Figure 6A). The extracts of all genotypes contained a substantial amount of fibrinolytic activity with an electrophoretic mobility corresponding to purified pKal (Figures 5B and 6A). No other fibrinolytic activity was observed. In zymograms without Plg, all fibrin-degrading activities in the extracts were absent (data not shown).

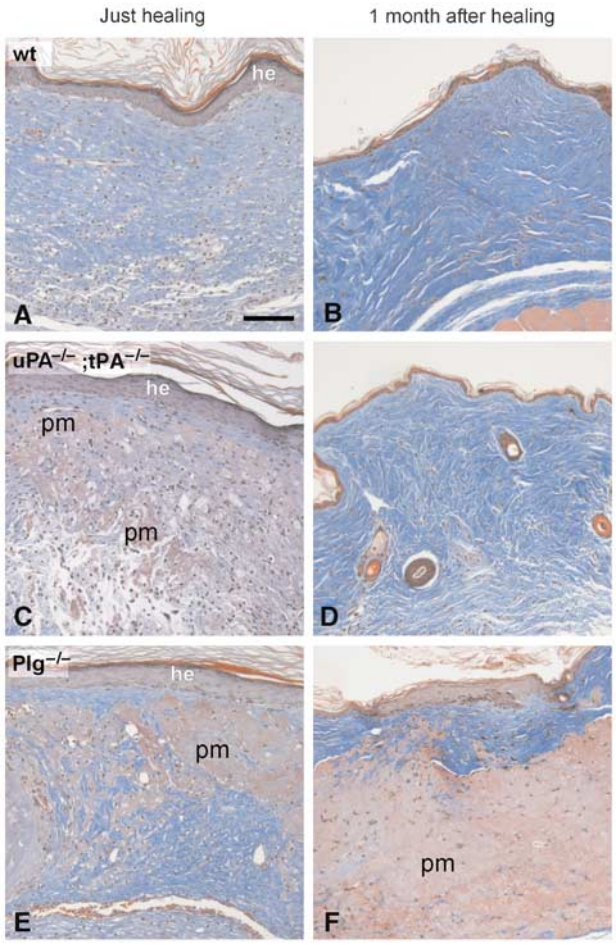

Figure 3 Analysis of skin wounds in wild-type, *uPA;tPA* double-deficient and *Plg*-deficient mice at the time of healing and 1 month post-healing Trichrome-stained sections of wounds from wild-type (**A, B**), *uPA;tPA* double-deficient (**C, D**) and *Plg*-deficient mice (**E, F**). Sections of tissue isolated just after healing reveal an intact, but hyperplastic epidermis (he), In wild-type mice (A), the provisional matrix has been completely replaced by granulation tissue, whereas in *uPA;tPA* double-deficient and *Plg*-deficient mice, larger areas of nondegraded provisional matrix (pm) were interspersed in the granulation tissue (C, E). At 1 month after healing, wild-type (B) and *uPA;tPA* double-deficient (D) mice all reveal a normal-looking epidermis and dermis, whereas in the *Plg*-deficient mice the epidermis is hyperplastic and the dermis is abnormal with abundant accumulations of undegraded provisional matrix (F). Bar: 60 μm.

We used a modified form of the bacterial serine protease inhibitor ecotin$^{7-29}$ that is highly selective for pKal and has no inhibitory effect towards, for example, plasmin, uPA, tPA or six other closely related serine proteases, for all of which the K_i is 4–7 orders of magnitude higher (Stoop and Craik, 2003). The activity corresponding to pKal in wound lysates was completely inhibited by ecotin$^{7-29}$, whereas the inhibitor did not block the activity ascribed to either uPA or the corresponding plasmin activity generated by uPA (Figure 6A). To demonstrate directly that pKal can activate Plg, we next analyzed Plg conversion *in vitro* by Western blot analysis. Both uPA and pKal convert Plg to two-chain plasmin, whereas only trace amounts of Plg are cleaved by prekallikrein. The Plg activation by pKal was not caused by trace impurities in the enzyme preparation as it was inhibited by the pKal-specific ecotin$^{7-29}$ (Figure 5C).

Detection of plasmin in wound extracts from uPA;tPA double-deficient mice

Western blot analysis reveals comparable levels of Plg in the crude extracts from wild-type, *uPA* single-deficient, *tPA* single-deficient and *uPA;tPA* double-deficient mice. As expected, no Plg was detected in *Plg*-deficient mice (Figure 5D, lanes 3–7). Similar amounts of plasmin A- and B-chains were found in wound extracts prepared from wild-type mice and *tPA*-deficient mice, whereas only low levels of plasmin chains were observed in the crude extract of *uPA*-deficient mice. However, in *uPA;tPA* double-deficient mice, no plasminogen conversion was directly detectable in the crude extracts (Figure 5D, lanes 3–7). To improve sensitivity, we subsequently performed a one-step enrichment of Plg/plasmin in wound extracts by lysine-Sepharose affinity chromatography. This provided the required sensitivity that enabled the detection of trace amounts of the individual plasmin chains present in some of the genotypes. As evident in Figure 5D, lanes 12 and 16, both A- and B-chains of plasmin were indeed detectable in extracts from *uPA;tPA* double-deficient mice demonstrating that Plg can be converted *in vivo* independently of uPA and tPA. Importantly, neither A- nor B-chains were detectable when extract from noninjured skin or plasma from wild-type mice were tested (Figure 5D, lanes 8, 14 and 15), emphasizing that Plg is activated *in vivo* during active tissue remodeling, and that no conversion occurs during the extraction or purification procedures.

The serine protease inhibitor ecotin$^{7-29}$ exacerbates the healing impairment in uPA;tPA double-deficient mice

To examine whether pKal has a physiological role during wound healing, we next treated wounded *uPA;tPA*-deficient or *Plg*-deficient mice systemically for 30 days with either vehicle (PBS) or ecotin$^{7-29}$. Ecotin$^{7-29}$ treatment of the *Plg*-deficient mice had no effect on the average wound length (Figure 6C). In contrast, ecotin$^{7-29}$ treatment of *uPA;tPA* double-deficient mice significantly delayed wound healing compared to vehicle control, as measured by the average wound length at the end of treatment 30 days post-wounding ($P<0.03$) (Figure 6C). In fact, the wound lengths of ecotin$^{7-29}$-treated *uPA;tPA* double-deficient mice, mock-treated *Plg*-deficient mice and ecotin$^{7-29}$-treated *Plg*-deficient mice were indistinguishable, which indicates that ecotin$^{7-29}$ blocks virtually all remaining plasminogen activation in the *uPA;tPA* double-deficient mice. At the end of ecotin$^{7-29}$ treatment at day 30 none of the *uPA;tPA* double-deficient wounds (0%) were healed as opposed to 3 out of 8 healed wounds (38%) in the PBS-treated *uPA;tPA* double-deficient mice (Figure 6B). Immediately after discontinuation of the treatment, a rapid completion of healing was observed in the ecotin$^{7-29}$-treated *uPA;tPA* double-deficient mice.

Discussion

Skin wound healing is impaired in *Plg*-deficient mice (Rømer *et al*, 1996). Through a direct comparison of *Plg* deficiency versus *uPA;tPA* double deficiency, we now show that the healing in mice that lack both *uPA* and *tPA* is significantly less impaired as compared to *Plg*-deficient mice. This difference is based on observations of attenuated impairments in gross healing times as well as re-epithelialization in the *uPA;tPA* double-deficient mice. We have found that gross skin wound

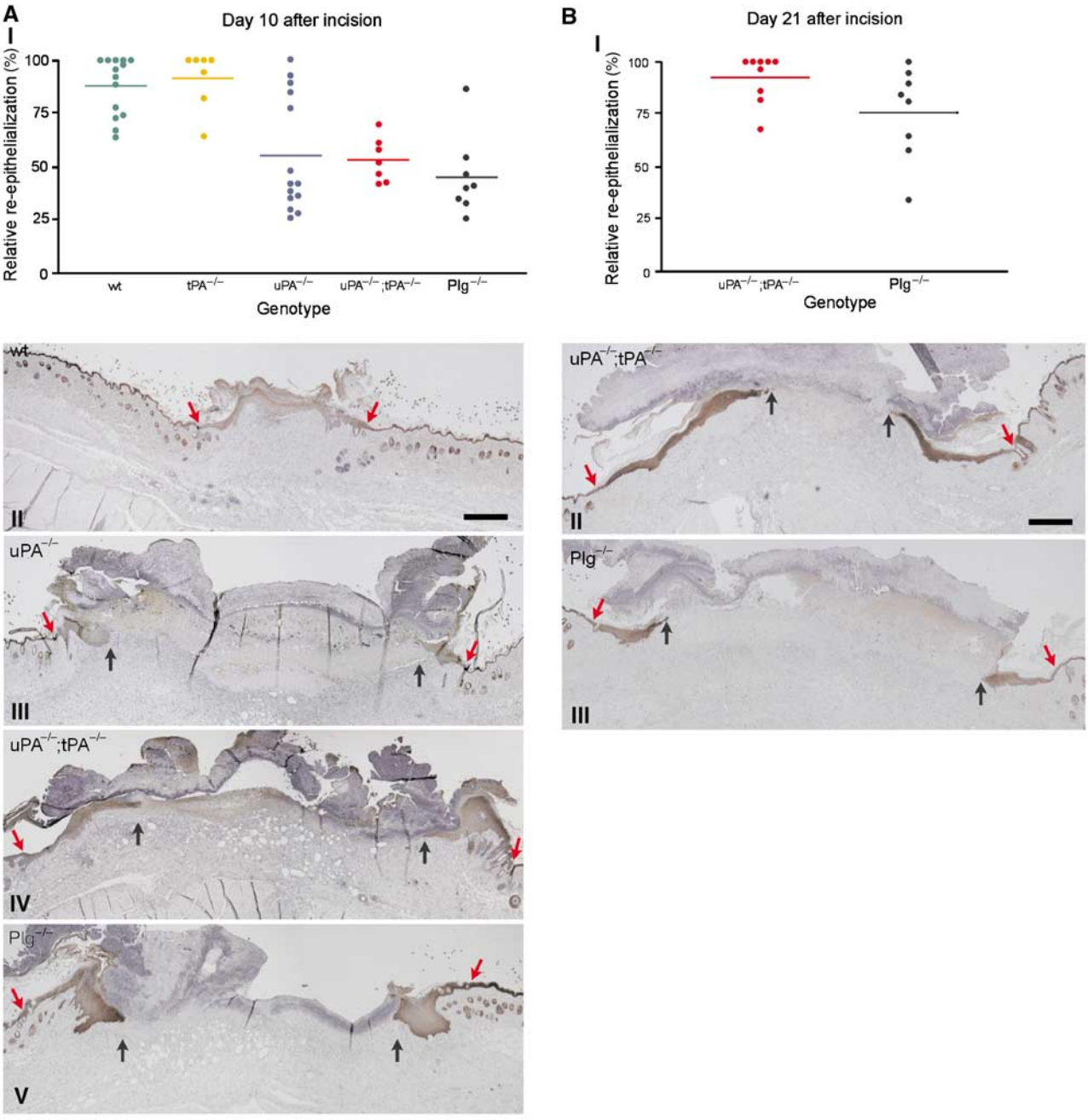

Figure 4 Morphometric analysis of wound re-epithelialization in wild-type, *tPA*-deficient, *uPA*-deficient, *uPA;tPA* double-deficient and *Plg*-deficient mice. (**A**) Scatter plot of the relative re-epithelialization of wounds day 10 after incision in wild-type mice, *tPA*-deficient mice, *uPA*-deficient mice, *uPA;tPA* double-deficient mice and *Plg*-deficient mice (AI). The relative re-epithelialization was determined as the distance from the wound edge to the front of the leading-edge keratinocytes, divided by the distance between the two wound edges. Examples of keratin-stained sections of day 10 wounds from wild-type mice (AII), *uPA*-deficient mice (AIII), *uPA;tPA* double-deficient mice (AIV) and *Plg*-deficient mice (AV). The red arrows mark the wound edge and black arrows point to the tip of the leading-edge keratinocytes. Bar: II–V ~60 μm. (**B**) Scatter plot of the relative re-epithelialization of wounds day 21 after incision in *uPA;tPA* double-deficient mice and *Plg*-deficient mice (BI). Examples of keratin-stained sections of day 21 wounds from *uPA;tPA* double-deficient mice (BII) and *Plg*-deficient mice (BIII). Red arrows mark the wound edge and black arrows identify the tip of the leading-edge keratinocytes. Bar: II–III ~60 μm.

healing in both *uPA* single-deficient and *tPA* single-deficient mice is indistinguishable from the healing of wild-type mice. In contrast, the concomitant ablation of both *uPA* and *tPA* caused a significant delay in the healing, in agreement with our previous findings (Bugge *et al*, 1996a). These results clearly demonstrate a functional redundancy between uPA and tPA in skin wound healing.

The cellular architecture both during and after complete re-epithelialization of the wounds revealed a significant histological difference between *uPA;tPA* double-deficient and *Plg*-deficient mice. The higher residual healing capability of *uPA;tPA* double-deficient mice shows that Plg is playing a role in the healing process even in the absence of the two cognate Plg activators, uPA and tPA. *Plg*-deficient mice

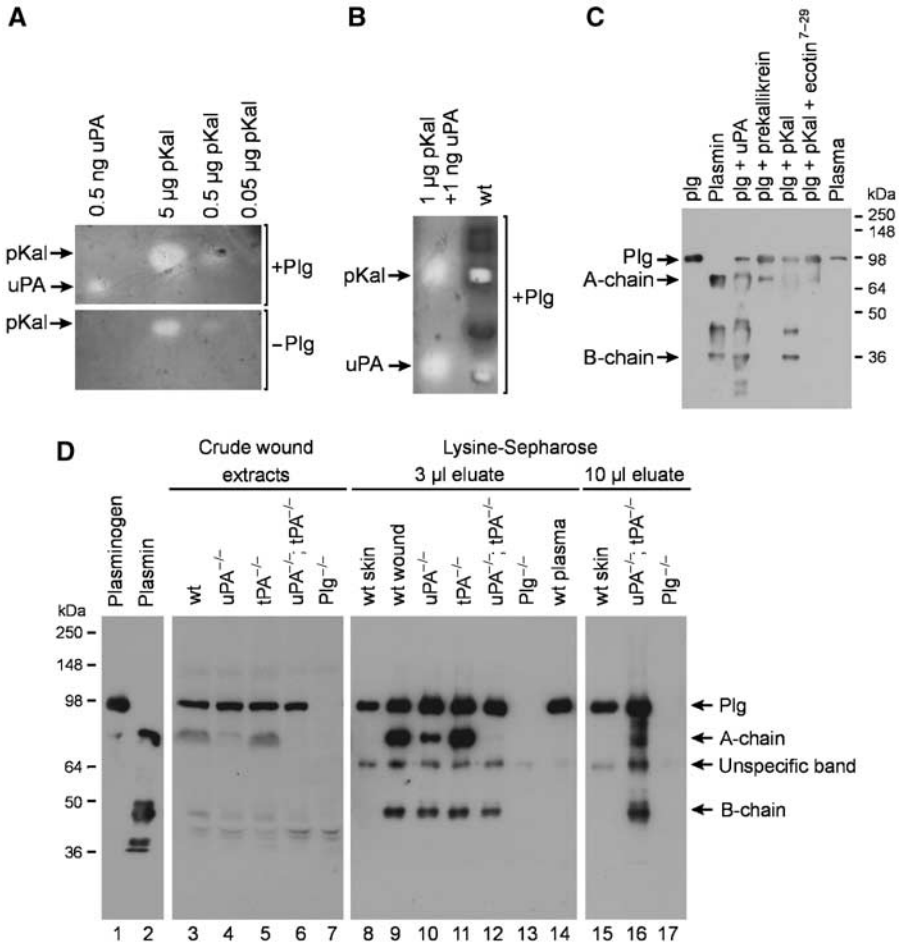

Figure 5 Detection of fibrinolytic activities and Plg/plasmin in wound extracts. (**A**) Fibrin/Plg overlay zymography of purified human pKal and murine uPA and without Plg. Note that the size of the lysis zones generated by pKal decreases in the absence of Plg. (**B**) Prolonged development of a zymogram with 1 µg of human pKal and 0.1 ng murine uPA in one lane and wild-type 7-day-old incisional wound extract in the second lane reveals activity comigrating with uPA and pKal in the wild-type wound extract. (**C**) Western blot analysis of 1 µg mouse Plg, 1 µg mouse plasmin and 1 µl of mouse plasma as controls. Generation of plasmin was detected in 1 µg Plg activated for 2 h at 37°C either by 10 ng uPA, 0.1 µg prekallikrein, 0.1 µg pKal or 0.1 µg pKal in the presence of Ecotin$^{7-29}$. (**D**) Western blot analysis for Plg and plasmin. 1 µg mouse Plg (lane 1), 1 µg mouse plasmin (lane 2). Lanes 3–7: 16 µl of crude wound extract prepared from 7-day-old incisions from either wild-type mice (lane 3), *uPA*-deficient mice (lane 4), *tPA*-deficient mice (lane 5), *uPA;tPA* double-deficient mice (lane 6) and *Plg*-deficient mice (lane 7). Lanes 8–14: 3 µl of eluate pool from Lysine-Sepharose columns, wild-type mice skin (lane 8), wild-type mice wounds (lane 9), *uPA*-deficient mice (lane 10), *tPA*-deficient mice (lane 11), *uPA;tPA* double-deficient mice (lane 12), *Plg*-deficient mice (lane 13) and plasma from wild-type mice (lane 14). Lanes 15–17: 10 µl of eluate pool from Lysine-Sepharose columns, wild-type mice skin (lane 15), *uPA;tPA* double-deficient mice (lane 16) and *Plg*-deficient mice (lane 17).

accumulate abundant fibrin, which disturbs the re-epithelialization process in particular (Rømer *et al*, 1996; Lund *et al*, 1999) and skin wound healing is rescued in double-deficient mice (Bugge *et al*, 1996b). This implies that the impaired healing in *Plg*-deficient mice is caused primarily by impaired fibrinolysis as a consequence of insufficient plasmin generation. Collectively, these data reveal that sufficient levels of plasmin must be generated despite the *uPA;tPA* deficiency in these mice, thus implying the presence of an additional Plg activator in these wounds. Accordingly, we have indeed demonstrated the presence of plasmin in wounds from *uPA;tPA* double-deficient mice thus providing the first biochemical evidence for an additional plasminogen activator *in vivo*.

A functional overlap exists between Plg and MMPs during skin wound healing (Lund *et al*, 1999) and trophoblast implantation (Solberg *et al*, 2003). We therefore compared the effect of MMP inhibitor treatment on the healing of skin wounds in *Plg*-deficient mice and *uPA;tPA* double-deficient mice. In agreement with our previous study we find that treatment with the MMP inhibitor galardin arrests healing in *Plg*-deficient mice. In *uPA;tPA* double-deficient mice, galardin treatment delays the healing process, whereas all the wounds do eventually heal with a mean healing time of 46 days. Two separate conclusions can be drawn from these findings.

Firstly, the further delay of healing in the *uPA;tPA* double-deficient mice by blocking MMP activity shows that MMPs contribute to fibrinolysis either directly or indirectly via Plg activation. In further consolidation of this interpretation, we found that galardin treatment of *Plg;fibrinogen* double-deficient wounds cause only a moderate delay in healing time (unpublished results) as opposed to the complete block of healing observed in the galardin-treated *Plg*-deficient mice (Lund *et al*, 1999). It remains however to be elucidated which MMP is responsible for fibrin degradation *in vivo*. MMP3, MMP8, MMP9, MMP12, MMP13 and MT1-MMP all have

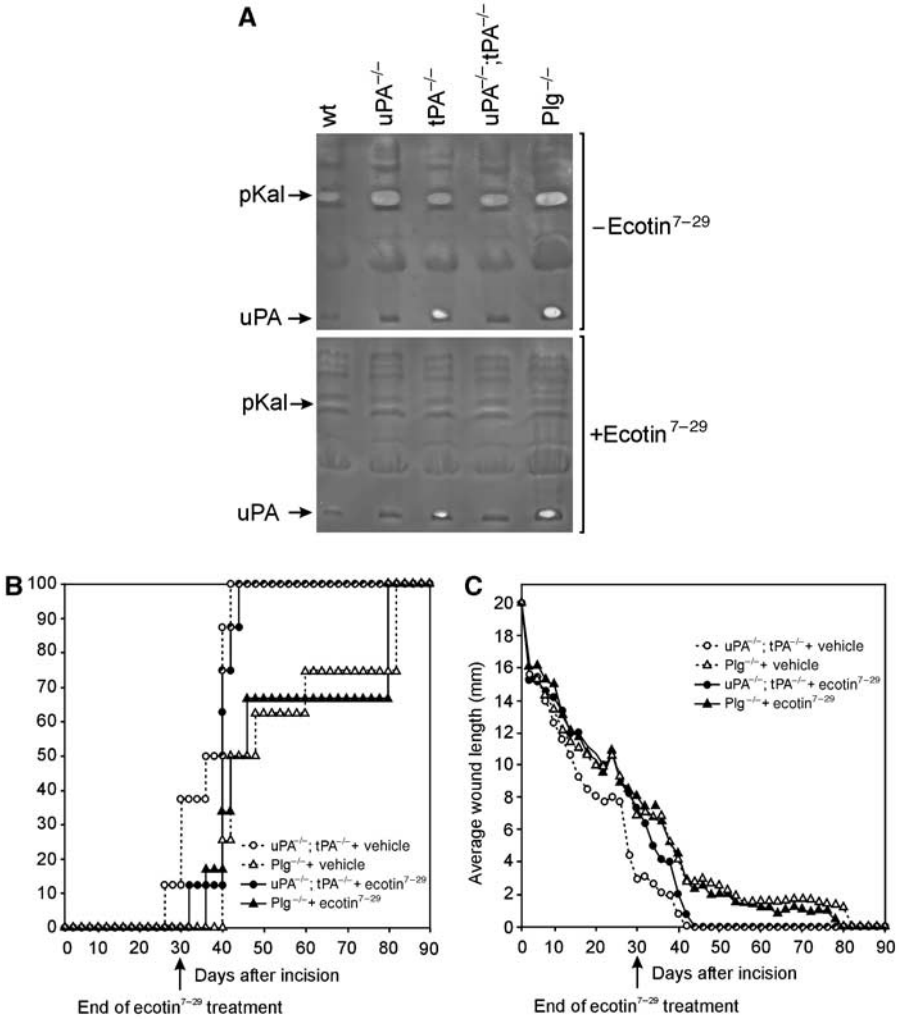

Figure 6 The pKal inhibitor ecotin$^{7-29}$ inhibits plasmin-mediated fibrinolysis and the healing of *uPA;tPA* double-deficient wounds. (**A**) Extracts of 7-day wounds from wild-type, *uPA*-deficient, *tPA*-deficient, *uPA;tPA* double-deficient and *Plg*-deficient mice (pooled from two mice per genotype) were subjected to fibrin/Plg overlay zymography with or without the serine protease inhibitor ecotin$^{7-29}$. Note the complete inhibition of activity corresponding to pKal by ecotin$^{7-29}$, whereas the uPA activity is not inhibited. (**B**) *uPA;tPA* double-deficient and *Plg*-deficient mice were treated with the serine protease inhibitor ecotin$^{7-29}$ or vehicle for 30 days ($n = 6$–8). The percentage fraction of mice with complete gross healing is plotted versus the time after the incision. (**C**) The wound length plotted versus the time after the incision. Until the end of treatment at day 30 after the incision, the wound length kinetics in ecotin$^{7-29}$-treated *uPA;tPA* double-deficient mice were indistinguishable from vehicle- or ecotin$^{7-29}$-treated *Plg*-deficient mice.

fibrinolytic activities *in vitro* (Bini *et al*, 1996; Hiller *et al*, 2000; Lelongt *et al*, 2001; Hotary *et al*, 2002), but no severe phenotypes after incisional wound healing are reported in the single-deficient mice tested so far; *MMP3*, *MMP9* or *MMP13* (Bullard *et al*, 1999; Mohan *et al*, 2002; Hartenstein *et al*, 2006). This suggests that the fibrinolytic potential of these MMPs should be tested *in vivo* in mice double-deficient in *Plg* and each of these *MMPs*. Secondly, the pharmacological blocking of MMP-mediated fibrinolysis in *uPA;tPA* double-deficient mice is not sufficient to arrest the healing process, demonstrating that these mice, in contrast to the galardin-treated *Plg*-deficient mice, still possess some residual fibrinolytic potential. This provides evidence of the existence of at least one Plg activator in addition to uPA and tPA, which is not galardin-sensitive.

A previous report suggested that pKal is a Plg activator during adipocyte differentiation (Selvarajan *et al*, 2001). We have now confirmed *in vitro* that purified human pKal has Plg-activating activities and, in addition, has some Plg-independent fibrinolytic activity. We observed an activity corresponding to pKal in murine wound extracts, and collectively these data suggest that pKal may be involved in fibrin degradation during skin wound healing both directly and through activation of Plg. To test this hypothesis, we treated *uPA;tPA* double-deficient mice with a mutated pKal-selective form of the serine protease inhibitor ecotin (Stoop and Craik, 2003), which decreased the healing rate, as measured by the wound length, to a level that was indistinguishable from vehicle-treated *Plg*-deficient wounds. In contrast, treatment of *Plg*-deficient mice with ecotin$^{7-29}$ did not lower their healing capacity further. This result suggests that ecotin$^{7-29}$ does not inhibit any rate-limiting proteases unrelated to plasminogen activators and the data do not support a biological role of plasminogen independent of its conversion to plasmin in wound healing. Ecotin$^{7-29}$ completely blocks the activity of pKal, but not the activity of uPA or tPA in wound extracts as

determined by fibrin/Plg zymography (Figure 6A and unpublished results). Thus, pKal most likely contributes to skin wound healing through Plg-dependent fibrinolysis.

Prekallikrein, the precursor of pKal is found at high concentrations (40–50 μg/ml) compared to 2–5 ng/ml of pro-uPA in plasma, which may enable its role as a Plg activator *in vivo* despite its relatively poor catalytic efficiency as Plg activator *in vitro* (Colman, 1969). The finding that pKal may play a significant role in Plg activation during skin wound healing suggests that pKal also has important and as yet unidentified physiological functions as a Plg activator in other tissue remodeling processes. Although our results obtained by ecotin$^{7-29}$ treatment of *uPA;tPA* double-deficient mice strongly suggest that pKal is an important Plg activator during skin wound healing, we cannot rule out a role for additional Plg activators. Ecotin$^{7-29}$ may inhibit other unidentified serine proteases with Plg activator activity, although our overlay zymography strongly support the conclusion that pKal is the additional Plg activator in wound healing. A definitive test of the role of pKal in skin wound healing and other tissue remodelling processes will be possible when *pKal*-deficient mice are available for generation of mice with triple-deficiency for *uPA*, *tPA* and *pKal*. Skin repair in these mice and *Plg*-deficient mice can then be compared directly.

We find it unlikely that the differences between the healing observed in *uPA;tPA* double-deficient and *Plg*-deficient mice can be explained by bacterial infection of the wounds and thereby contamination with prokaryotic Plg activators such as streptokinase or staphylokinase (Sun *et al*, 2004), as no signs of infection have been observed either macroscopically or microscopically in any mice in the experiments. Furthermore, we have observed a similar difference between the phenotypes of *uPA;tPA* double-deficient and *Plg*-deficient mice in a nonlesional tissue remodelling process, that is, post-lactational mammary gland involution, which is less impaired in *uPA;tPA* double-deficient than in *Plg*-deficient mice (unpublished results).

The demonstration of a third Plg activator, which at least partially accounts for the difference in wound healing time between *uPA;tPA*-deficient and *Plg*-deficient mice, has important implications for the understanding of Plg activation during normal and pathological tissue remodelling. It is well established that *Plg* deficiency results in serious physiological consequences in both humans and mice although with different degrees of penetrance (Bugge *et al*, 1995; Schuster *et al*, 1997; Drew *et al*, 1998). In several fundamental physiological processes involving normal as well as pathological tissue remodelling, Plg activation has been shown to play a pivotal role, and it will be interesting to define the individual and combined significance of uPA, tPA and pKal.

Numerous studies have revealed that uPA and uPAR are expressed either by invading cancer cells or by stromal cells in their vicinity (Johnsen *et al*, 1998). The ability of skin squamous carcinoma cells to mimic the 'invasive' phenotype of re-epithelializing keratinocytes with regard to their expression of components of the Plg activation system and MMPs is likely to reflect a general mechanism employed by invading cancer cells. Our demonstration of the involvement of at least three Plg activators and one or more MMPs in wound healing may thus have important implications for a therapeutic approach aiming at blocking invasion and metastasis in cancer. In order to obtain a complete inhibition of cancer invasion, it will thus be necessary to use combinations of protease inhibitors.

Materials and methods

Animals and animal treatment

uPA and *tPA* gene-targeted mice of a mixed 129/Black Swiss background (Carmeliet *et al*, 1994) backcrossed to C57Bl/6J (Panum Institute, Copenhagen) mice for 16 generations were crossed, followed by interbreeding of the double heterozygous offspring. *Plg* gene-targeted 129/Black Swiss mice (Bugge *et al*, 1995) were backcrossed into C57BL/6J (Panum Institute, Copenhagen) for 21 generations. The plasminogen genotype was determined as described (Lund *et al*, 1999). The uPA genotype was determined by multiplex PCR using the following three primers. muPA-7p (CTC CCG TGG CTG GGT AGT GG) hybridizing to position 7719–7738 in the mouse uPA gene (GenBank: M17922), and muPA-4m (AGA GGA CGG TCA GCA TGG GAA C) hybridizing to position 8029–8008 generate a 311 bp product specific for the endogenous allele. muPA-4m and mPGK-2m (GCC TTG GGA AAA GCG CCT C) hybridizing to position 1092–1074 in the mouse phosphoglycerate kinase-1 promoter (GenBank: X15339) generate a ~186 bp product specific for the targeted allele. The tPA genotype was determined by multiplex PCR using the following three primers; mtPA-3m (GTC TGT TCT TCC TCT CCG GGG AC) hybridizing to position 1673–1695 in the mouse tPA gene (GenBank: AC121835), and mtPA-4p (CTC ACA CCC TTG GCA GGC TG) hybridizing to position 1984–1965 generate a 312 bp product specific for the endogenous allele. mtPA-3m and mPGK-2m generate a ~243 bp product specific for the targeted allele.

All mice used for experiments were males between 6 and 8 weeks old at the start of the experiment. Wound healing experiments of *uPA;tPA*-deficient mice and *Plg*-deficient mice was carried out at the same time and in the same room. Investigators unaware of the mouse genotype performed all experimental evaluations, tissue isolations and microscopic analyses. The MMP inhibitor galardin was synthesized as described (Grobelny *et al*, 1992). Galardin inhibits the enzymatic activity of a number of MMPs, including MMP2, -3, -9 and -14 (as described in Lund *et al*, 1999). Galardin was formulated as a 20 mg/ml slurry in 4% carboxymethylcellulose (CMC) in PBS and was administered daily i.p. at 100 mg/kg body weight. Mock treatment included 4% CMC in PBS. The same batch of galardin was used for the treatment of *uPA*-, *tPA*- and *Plg*-deficient mice. A mutated form of ecotin rendered highly specific for plasma kallikrein (ecotin$^{7-29}$) was isolated from a phage display library as described (Stoop and Craik, 2003). Samples used for animal injections were diluted in PBS, and administered i.p. at a dose of 10 mg/kg/day (two daily injections for 30 days).

Tissue preparation

Incisional skin wounds were generated in 6- to 8-week-old mice and tissues were removed for histological analysis as described previously (Lund *et al*, 1999). A total of 133 mice were wounded and tissue isolated at day 10 post-wounding from 18 wild-type mice, 10 *tPA*-deficient, 17 *uPA*-deficient, 13 *uPA;tPA* double-deficient mice and nine *Plg*-deficient mice. At the time of healing, we isolated tissue from 10 wild-type, eight *tPA*-deficient, 11 *uPA*-deficient, six *uPA;tPA* double-deficient mice and five *Plg*-deficient mice. At 1 month post-healing, we isolated tissue from seven wild-type, five *tPA*-deficient, four *uPA*-deficient, five *uPA;tPA* double-deficient mice and five *Plg*-deficient mice. Animal care at The Department of Experimental Medicine, University of Copenhagen and Rigshospitalet, Copenhagen, Denmark was in accordance with the institutional and national guidelines.

Computer-assisted morphometry

Keratinocyte migration was measured microscopically on tissue sections stained immunohistochemically with anti-keratin IgG (Lund *et al*, 1999). The length of the epidermal tongue was measured as the distance between the tip of the leading-edge keratinocytes and the edge of the wound, defined as the point in the zone of proliferation where a shift from two to three layers of keratinocytes could be identified. The relative migration was determined as the sum of the lengths of both epidermal tongues divided by the width of the wound, defined as the distance between

the wound edges. Indication of this point in the proliferation zone and the tip of the epidermal wedge by image analysis (Olympus AX70 system) were performed by an observer unaware of the genotype of the mice. The mean fraction of migration, the standard error (s.e.) was determined for each group of animals.

Statistical analysis

The SAS® software package (version 8.2; SAS Institute, Cary, NC) was used to manage data and for statistical analysis. The distribution of time to wound closure was found to be normal. Prespecified tests of hypothesis comparing experimental groups to the control group of mice were carried out using two sample *t*-tests. The assumption of variance homogeneity was tested by the folded *F*-test and the two sample *t*-test assuming unequal variances was used if the hypothesis of variance homogeneity was rejected. Incomplete data were discarded. Power calculations demonstrated that at least eight mice should be included in each group in order to detect a difference in time to wound closure of 5 days with 80% power. Plots of time to complete re-epithelialization were carried out using Kaplan–Meier estimates. The level of significance was set at 5%.

Zymography

Wound tissue containing both the wound rim and granulation tissue was lysed in 5 μl of 0.1 M Tris/HCl, 1% Triton X-100, pH 7.4 per mg wet weight of tissue. The extracts were used for fibrin/Plg overlay zymograms with and without plasminogen as described (Lund *et al*, 1996) and with and without ecotin$^{7-29}$ (10 μg/ml) followed by incubation at 37°C for 16–28 h or in prolonged development for 40 h. Recombinant mouse pro-uPA (produced by Schneider cells, as described previously (Ploug *et al*, 2001)) and human plasma kallikrein (Kordia Life Sciences, The Netherlands) were used as controls.

Western blot analysis

Frozen tissue powder containing both the wound rim and granulation tissue (pool of three mice per genotype) was resuspended in 5 μl of 0.1 M Tris/HCl, pH 7.4, 10 μg/ml of aprotinin per mg wet weight of tissue, treated for 2 × 8 min on an Ultrasound bath and the resulting supernatants were collected after centrifugation at 12 000 *g* for 30 min at 4°C. Samples were reduced and alkylated before SDS–PAGE and transferred to PVDF membranes by electroblotting. Additional binding was blocked by incubation for 1 h at room temperature with 5% nonfat-dried milk in phosphate-buffered saline containing 0.05% Tween-20 (PBS-T). Incubation with the primary antibody was overnight at 4°C with 0.5 μg/ml polyclonal rabbit anti-human plasminogen antibody (DAKO, A0081). After washing in PBS-T (5 × 5 min), membranes were incubated for $1\frac{1}{2}$ h at room temperature with HRP-linked secondary antibody (DAKO, P0217) diluted 1:5000 in blocking buffer. After washing in PBS-T and PBS, HRP activity was detected using enhanced chemiluminescence's reagents (Amersham Biosciences, Hillerød, Denmark). Purified mouse Plg and plasmin (Innovative Research, Inc., Hilltop, MI) were used as controls. A negative control without primary antibody included was carried out in parallel.

One-step affinity purification of Plg/plasmin was accomplished by application of 1500 μl wound extract onto 100 μl lysine Sepharose 4B gel (Amersham Bioscience) settled in a disposable column. After sample application, the columns were washed extensively with more than 10 column volumes of 0.1 M phosphate buffer, pH 7.4. The bound Plg/plasmin were eluted by 250 μl 0.1 M 6-aminohexanoic acid in 0.1 M phosphate buffer, pH 7.4 and fractions of approximately 25 μl were collected. All manipulations were performed at 4°C with buffers containing 10 μg/ml aprotinin.

Double immunofluorescence

Tissue sections were deparaffinized in xylene and hydrated through graded ethanol/water dilutions. Antigen retrieval was carried out by incubation with proteinase K for 15 min at 37°C. Sections were washed in running tap water for 5 min and Tris-buffered saline (TBS: 50 mM Tris, 150 mM NaCl, pH 7.6) for 5 min. Sections were incubated overnight simultaneously with both rabbit anti-mouse fibrin(ogen) antibody (1:2000; Bugge *et al*, 1995) and rat anti-mouse Troma1 antibody (detects cytokeratin 8; 1:100 Kemler *et al*, 1981), in TBS containing 0.25% BSA at 4°C. Rabbit anti-fibrin(ogen) antibody was detected with Alexa Fluor 488-linked donkey anti-rabbit antibody (1:200, Molecular Probes, CA, A21206) and rat anti-Troma-1 antibody was detected with Alexa Fluor 594-linked goat anti-rat antibody (1:200, Molecular Probes, A11007) diluted together in TBS containing 0.25% BSA and incubated for 45 min at room temperature. Antibody incubations were followed by washes in TBS. Controls without anti-fibrin(ogen) primary antibody were negative for unspecific staining.

Acknowledgements

We thank Dr Thomas Bugge for the *Plg*-deficient mice and Dr Peter Carmeliet for the *uPA*- and *tPA*-deficient mice. We are grateful to Mette M Andersen, Lotte Frederiksen, Kirsten L Jakobsen, Charlotte Lønborg and John Post for excellent technical assistance. This work was supported financially by the European Commission: Grant number QLG1-CT-2000-01131 and LSHC-CT-2003-503297, European Union research training grant for mammary gland biology RTN-2002-00246, Aage Bangs Foundation, the Danish Biotechnology Program, Centre for Medical Biotechnology, the Danish Cancer Society, the Danish Medical Research Council, the Danish Cancer Research Foundation, Agnes and Poul Friis Foundation and a grant from the National Cancer Institute (USA) P01 CA072006.

References

Beare AHM, O'Kane S, Krane SM, Ferguson MWJ (2003) Severely impaired wound healing in the collagenase-resistant mouse. *J Invest Dermatol* **120:** 153–163

Bini A, Itoh Y, Kudryk BJ, Nagase H (1996) Degradation of cross-linked fibrin by matrix metalloproteinase 3 (stromelysin 1): hydrolysis of the gamma Gly 404-Ala 405 peptide bond. *Biochemistry* **35:** 13056–13063

Bugge TH, Flick MJ, Danton MJ, Daugherty CC, Rømer J, Danø K, Carmeliet P, Collen D, Degen JL (1996a) Urokinase-type plasminogen activator is effective in fibrin clearance in the absence of its receptor or tissue-type plasminogen activator. *Proc Natl Acad Sci USA* **93:** 5899–5904

Bugge TH, Flick MJ, Daugherty CC, Degen JL (1995) Plasminogen deficiency causes severe thrombosis but is compatible with development and reproduction. *Genes Dev* **9:** 794–807

Bugge TH, Kombrinck KW, Flick MJ, Daugherty CC, Danton MJ, Degen JL (1996b) Loss of fibrinogen rescues mice from the pleiotropic effects of plasminogen deficiency. *Cell* **87:** 709–719

Bugge TH, Lund LR, Kombrinck KK, Nielsen BS, Holmback K, Drew AF, Flick MJ, Witte DP, Danø K, Degen JL (1998) Reduced metastasis of Polyoma virus middle T antigen-induced mammary cancer in plasminogen-deficient mice. *Oncogene* **16:** 3097–3104

Bullard KM, Lund L, Mudgett JS, Mellin TN, Murphy B, Ronan J, Banda MJ (1999) Impaired wound contraction in stromelysin-1 deficient mice. *Ann Surg* **230:** 260–265

Carmeliet P, Schoonjans L, Kieckens L, Ream B, Degen J, Bronson R, De Vos R, van den Oord JJ, Collen D, Mulligan RC (1994) Physiological consequences of loss of plasminogen activator gene function in mice. *Nature* **368:** 419–424

Collen D, Lijnen HR (2005) Thrombolytic agents. *Thromb Haemost* **93:** 627–630

Colman RW (1969) Activation of plasminogen by human plasma kallikrein. *Biochem Biophys Res Commun* **35:** 273–279

Danø K, Andreasen PA, Grondahl-Hansen J, Kristensen P, Nielsen LS, Skriver L (1985) Plasminogen activators, tissue degradation, and cancer. *Adv Cancer Res* **44:** 139–266

Danø K, Behrendt N, Hoyer-Hansen G, Johnsen M, Lund LR, Ploug M, Romer J (2005) Plasminogen activation and cancer. *Thromb Haemost* **93:** 676–681

Danø K, Romer J, Nielsen BS, Bjorn S, Pyke C, Rygaard J, Lund LR (1999) Cancer invasion and tissue remodeling—cooperation of protease systems and cell types. *Apmis* **107:** 120–127

Drew AF, Kaufman AH, Kombrinck KW, Danton MJ, Daugherty CC, Degen JL, Bugge TH (1998) Ligneous conjunctivitis in plasminogen-deficient mice. *Blood* **91:** 1616–1624

Egeblad M, Werb Z (2002) New functions for the matrix metalloproteinases in cancer progression. *Nat Rev Cancer* **2:** 161–174

Ellis V, Behrendt N, Dano K (1991) Plasminogen activation by receptor-bound urokinase. A kinetic study with both cell-associated and isolated receptor. *J Biol Chem* **266:** 12752–12758

Grobelny D, Ponez L, Galardy RE (1992) Inhibition of human skin fibroblast collagenase, thermolysin and *Pseudomonas aeruginosa* elastase by peptide hydroxamic acids. *Biochemistry* **31:** 7152–7154

Hartenstein B, Dittrich BT, Stickens D, Heyer B, Vu TH, Teurich S, Schorpp-Kistner M, Werb Z, Angel P (2006) Epidermal development and wound healing in matrix metalloproteinase 13-deficient mice. *J Invest Dermatol* **126:** 486–496

Hiller O, Lichte A, Oberpichler A, Kocourek A, Tschesche H (2000) Matrix metalloproteinases collagenase-2, macrophage elastase, collagenase-3, and membrane type 1-matrix metalloproteinase impair clotting by degradation of fibrinogen and factor XII. *J Biol Chem* **275:** 33008–33013

Hotary KB, Yana I, Sabeh F, Li XY, Holmbeck K, Birkedal-Hansen H, Allen ED, Hiraoka N, Weiss SJ (2002) Matrix metalloproteinases (MMPs) regulate fibrin-invasive activity via MT1–MMP-dependent and -independent processes. *J Exp Med* **195:** 295–308

Johnsen M, Lund LR, Rømer J, Almholt K, Danø K (1998) Cancer invasion and tissue remodeling: common themes in proteolytic matrix degradation. *Curr Opin Cell Biol* **10:** 667–671

Kemler R, Brulet P, Schnebelen M T, Gaillard J, Jacob F (1981) Reactivity of monoclonal antibodies against intermediate filament proteins during embryonic development. *J Embryol Exp Morphol* **64:** 45–60

Lelongt B, Bengatta S, Delauche M, Lund LR, Werb Z, Ronco PM (2001) Matrix metalloproteinase 9 protects mice from anti-glomerular basement membrane nephritis through its fibrinolytic activity. *J Exp Med* **193:** 793–802

Llinas P, Le Du MH, Gardsvoll H, Dano K, Ploug M, Gilquin B, Stura EA, Menez A (2005) Crystal structure of the human urokinase plasminogen activator receptor bound to an antagonist peptide. *EMBO J* **24:** 1655–1663

Lund LR, Bjørn SF, Sternlicht MD, Nielsen BS, Solberg H, Usher PA, Osterby R, Christensen IJ, Stephens RW, Bugge TH, Dano K, Werb Z (2000) Lactational competence and involution of the mouse mammary gland require plasminogen. *Development* **127:** 4481–4492

Lund LR, Rømer J, Bugge TH, Nielsen BS, Frandsen TL, Degen JL, Stephens RW, Danø K (1999) Functional overlap between two classes of matrix-degrading proteases in wound healing. *EMBO J* **18:** 4645–4656

Lund LR, Rømer J, Thomasset N, Solberg H, Pyke C, Bissell MJ, Danø K, Werb Z (1996) Two distinct phases of apoptosis in mammary gland involution: proteinase-independent and -dependent pathways. *Development* **122:** 181–193

Madlener M, Parks WC, Werner S (1998) Matrix metalloproteinases (MMPs) and their physiological inhibitors (TIMPs) are differentially expressed during excisional skin wound repair. *Exp Cell Res* **242:** 201–210

Mohan R, Chintala SK, Jung JC, Villar WV, McCAbe F, Russo LA, Lee Y, McCarthy BE, Wollenberg KR, Jester JV, Wang M, Welgus HG, Shipley JM, Senior RM, Fini ME (2002) Matrix metalloproteinase gelatinase B (MMP-9) coordinates and effects epithelial regeneration. *J Biol Chem* **277:** 2065–2072

Ploug M (2003) Structure–function relationships in the interaction between the urokinase-type plasminogen activator and its receptor. *Curr Pharm Des* **9:** 1499–1528

Ploug M, Ostergaard S, Gardsvoll H, Kovalski K, Holst-Hansen C, Holm A, Ossowski L, Danø K (2001) Peptide-derived antagonists of the urokinase receptor. Affinity maturation by combinatorial chemistry, identification of functional epitopes, and inhibitory effect on cancer cell intravasation. *Biochemistry* **40:** 12157–12168

Rømer J (2003) Skin cancer and wound healing: tissue-specific similarities in extracellular proteolysis. *APMIS* **111** (Suppl 107)**:** 1–36

Rømer J, Bugge TH, Pyke C, Lund LR, Flick MJ, Degen JL, Dano K (1996) Impaired wound healing in mice with a disrupted plasminogen gene. *Nat Med* **2:** 287–292

Schuster V, Mingers AM, Seidenspinner S, Nussgens Z, Pukrop T, Kreth HW (1997) Homozygous mutations in the plasminogen gene of two unrelated girls with ligneous conjunctivitis. *Blood* **90:** 958–966

Selvarajan S, Lund LR, Takeuchi T, Craik CS, Werb Z (2001) A plasma kallikrein-dependent plasminogen cascade required for adipocyte differentiation. *Nat Cell Biol* **3:** 267–275

Solberg H, Rinkenberger J, Danø K, Werb Z, Lund LR (2003) A functional overlap of plasminogen and MMPs regulates vascularization during placental development. *Development* **130:** 4439–4450

Stoop AA, Craik CS (2003) Engineering of a macromolecular scaffold to develop specific protease inhibitors. *Nat Biotechnol* **21:** 1063–1068

Sun H, Ringdahl U, Homeister JW, Fay WP, Engleberg NC, Yang AY, Rozek LS, Wang X, Sjobring U, Ginsburg D (2004) Plasminogen is a critical host pathogenicity factor for group A streptococcal infection. *Science* **305:** 1283–1286

This page contains unpublished data which should be protected.

APPENDIX 3: Mast cells are required for postnatal mammary gland development.

PLEASE NOTE: This appendix represents unpublished data that are being prepared for publication and therefore should be protected.

INTRODUCTION

Long known as potent effectors of the immune response, mast cells ordinarily house and release factors capable of influencing their extracellular environment, including many serine proteases (Metcalfe et al., 1997). Mast cells are capable of producing thousands of different chemicals, and may secrete them selectively or in large amounts through the exocytotic process of degranulation (Galli and Tsai, 2008). Mast cells are derived from hematopoietic progenitors in bone marrow and circulate through the blood to tissues where they mature into a mast cell with a specific granule phenotype; the content of their granules and/or phenotype differs depending on factors in their destination's environment (Galli, 2000; Galli et al., 2005; Kitamura, 1989; Metcalfe et al., 1997). Mast cells are found in any vascularized tissues, though they tend to reside around blood vessels, nerves, epithelial cells, and smooth muscle cells, where they can exert a variety of influences on their environment (Galli and Tsai, 2008; Kitamura, 1989; Metcalfe et al., 1997).

Best known for their role in releasing histamine, causing vasodilation and blood vessel leakiness, mast cells also produce a host of proteases, proinflammatory cytokines, proangiogenic factors (such as vascular endothelial growth factor) and chemokines known to contribute to the metastatic potential of tumors (Coussens and Werb, 2002; Metcalfe et al., 1997). Thus, the presence and activity of mast cells may have numerous consequences on the normal and pathological development and maintenance of the tissues that house them.

The growth and invasion of the developing mammary ductal epithelium into the mammary fat pad has been extensively described (Cunha et al., 2000; Richert et al., 2000; Wiseman and Werb, 2002). At birth, the mammary gland consists of a fatty, highly vascularized pad of tissue with a rudimentary ductal epithelial tree descending into it from the overlying nipple. These structures parallel the growth of the mouse until the start of puberty (around 3 weeks of age), when a host of ovarian hormones stimulates the development of terminal end buds (TEBs), multilayered bulbous structures at the tips of growing and branching ducts (Richert et al., 2000; Wiseman and Werb, 2002). Proliferation of TEB cells leads to the bifurcation and elongation of duct structures towards the outer edges of the fat pad by 10-12 weeks of age, when the TEBs then regress and become terminal duct ends (Richert et al., 2000; Topper and Freeman, 1980). The end of mammary gland development is realized by the cycle of pregnancy, lactation, and involution, where the mammary gland returns to its prepregnant state.

Though hormones are responsible for the initiation and maintenance of TEB formation and duct elongation, mammary epithelial development is regulated by the mammary stroma, the various components of which include mesenchymal-derived cells such as fibroblasts and adipocytes, growth and survival factors, extracellular matrix

proteins and their degrading proteases, blood vessels, and inflammatory cells. Previous studies have demonstrated that components of the fatty mammary stroma are essential for proper development of the epithelium of the mammary gland (Cunha and Hom, 1996; Cunha et al., 2000; Wiseman and Werb, 2002), and that resident macrophages and eosinophils are included in this phenomenon (Gouon-Evans et al., 2002; Gouon-Evans et al., 2000; Ingman et al., 2006). Like other innate immune cells, here we show that mast cells are present in the stroma of the murine mammary gland throughout its postnatal development.

Given that mast cells are present in the mammary stroma and have multiple means of influence over the tissues in which they reside, this study addresses the hypothesis that mast cells exert an effect on normal mammary development. To this end, we use both genetic and pharmacological models to disrupt mast cell function in the mammary gland to show that mast cells must be present, able to degranulate, and produce active proteases for normal development to occur.

METHODS

Experimental animal models

Care of animals and animal experiments were performed in accordance with protocols approved by the UCSF Institutional Animal Use and Care Committee (IACUC). C57BL/6J-*Kit*$^{W\text{-}sh/W\text{-}sh}$ mice (Duttlinger et al., 1993) were obtained from the Jackson Laboratory and C57BL/6 mice were obtained from Charles River Laboratories (Wilmington, MA). At each time point, we examined offspring from *Kit*$^{W\text{-}sh/W\text{-}sh}$, *Kit*$^{+/W\text{-}sh}$, and *Kit*$^{+/+}$ siblings. DPPI -/- mice (Pham and Ley, 1999) were provided by L. Coussens (UCSF). Wild-type FVB mice were obtained from Charles River Laboratories.

To stabilize mast cells from degranulating, CD1 (Charles River Laboratories) female mice were intraperitoneally injected as previously described (Jamieson et al., 2005) daily with 50 mg/kg body weight sodium cromoglycate (Sigma, St. Louis, MO, USA) dissolved in saline from 3 to 5 weeks of age.

Estrus stage was determined for every mouse by vaginal smear (Rugh, 1968) and only mice in similar estrus phases were compared at each time point.

Whole mount mammary gland preparation and analysis

For whole mount analysis, abdominal mammary glands were removed at 3, 5, 8, and 12 weeks of age, stretched on a glass slide, and fixed overnight in Bouin's fixative (75% ethanol, 25% glacial acetic acid). They were then rehydrated and stained overnight at 4 degrees in Alum Carmine stain [2 g/l carmine dye (Sigma, St. Louis, MO, USA) and 5 g/l aluminum potassium sulfate in distilled water]. The glands were then dehydrated and immersed in Histoclear (Fisher Scientific) for lipid removal and storage. Images were acquired using Nikon ACT-1 software on a Leica dissecting microscope and analyzed using Adobe Photoshop and NIH Image (ImageJ) software. Duct lengths (in mm) were measured from the nipple base to the tips of the 3 longest ducts and averaged. Numbers of terminal end buds in the invasion front were counted past half-way through the lymph node. Total numbers of branches in the invasion front were counted past half-way through the lymph node. Two-tailed Student's *t*-tests and one-way ANOVAs were used to determine statistical significance between groups (n = 5 to 8 mice/group). Significance was considered when probabilities were ≤0.05.

Histology, enzyme histochemistry, and immunofluorescence

Contralateral abdominal mammary glands were removed at 3, 5, 8, and 12 weeks of age and immediately embedded in OCT (Sakura) medium on dry ice. 5 μm frozen sections were cut for use in histology, enzyme histochemistry, and immunohistochemistry. To visualize mast cells, frozen sections were air-dried for ≥30 minutes, post-fixed in ice-cold acetone for 10 minutes, rinsed in PBS, and then stained in either Toluidine blue [a metachromatic dye for mast cells, made up as 0.1% Toluidine blue O (Sigma) in 1% sodium chloride, pH 2.3] or by using an enzymatic reaction with naphthol AS-D chloroacetate esterase (Sigma) to detect chymase activity (Moloney et al., 1960) then counterstained with Gill's hematoxylin or DAPI. To examine collagen deposition and overall morphology of the glands, Masson's Trichrome (Sigma) was used on frozen sections dried and fixed as described above. Lipid content was determined by Oil Red O (Sigma) staining. Frozen sections were fixed for 1-2 days in 4% parafomaldehyde at 4º, rinsed in distilled water, air-dried for ≥90 minutes, then stained in working Oil Red [60% saturated Oil red O (Sigma, 0.5% in isopropanol); 40% dextrin (1% typeIII corn dextrin (Sigma) in distilled water)] for 20 minutes and counterstained with Gill's hematoxylin (Sigma) and stored in PBS.

Frozen sections were also used to identify macrophages in mammary glands using an rat monoclonal antibody to mouse F4/80 (Caltag Laboratories, Invitrogen, Carlsbad, CA), a macrophage-specific cell surface glycoprotein (Malorny et al., 1986). Slides were blocked in 4% goat serum and 2% BSA (Sigma) in PBS, then incubated overnight with 1:200 anti-mouse F4/80 at 4º. F4/80$^+$ cells were detected using an Alexa 488-conjugated goat anti-rat IgG (Molecular Probes, Invitrogen) with a DAPI (Vector Laboratories, Burlingame, CA) counterstain. Control tissues were treated with an isotype in lieu of primary antibody or by omission of the primary antibody. Frozen sections were also used to identify mitotic cells using a 1:500 dilution of polyclonal antibody against human phospho-Histone H3 (Ser10; Upstate, Millipore, Billerica, MA). Slides were blocked in 4% goat serum and 2% BSA (Sigma) in PBS, then incubated overnight with anti-human phospho-Histone H3 antibody at 4º. Phospho-Histone H3$^+$ cells were detected using an Alexa 594-conjugated goat anti-rabbit IgG (Molecular Probes, Invitrogen) with a DAPI (Vector Laboratories, Burlingame, CA) counterstain. Controls were performed as described above. Immunofluorescence images were acquired at 200x using a Leica DMR microscope and Leica FireCam with accompanying software. Quantification of percentages of mitotic cells in mammary ducts and TEBs was performed by excising duct or TEB structures from images using Adobe Photoshop 7, counting the number of DAPI$^+$ pixels (blue), counting the number of phospho-Histone H3$^+$ pixels (red), and expressing the ratio as a percentage of phospho-Histone H3$^+$ nuclei per structure. A minimum of 10 images of ducts and TEBs apiece were analyzed per W-*sash* phenotype at both 5 and 8 weeks of age.

RESULTS

Mast cells are present in the murine postnatal mammary gland

At 1 and 3 weeks of age, the prepubertal mammary gland consists of a rudimentary epithelial tree at one end of a largely fatty stroma, consisting largely of

unilocular adipoctyes, fibroblasts, blood vessels, nerves, and in some cases, lymph tissue, all surrounded by loose areolar connective tissue. We identified a population of histamine- and chymase-positive mast cells present in the developing mammary gland using several histological methods. Mast cells were scattered throughout this stromal tissue, though in relatively small numbers, and did not appear to localize to any particular features of the prepubertal gland (Figures 1A-B). By 5 weeks of age, the mammary gland has begun to proliferate and grow in response to ovarian hormones, and the advancing ductal front is characterized by the presence of TEBs. At this age, mast cells were still scattered throughout the mammary stroma, but more were found around blood vessels and around the invading ducts (Figure 1C). In particular, mast cells were frequently observed in the stroma immediately surrounding TEBs, adjacent to the periductal stroma or just ahead of the advancing TEB. At 8 weeks, mammary glands have the same pattern of mast cell localization. Mast cells were also observed in pregnant, lactating, and involuting mammary glands as reported previously by others (Figures 1D-E, and data not shown). At all ages, mast cells also were observed at the periphery of the mammary lymph node. These observations of mast cells throughout mammary gland development, and their increased number and proximity to the growing ducts, led us to hypothesize that mast cells play a role in normal mammary epithelial development.

Mast cells are required for normal postnatal mammary gland development

To test the hypothesis that mast cells are involved in pubertal mammary gland development, we used the W-*sash* mast cell-deficient mouse line ($Kit^{W\text{-}sh}$). This mutation is the result of a spontaneous inversion mutation in the regulatory region of the c-*kit* gene (Nagle et al., 1995), resulting in profound deficiency of mast cells in all tissues and significant deficits in melanocytes without affecting other c-*kit*-dependent cell types (Duttlinger et al., 1993; Grimbaldeston et al., 2005). Furthermore, in most tissues, heterozygous $Kit^{+/W\text{-}sh}$ mice have significantly fewer mast cells than wild-type littermates (Grimbaldeston et al., 2005), providing a useful tool for examining the potential “dosage effect” of mast cells in physiological conditions. By histology and enzyme histochemistry, we determined that mast cells were completely absent from the mammary glands of $Kit^{W\text{-}sh/W\text{-}sh}$ mice, and were present in both $Kit^{+/W\text{-}sh}$ and wild-type littermates throughout development (Figure 2A and data not shown). The localization of mast cells in $Kit^{+/W\text{-}sh}$ and wild-type did not differ.

We analyzed mammary gland ductal growth in $Kit^{W\text{-}sh/W\text{-}sh}$, $Kit^{+/W\text{-}sh}$, and $Kit^{+/+}$mice at 3, 5, and 8 weeks of age by comparing whole-mounts of abdominal mammary glands for ductal outgrowth (Figure 2B). At 3 weeks, just before the hormone-driven onset of pubertal development, the number of duct ends and TEBs did not differ by genotype. However, by 5 weeks of age, mast-cell deficient $Kit^{W\text{-}sh/W\text{-}sh}$ mice had significantly fewer duct ends in the invasion front as well as fewer TEBs than wild-type controls, while $Kit^{+/W\text{-}sh}$ had an intermediate phenotype (Figures 2C-E). Presumably, the fewer number of TEBs directly correlated to the reduced number of ducts. This effect on duct end and TEB number persisted into 8 weeks of age, when the advancing duct ends are nearing the boundaries of the mammary fat pad (Figures 2C-E). Additionally, at both 5 and 8 weeks of age, duct lengths were reduced in $Kit^{W\text{-}sh/W\text{-}sh}$ mice when compared to wild-type, and $Kit^{+/W\text{-}sh}$ had intermediate mean lengths, though these differences were not

statistically significant (data not shown), suggesting that mast cells contribute more significantly to the induction or maintenance of TEB formation than the ability of the ducts to migrate and extend into the mammary fat pad. Early observations of littermates at 12 weeks of age (*n*=2/genotype) indicate that the developmental defects persist in adult virgin W-*sash* mutants and heterozygotes, with reduced duct lengths and duct end numbers. However, as $Kit^{W\text{-}sh/W\text{-}sh}$ and $Kit^{+/W\text{-}sh}$ are capable of normal lactation and supporting average-sized litters, these deficits do not impair later mammary gland function.

To make certain that these mast cell-dependent differences were not due to an overall reduction in body growth or relative mammary fat pad sizes somehow related to mast cell deficiency, we monitored mouse body weights as well as the ratio of mammary gland weights to body weight and found no significant differences between the different W-*sash* genotypes at any of the ages analyzed (data not shown). Therefore, these data indicate that the impairment in TEB formation and fewer ducts observed in W-*sash* mutant and heterozygous as compared to wild-type mice are due to mast cell-deficiency and reduced mast cell numbers, respectively. These observations point to a requirement for mast cells for normal postnatal mammary gland development.

Mast cells in mammary gland are not required for macrophage recruitment or collagen deposition around TEBs

Macrophages have been described as having similar effects on mammary gland development as those reported in our study (Gouon-Evans et al., 2002; Gouon-Evans et al., 2000; Ingman et al., 2006). Analysis of mice null for a major macrophage growth marker, CSF1, showed that macrophage-deficient mammary glands had delayed and reduced duct outgrowth (Gouon-Evans et al., 2000). As mast cells have been identified as key recruiters of leukocytes *in vivo* (Gaboury et al., 1995; Kubes and Kanwar, 1994; Metz et al., 2007; Walsh et al., 1991), it was important to determine whether the impaired mammary gland development of W-*sash* mice was due to mast cell deficiency or as a secondary effect of loss of mast cell recruitment of macrophages to the mammary gland. Thus, we performed immunofluorescence on $Kit^{W\text{-}sh}$ mutant, heterozygote, and *Kit* wild-type mammary glands at 5 and 8 weeks of age using an anti-F4/80 antibody, which had previously been used to localize macrophages and eosinophils around the necks and proximal ducts of TEBs in the developing mammary gland (Gouon-Evans et al., 2000; Ingman et al., 2006). We found that mast cell deficiency did not result in loss of $F4/80^{+}$ cells around TEBs (Figure 3A), as staining was similarly distributed and intense in mammary glands of each of the W-*sash* genotypes. Therefore, macrophage loss subsequent to mast cell deficiency cannot be the cause of the W-*sash* mutant mammary developmental defect.

Furthermore, it has been suggested that the role of macrophages around TEBs during mammary development is to organize the collagen-rich matrix surrounding these structures (Ingman et al., 2006). As mammary gland duct elongation requires an exquisite coordination of proper epithelial-ECM signals along the invading duct edges (Wiseman and Werb, 2002), we performed Masson's trichrome staining to look at collagen deposition around TEBs in mast cell-deficient or –reduced mice. At both 5 and 8 weeks of age, we saw no noticeable difference in collagen deposition (Figure 3B), or overall morphology of the TEBs and surrounding stroma, confirming that the mast cell-

dependent mammary development phenotype is independent of macrophage-mediated effects or collagen deposition and TEB shape.

Mast cells are required for normal levels of proliferation in ducts and TEBs in developing mammary glands

In order to determine how mast cell deficiency might result in fewer duct ends and TEBs, we next assessed the proliferative capacity of epithelial cells in the developing mammary gland. We performed immunofluorescence on 5 and 8 week old mammary glands with an antibody against the phosphorylated serine 10 residue of human histone H3, which acts as a specific marker for cells entering mitosis (Hendzel et al., 1997). We then determined the percentage of phospho-Histone $H3^+$ cells in both mammary ducts and TEBs at 5 and 8 weeks of age as indicators of proliferation for $Kit^{W\text{-}sh/W\text{-}sh}$, $Kit^{+/W\text{-}sh}$, and $Kit^{+/+}$ mice. We found fewer mitotic cells in both ducts and TEBs of *Kit* mutant mice than in wild-type (Figures 4A-B). Furthermore, $Kit^{+/W\text{-}sh}$ mice had an intermediate percentage of mitotic ducts and TEB cells, consistent with the observation that the mast cell-reduced W-*sash* heterozygotes had a deficiency in TEB and duct ends intermediate to that of the mast cell-deficient mice and wild-type controls. These data indicate that mammary gland mast cells exert a regulatory influence over TEB and duct cell proliferation required for normal TEB and duct end numbers during pubertal mammary gland development.

Mast cells must be able to degranulate to exert their regulatory effect over mammary gland development

Mast cells may influence their environments in a variety of ways. Conventionally, “activated” mast cells either degranulate and release a host of factors, or they secrete specific factors more selectively; in either case, mast cell products are largely identified as inflammatory mediators, and may include cytokines, growth and survival factors, proteases, histamine, and chemokines (Galli and Tsai, 2008; Metcalfe et al., 1997). Therefore, it was necessary to test that the requirement for mast cells in mammary gland development involves their activation or actual degranulation to exert their effects on ductal growth.

To assess whether mast cell degranulation was required for normal mammary gland development, we treated CD1 outbred mice from the onset of puberty at 3 weeks of age until 5 weeks of age with sodium cromoglycate (cromolyn sodium), which is thought to stabilize mast cells and prevent degranulation by blocking the calcium ion influx required to trigger granule release from the cell (McIntyre et al., 1981). This time period represents the first two weeks of pubertal development, when TEBs are formed and the mammary ductal tree elongates from its prepubertal rudiment and begins to fill the mammary fat pad. We found that cromolyn sodium treatment during these first two weeks of puberty significantly inhibited TEB formation and mammary duct end number (Figures 5A-C). These data indicate that not only is mast cell presence necessary for mammary gland pubertal development, but the mast cells must degranulate to exert their effect during this period of mammary duct growth. Thus, during development, mast cell activation in the mammary gland must be sufficient to induce release of granules that contain some TEB-promoting mediator(s). This does not preclude the possibility

that other, long-term degranulation-independent mediator secretion is also involved in mammary gland development.

Mast cell protease activation is necessary for normal mammary gland development

To begin to identify which mast cell mediators are responsible for these cells' effects on mammary gland development, we next examined the mammary gland development phenotype of mice deficient for dipeptidyl peptidase I (DPPI). Mice deficient for DPPI are healthy and fertile, yet have many inactivated proteases in granulocytic lymphocytes (Pham and Ley, 1999). DPPI, also known as murine cathepsin C, is the *in vivo* activator of mast cell granule serine proteases including chymase, as well as acts as a regulator of the amount of active tryptase in mast cells (Wolters et al., 2001). Thus, to determine whether activated serine proteases in mast cells are required for mammary gland development, we examined whole-mount mammary glands from 5 and 8 week old *DPPI* $^{-/-}$ mice and compared them to wild-type controls. We found that at both of these ages, lack of activated serine proteases in mast cells significantly inhibited TEB and duct end formation (Figures 6A-C). These data indicate that DPPI-dependent mast cell granule protease activation is necessary for mast cells to regulate normal mammary gland duct development.

DISCUSSION

Previous work has established that stromal cells, including some leukocytes, are necessary for pubertal development of the mammary gland ductal epithelium. In this study, we have demonstrated that mast cells should be included in the list of stromal cells that regulate mammary gland development. Mast cells are positioned all over the mammary stroma and around resident lymph nodes and large blood vessels throughout postnatal development; during pubertal expansion of the rudimentary duct, mast cells also are stationed around the invading TEBs ahead of and beside the advancing end buds. As TEBs are the functional unit of mammary gland duct elongation and branching, regulation of their cell proliferation and differentiation, shape, and extracellular matrix is essential for proper TEB formation and duct invasion into the mammary stroma. Coordination of cell proliferation, differentiation, and apoptosis in the TEBs allows them to push forward into the adipocyte- and fibroblast-rich stroma, resulting in duct elongation, as well as allows the TEB to bifurcate, resulting in duct branching (Richert et al., 2000). Given their diverse functions and potent effects on the tissues that house them, the proximity of mast cells near TEBs during this phase of pubertal development suggests that mast cells play an intriguing role in the regulation of mammary gland development.

Resident mast cells in the mammary gland could arise from precursors recruited to the mammary stroma proper where they mature locally, or could migrate as mature cells to the mammary gland from the surrounding subdermal connective tissue. As mast cells have been shown to be involved in leukocyte recruitment (Gaboury et al., 1995; Kubes and Kanwar, 1994; Metz et al., 2007), it is not clear whether the mast cells localized to the mammary lymph nodes have the same function as the mast cells found

throughout the rest of the mammary fat pad, especially those that are found around the developing gland.

W-*sash* mice, whose altered c-*kit* expression leads to loss of mast cells in all tissues, provided us a genetic model for mast cell ablation in the mammary gland. Examination of W-*sash* mammary glands and comparison with W-*sash* heterozygotes and wild-type glands revealed that mast cells are necessary for proper TEB formation and subsequent duct numbers. Furthermore, proper numbers of mast cells are necessary to mammary development, as W-*sash* heterozygote glands have fewer mast cells than wild-type, and heterozygous glands had an impairment in development intermediate to that of the mast cell-deficient and wild-type glands. Although duct lengths in the W-*sash* mutant glands were shorter than in wild-type, the difference did not reach statistical significance (data not shown; P=0.07-0.09). This suggests that mast cells play a more significant role in TEB formation and/or maintenance than in duct extension, even though the processes are coordinated in ductal morphogenesis. Although fewer in number, the TEBs observed in mast cell-deficient mice appeared normal in shape and size. We attempted rescue of the W-*sash* phenotype by intraperitoneal injection of C57Bl/6 $Kit^{+/+}$ β-actin-CFP bone marrow cells into $Kit^{W\text{-}sh/W\text{-}sh}$ animals at 3 weeks of age but results were inconclusive due to poor mast cell reconstitution in the mammary glands (data not shown).

Reduced TEB number and duct branching has been reported in many mouse models (for review, see (Howlin et al., 2006)), implicating hormones, cytokines, extracellular matrix proteins and their receptors and proteases, and growth and transcription factors. Our observations that mammary glands without or with fewer mast cells had a lower percentage of proliferating cells in both TEBs and ducts during pubertal development suggest that mast cells are part of the complex regulation of proliferation in TEB and duct development. Therefore, the requirement for mast cells implies a direct or indirect ability of mast cells to affect the proliferative capacity of the dividing epithelial cells of the growing mammary gland despite their distance from one another.

There are two potential mechanisms for this effect: first, mast cells recruit other cells known to affect mammary development; second, mast cells alter the stromal ECM immediately surrounding the invading ducts where they reside. We tested the first possibility by staining W-*sash* mammary glands for the F4/80 antigen, a marker of macrophages, because mast cells are known to recruit leukocytes to tissues *in vivo* (Gaboury et al., 1995; Kubes and Kanwar, 1994; Walsh et al., 1991) and macrophages have been shown to influence mammary gland development to similar effect as that reported in this study (Gouon-Evans et al., 2000). Therefore, it was possible that mast cell effects we observed were solely due to their recruitment of macrophages to the developing mammary gland. However, there was no difference in $F4/80^{+}$ cells localized around TEBs in mast cell-deficient or mast cell-reduced mammary glands at 3, 5, and 8 weeks of age, suggesting that the effects of mast cells on mammary gland development are macrophage-independent. Furthermore, it has been reported that macrophages are responsible not for the amount, but rather the organization of collagen around TEBs, resulting in altered TEB shape (Ingman et al., 2006). We observed that collagen deposition around TEBs appeared unaffected by mast cell loss, and unlike the macrophage effect, TEB shape also was unaffected by mast cell loss. However, it is

important to note that neither of these results rules out other relationships between inflammatory cells or stromal matrix proteins and mast cells and their products in mammary gland development. Interestingly, a genetic model for eosinophil overabundance through transgenic overexpression of interleukin-5 also results in reduced TEB and duct formation (Sferruzzi-Perri et al., 2003), suggesting that leukocyte recruitment and regulation must be finely controlled to promote mammary duct development.

The W-*sash* model revealed a requirement solely for the presence of stromal mast cells during mammary gland development for proper epithelial cell proliferation, resulting in normal TEB formation and duct branching. We next sought to determine more specifically whether mammary mast cells have to be able to degranulate, and then whether those granules must have active and normal levels of proteases within those granules to exert their effects on mammary gland development. We used cromolyn sodium to stabilize mast cells during the first two weeks of puberty and found that TEB and duct numbers were reduced comparably to the W-*sash* phenotype at 5 weeks of age. This result shows that, at least during the first two weeks of puberty, mast cell degranulation is required to promote TEB formation and duct branching in the early phases of mammary gland growth. As murine mast cell granules contain histamine, proteoglycans, and any number of proteases (including serine proteases such as chymases and tryptases) (Galli and Tsai, 2008; Metcalfe et al., 1997), there are many possible granule components that could contribute to regulation of mammary gland development.

Tissue-type mast cell proteases have been implicated in angiogenesis (Blair et al., 1997; Coussens et al., 1999) and extracellular matrix protein degradation either directly (Vartio et al., 1981; Wolters et al., 2000) or by activation of other ECM proteases (Johnson et al., 1998). As such, they are strong candidates for the mechanism by which mast cells affect the developing mammary gland. To test whether mast cell protease activity is required in mammary development, we examined mammary glands from DPPI (cathepsin C) knockout mice at 5 and 8 weeks of age. DPPI -/- mice have mast cells that may be activated and can degranulate normally, however have no active chymases and have greatly reduced amounts of active tryptase, rendering the majority of their granule proteases functionally inactive (Wolters et al., 2001). We found that at both time points, normal activation of mast cell proteases is required for TEB formation and duct branching in mammary gland development. As cathepsin C has been reported to have its own proteolytic activity towards ECM proteins such as fibronectin and collagens I and IV ((Wolters et al., 2000) it is possible that the loss of cathepsin C could account for the mammary gland phenotype reported here. However, as cathepsin C is required for normal tryptase expression and chymase activation in mast cells (Wolters et al., 2001), it is also possible that tryptase and chymase are required in mammary gland development, either for their own activity or as activators of other proteases such as matrix metalloproteinases. It is important to note that both the cromolyn sodium treatment experiment and the DPPI knockout mammary phenotypes also rule out the possibility that the W-*sash* mammary gland defects were secondary to effects of c-*kit* hypomorphism on other cell types (such as the mammary epithelium) rather than directly by loss of mammary tissue mast cells.

Though our study implicates mast cell proteases as likely effectors of mast cell activity on the developing mammary gland, other mast cell mediators could also be involved. For example, histamine and some of its receptors are highly expressed by mammary alveolar epithelium during pregnancy and lactation, and these expression levels change significantly during the estrus cycle (Maslinski et al., 1993; Wagner et al., 2003), suggesting a role for histamine in later mammary gland differentiation. Mice null for histidine decarboxylase (HDC), the major enzyme responsible for histamine synthesis, are reportedly fertile, yet have reduced numbers of tissue mast cells, and the mast cells have reduced granular content (Ohtsu et al., 2001). It would be interesting to examine HDC-null mammary glands to determine whether histamine is a crucial contributor to mammary gland development. It is also possible that mast cell-produced chemokines, cytokines, growth factors, or lipid-derived mediators contribute to mast cell effects on mammary gland development. Two intriguing candidates would be transforming growth factor-beta (TGF-β) and prostaglandin D_2, both well-established mast cell products. However, as TGF-β and prostaglandin D_2 have been reported to inhibit mammary epithelial proliferation (Silberstein et al., 1992; Yee et al., 2003), it is unlikely that loss of these mast cell mediators would account for the negative effects on mammary development we observed in our study. More specific characterization of the mammary gland mast cell phenotype would be necessary to identify which mediators may be strongly implicated in regulation of mammary gland morphogenesis.

In total, our results indicate that mast cells must be present, capable of degranulation, and have activated granule-associated proteases to facilitate normal mammary gland pubertal development in the mouse. Mast cells are located near the advancing ducts throughout development, and affect TEB formation and duct branching by promoting cell proliferation in the growing mammary gland. Eosinophils and macrophages have been shown to promote mammary gland development (Gouon-Evans et al., 2000), and it was conceivable that mast cells are responsible for their recruitment to mammary gland TEBs, however, we found that $F4/80^+$ cells were present in normal numbers despite mast cell deficiency. Thus, the effect of mast cells on mammary gland growth is either independent or upstream of the action of other leukocytes during mammary development. Therefore, this study demonstrates for the first time that mast cells directly affect mammary gland growth during puberty.

REFERENCES

Blair, R.J., H. Meng, M.J. Marchese, S. Ren, L.B. Schwartz, M.G. Tonnesen, and B.L. Gruber. 1997. Human mast cells stimulate vascular tube formation. Tryptase is a novel, potent angiogenic factor. *The Journal of clinical investigation*. 99:2691-700.

Coussens, L.M., W.W. Raymond, G. Bergers, M. Laig-Webster, O. Behrendtsen, Z. Werb, G.H. Caughey, and D. Hanahan. 1999. Inflammatory mast cells up-regulate angiogenesis during squamous epithelial carcinogenesis. *Genes Dev*. 13:1382-97.

Coussens, L.M., and Z. Werb. 2002. Inflammation and cancer. *Nature*. 420:860-7.

Cunha, G.R., and Y.K. Hom. 1996. Role of mesenchymal-epithelial interactions in mammary gland development. *Journal of mammary gland biology and neoplasia*. 1:21-35.

Cunha, G.R., J.F. Wiesen, Z. Werb, P. Young, Y.K. Hom, P.S. Cooke, and D.B. Lubahn. 2000. Paracrine mechanisms of mouse mammary ductal growth. *Advances in experimental medicine and biology*. 480:93-7.

Duttlinger, R., K. Manova, T.Y. Chu, C. Gyssler, A.D. Zelenetz, R.F. Bachvarova, and P. Besmer. 1993. W-sash affects positive and negative elements controlling c-kit expression: ectopic c-kit expression at sites of kit-ligand expression affects melanogenesis. *Development*. 118:705-17.

Gaboury, J.P., B. Johnston, X.F. Niu, and P. Kubes. 1995. Mechanisms underlying acute mast cell-induced leukocyte rolling and adhesion in vivo. *Journal of immunology (Baltimore, Md.* 154:804-13.

Galli, S.J. 2000. Mast cells and basophils. *Curr Opin Hematol*. 7:32-9.

Galli, S.J., J. Kalesnikoff, M.A. Grimbaldeston, A.M. Piliponsky, C.M. Williams, and M. Tsai. 2005. Mast cells as "tunable" effector and immunoregulatory cells: recent advances. *Annu Rev Immunol*. 23:749-86.

Galli, S.J., and M. Tsai. 2008. Mast cells: Versatile regulators of inflammation, tissue remodeling, host defense and homeostasis. *Journal of dermatological science*. 49:7-19.

Gouon-Evans, V., E.Y. Lin, and J.W. Pollard. 2002. Requirement of macrophages and eosinophils and their cytokines/chemokines for mammary gland development. *Breast cancer research*. 4:155-64.

Gouon-Evans, V., M.E. Rothenberg, and J.W. Pollard. 2000. Postnatal mammary gland development requires macrophages and eosinophils. *Development (Cambridge, England)*. 127:2269-82.

Grimbaldeston, M.A., C.-C. Chen, A.M. Piliponsky, M. Tsai, S.-Y. Tam, and S.J. Galli. 2005. Mast Cell-Deficient W-sash c-kit Mutant KitW-sh/W-sh Mice as a Model for Investigating Mast Cell Biology in Vivo. *Am J Pathol*. 167:835-848.

Hendzel, M.J., Y. Wei, M.A. Mancini, A. Van Hooser, T. Ranalli, B.R. Brinkley, D.P. Bazett-Jones, and C.D. Allis. 1997. Mitosis-specific phosphorylation of histone H3 initiates primarily within pericentromeric heterochromatin during G2 and spreads in an ordered fashion coincident with mitotic chromosome condensation. *Chromosoma*. 106:348-60.

Howlin, J., J. McBryan, and F. Martin. 2006. Pubertal mammary gland development: insights from mouse models. *Journal of mammary gland biology and neoplasia*. 11:283-97.

Ingman, W.V., J. Wyckoff, V. Gouon-Evans, J. Condeelis, and J.W. Pollard. 2006. Macrophages promote collagen fibrillogenesis around terminal end buds of the developing mammary gland. *Developmental dynamics*. 235:3222-9.

Jamieson, T., D.N. Cook, R.J. Nibbs, A. Rot, C. Nixon, P. McLean, A. Alcami, S.A. Lira, M. Wiekowski, and G.J. Graham. 2005. The chemokine receptor D6 limits the inflammatory response in vivo. *Nature immunology*. 6:403-11.

Johnson, J.L., C.L. Jackson, G.D. Angelini, and S.J. George. 1998. Activation of matrix-degrading metalloproteinases by mast cell proteases in atherosclerotic plaques. *Arteriosclerosis, thrombosis, and vascular biology*. 18:1707-15.

Kitamura, Y. 1989. Heterogeneity of mast cells and phenotypic change between subpopulations. *Annu Rev Immunol*. 7:59-76.

Kubes, P., and S. Kanwar. 1994. Histamine induces leukocyte rolling in post-capillary venules. A P-selectin-mediated event. *Journal of immunology (Baltimore, Md.* 152:3570-7.

Malorny, U., E. Michels, and C. Sorg. 1986. A monoclonal antibody against an antigen present on mouse macrophages and absent from monocytes. *Cell and tissue research*. 243:421-8.

Maslinski, C., D. Kierska, W.A. Fogel, A. Kinnunen, and P. Panula. 1993. Histamine: its metabolism and localization in mammary gland. *Comparative biochemistry and physiology*. 105:269-73.

McIntyre, J.A., E.D. Neerunjun, W.P. Faulk, and M. Papamichail. 1981. Inhibition of in vitro allogeneic reactions with disodium cromoglycate. *International archives of allergy and applied immunology*. 66:244-50.

Metcalfe, D.D., D. Baram, and Y.A. Mekori. 1997. Mast cells. *Physiol Rev*. 77:1033-79.

Metz, M., M.A. Grimbaldeston, S. Nakae, A.M. Piliponsky, M. Tsai, and S.J. Galli. 2007. Mast cells in the promotion and limitation of chronic inflammation. *Immunological reviews*. 217:304-28.

Moloney, W.C., K. McPherson, and L. Fliegelman. 1960. Esterase activity in leukocytes demonstrated by the use of naphthol AS-D chloroacetate substrate. *The journal of histochemistry and cytochemistry*. 8:200-7.

Nagle, D.L., C.A. Kozak, H. Mano, V.M. Chapman, and M. Bucan. 1995. Physical mapping of the Tec and Gabrb1 loci reveals that the Wsh mutation on mouse chromosome 5 is associated with an inversion. *Human molecular genetics*. 4:2073-9.

Ohtsu, H., S. Tanaka, T. Terui, Y. Hori, Y. Makabe-Kobayashi, G. Pejler, E. Tchougounova, L. Hellman, M. Gertsenstein, N. Hirasawa, E. Sakurai, E. Buzas, P. Kovacs, G. Csaba, A. Kittel, M. Okada, M. Hara, L. Mar, K. Numayama-Tsuruta, S. Ishigaki-Suzuki, K. Ohuchi, A. Ichikawa, A. Falus, T. Watanabe, and A. Nagy. 2001. Mice lacking histidine decarboxylase exhibit abnormal mast cells. *FEBS letters*. 502:53-6.

Pham, C.T., and T.J. Ley. 1999. Dipeptidyl peptidase I is required for the processing and activation of granzymes A and B in vivo. *Proceedings of the National Academy of Sciences of the United States of America*. 96:8627-32.

Richert, M.M., K.L. Schwertfeger, J.W. Ryder, and S.M. Anderson. 2000. An atlas of mouse mammary gland development. *J Mammary Gland Biol Neoplasia*. 5:227-41.

Rugh, R. 1968. The mouse; its reproduction and development. Burgess Pub. Co., Minneapolis,. iv, 430 pp.

Sferruzzi-Perri, A.N., S.A. Robertson, and L.A. Dent. 2003. Interleukin-5 transgene expression and eosinophilia are associated with retarded mammary gland development in mice. *Biology of reproduction*. 69:224-33.

Silberstein, G.B., K.C. Flanders, A.B. Roberts, and C.W. Daniel. 1992. Regulation of mammary morphogenesis: evidence for extracellular matrix-mediated inhibition of ductal budding by transforming growth factor-beta 1. *Developmental biology*. 152:354-62.

Topper, Y.J., and C.S. Freeman. 1980. Multiple hormone interactions in the developmental biology of the mammary gland. *Physiological reviews*. 60:1049-106.

Vartio, T., H. Seppa, and A. Vaheri. 1981. Susceptibility of soluble and matrix fibronectins to degradation by tissue proteinases, mast cell chymase and cathepsin G. *The Journal of biological chemistry*. 256:471-7.

Wagner, W., A. Ichikawa, S. Tanaka, P. Panula, and W.A. Fogel. 2003. Mouse mammary epithelial histamine system. *Journal of physiology and pharmacology*. 54:211-23.

Walsh, L.J., G. Trinchieri, H.A. Waldorf, D. Whitaker, and G.F. Murphy. 1991. Human dermal mast cells contain and release tumor necrosis factor alpha, which induces endothelial leukocyte adhesion molecule 1. *Proceedings of the National Academy of Sciences of the United States of America*. 88:4220-4.

Wiseman, B.S., and Z. Werb. 2002. Stromal effects on mammary gland development and breast cancer. *Science*. 296:1046-9.

Wolters, P.J., M. Laig-Webster, and G.H. Caughey. 2000. Dipeptidyl peptidase I cleaves matrix-associated proteins and is expressed mainly by mast cells in normal dog airways. *American journal of respiratory cell and molecular biology*. 22:183-90.

This page contains unpublished data which should be protected.

Wolters, P.J., C.T. Pham, D.J. Muilenburg, T.J. Ley, and G.H. Caughey. 2001. Dipeptidyl peptidase I is essential for activation of mast cell chymases, but not tryptases, in mice. *The Journal of biological chemistry*. 276:18551-6.

Yee, L.D., Y. Guo, J. Bradbury, S. Suster, S.K. Clinton, and V.L. Seewaldt. 2003. The antiproliferative effects of PPARgamma ligands in normal human mammary epithelial cells. *Breast cancer research and treatment*. 78:179-92.

This page contains unpublished data which should be protected.

FIGURES

Figure 1. Mast cells are present in the mammary stroma during postnatal development. Frozen 5 μm sections of abdominal mammary glands stained by enzymatic reaction with naphthol AS-D chloroacetate esterase (CAE, red) to detect chymase activity (Moloney et al., 1960) then counterstained with Gill's hematoxylin. A) 1 week; B) 3 week; C) 5 week; D) 20 days lactating; E) 4 days involuting. Scale bar for A-E = 100 μm.

Figure 1

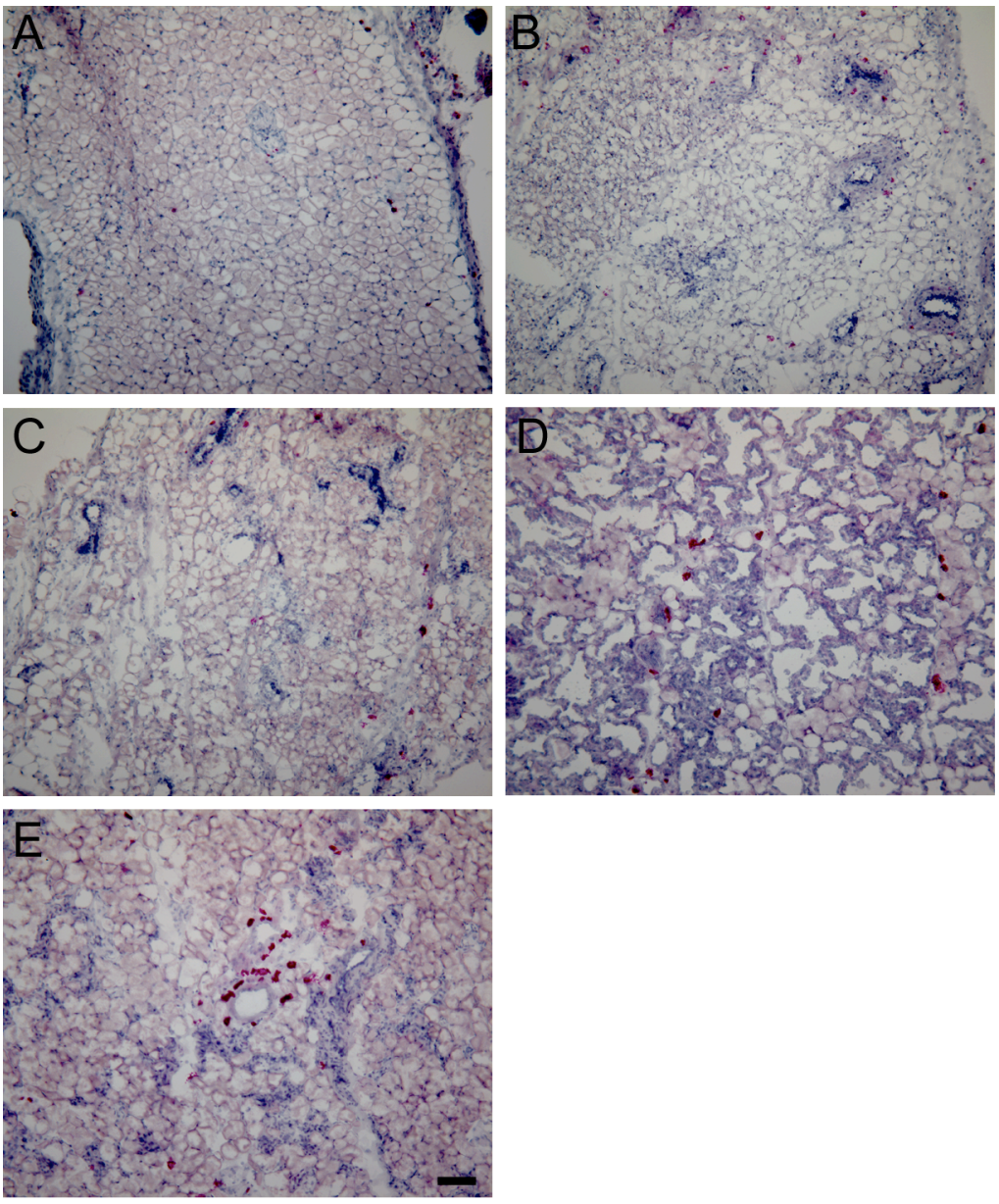

Figure 2. Mast cells are required for normal mammary gland development.

A) Mast cells are present in wild-type mammary gland but absent in W-*sash* mutant mice. Frozen 5 μm sections of abdominal mammary glands from 5 week old littermates stained with CAE. Scale bar = 100 μm. B) Analysis of carmine-stained mammary gland whole mounts required counting of TEBs (black arrowhead) and duct ends (white arrowhead) past the mid-lymph node (denoted by line, LN=lymph node). The nipple is indicated by an asterisk. Scale bar = 1 mm. C) Comparison of carmine-stained whole mounts of left abdominal mammary glands from W-*sash* wild-type, heterozygote, and mutant mice at 5 and 8 weeks of age, 10x. D) Counts of TEBs past the mid-lymph node from whole mount analysis reveal that mast cells are required for TEB formation in the pubertal mammary gland. *n*=8 mice/group. Error bars represent standard error. ANOVA values: *5 weeks, p=0.038; **8 weeks, p=0.024. E) Counts of duct ends (primary and secondary branching) past the mid-lymph node from whole mount analysis reveal that mast cells are required for duct end numbers in the pubertal mammary gland. *n*=8 mice/group. Error bars represent standard error. ANOVA values: ***5 weeks, p=0.0003; *8 weeks, p=0.0325.

Figure 2

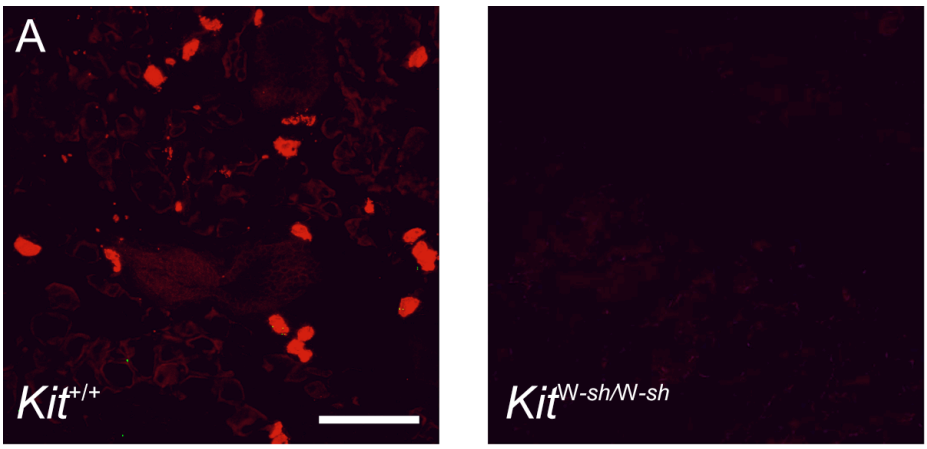

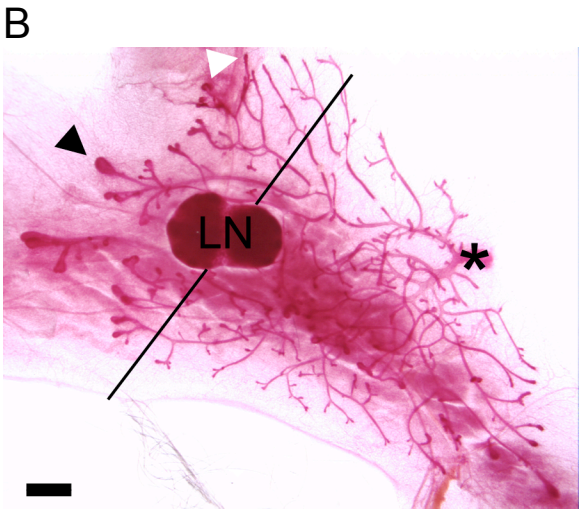

Figure 2, continued

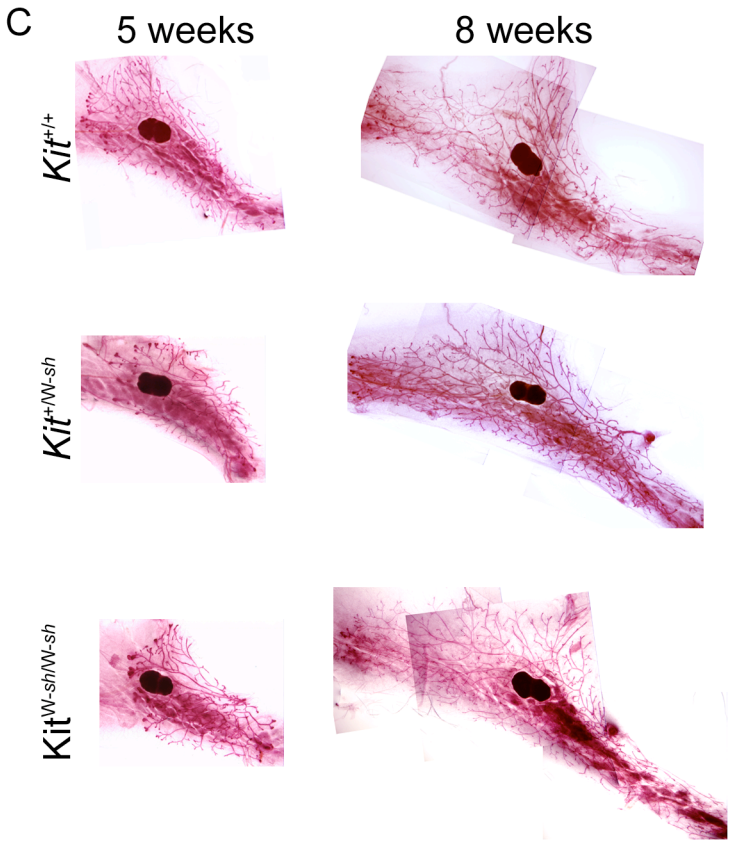

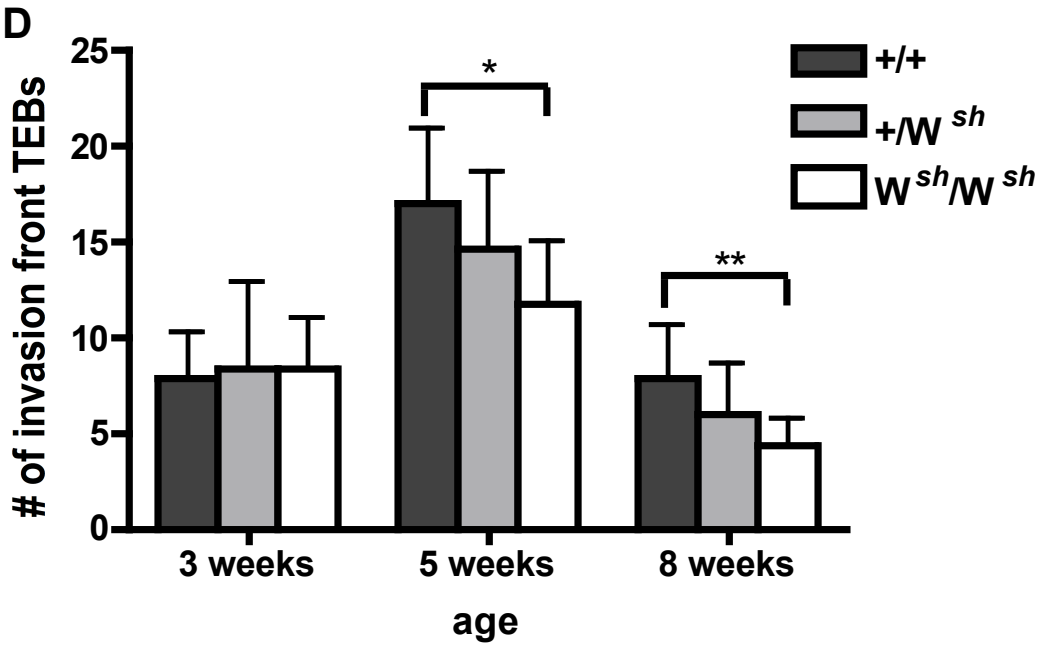

Figure 2, continued

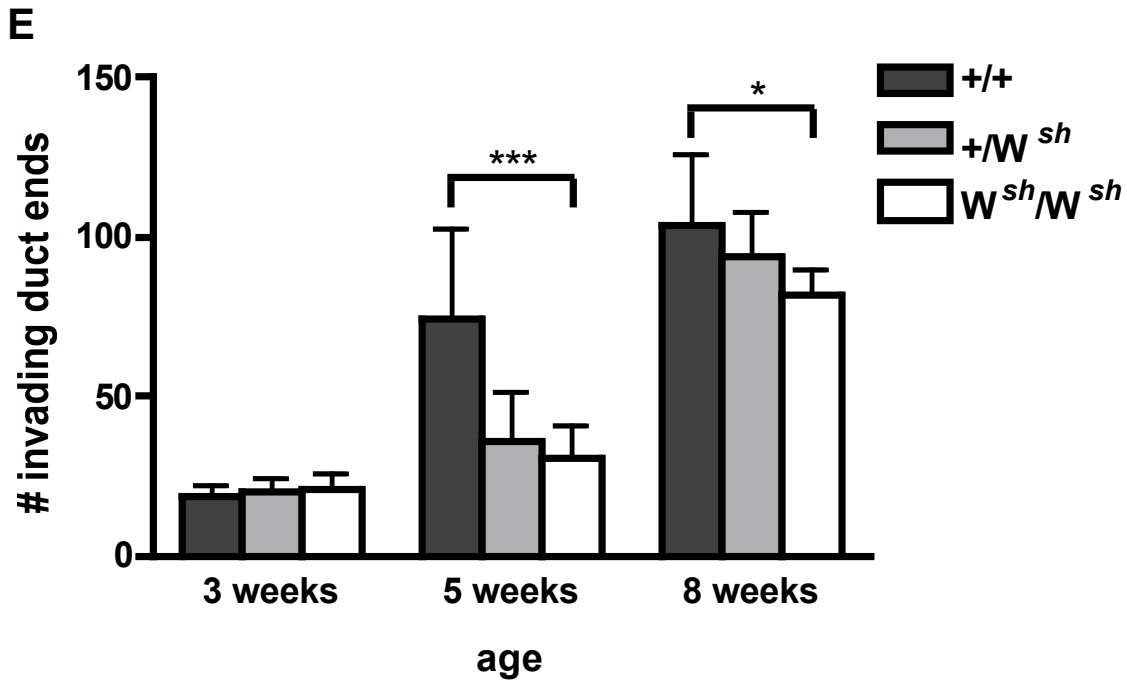

This page contains unpublished data which should be protected.

Figure 3. Mammary gland mast cells are not responsible for F4/80^{+} cell recruitment and TEB shape in the mammary gland. A) Immunofluorescence on *Kit*$^{W\text{-}sh}$ mutant, heterozygote, and *Kit* wild-type mammary glands at 5 weeks of age using anti-F4/80 antibody with Alexa 488-conjugated secondary antibody (green), used to localize macrophages (and eosinophils), DAPI counterstain (blue), scale bar = 100 μm. B) Masson's trichrome staining of stromal collagen deposition (blue) around TEBs in mast cell-deficient or –reduced mice at 5 weeks of age**,** 200x.

Figure 3

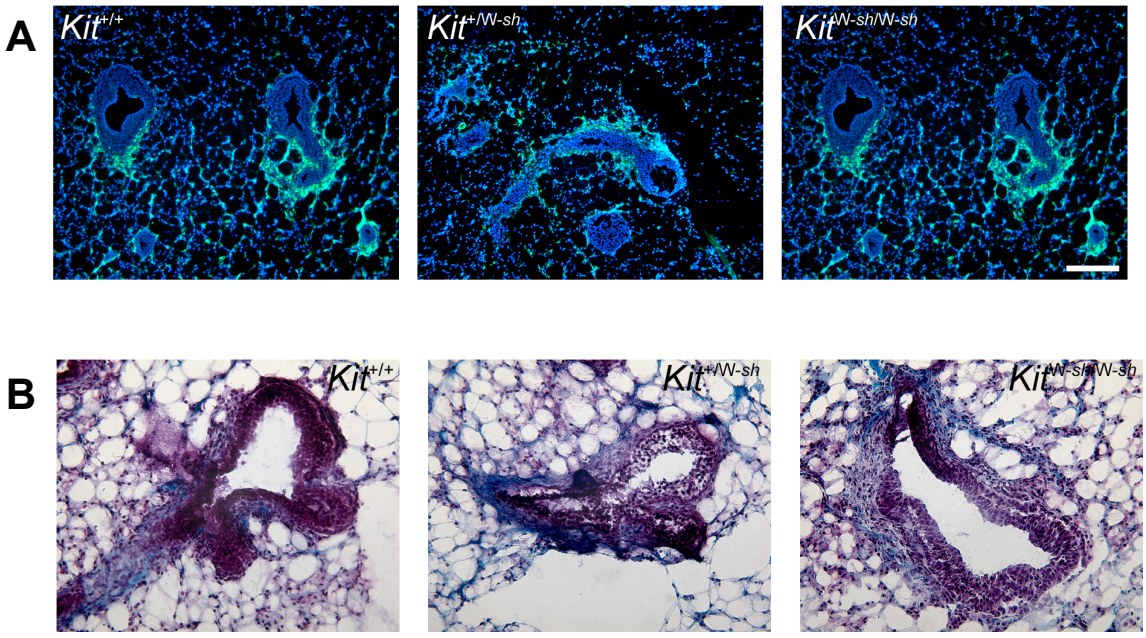

Figure 4. Mast cells are required for proper epithelial cell proliferation in TEBs and ducts in the developing mammary gland. Immunofluorescence was performed on frozen sections of *Kit*$^{W\text{-}sh}$ mutant, heterozygote, and *Kit* wild-type mammary glands at 5 and 8 weeks of age using an antibody against phospho-histone H3, a mitotic marker, and counterstained with DAPI. Phospho-histone H3^{+} cells were counted and expressed as a percentage of mitotic cells per TEB or duct, respectively. *n*=8 mice/group. A) Mast cells are required for proper epithelial cell proliferation in mammary gland TEBs at 5 weeks. Error bars represent standard error. *ANOVA: $p<0.0001$. B) Mast cells are required for proper epithelial cell proliferation in mammary gland TEBs and ducts at 8 weeks. Error bars represent standard error. ANOVA values: *5 weeks, $p=0.0025$; **8 weeks, $p=0.0013$.

Figure 4

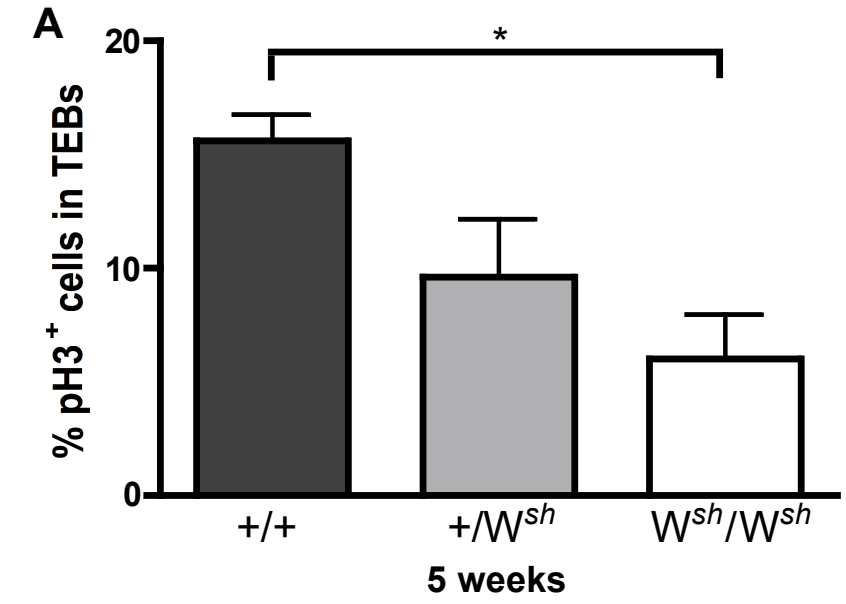

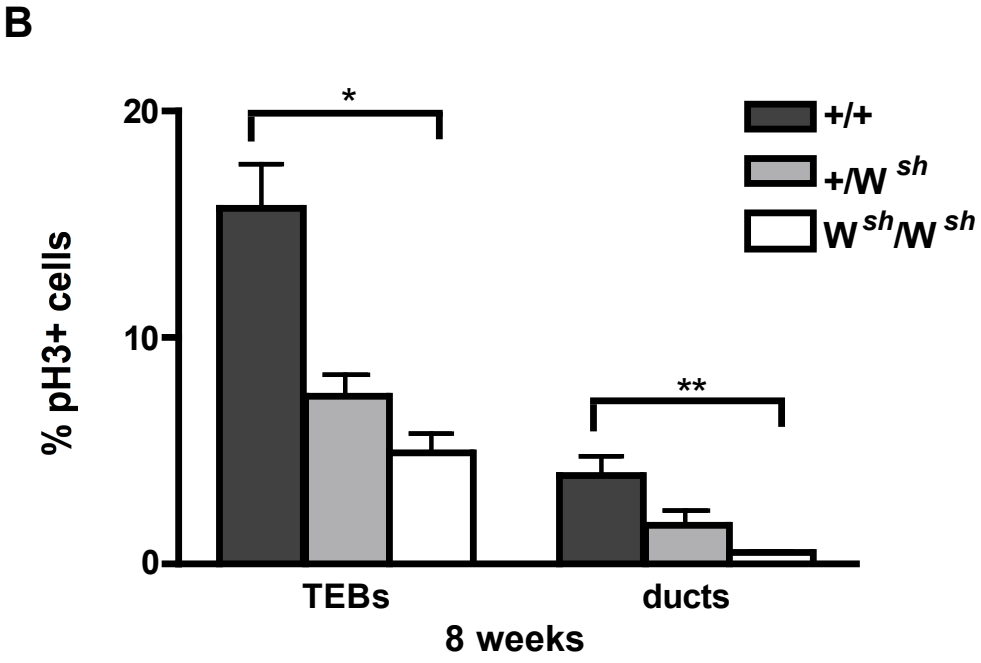

This page contains unpublished data which should be protected.

Figure 5. Mast cell degranulation is required for their effect on mammary gland pubertal development. Mice were treated daily with cromolyn sodium, a mast cell degranulation inhibitor, or saline control from weeks 3 to 5 of age. *n*=7 mice/group. A) Carmine-stained whole mounts of saline- and cromolyn sodium-treated mammary glands at 5 weeks, 10x. B) Cromolyn sodium-treated mammary glands have fewer TEBs after two weeks of treatment. Student's t-test: P=0.0047. Error bars represent standard deviation. C) Cromolyn sodium-treated mammary glands have fewer duct ends after two weeks of treatment. Student's t-test: P=0.049. Error bars represent standard deviation.

Figure 5

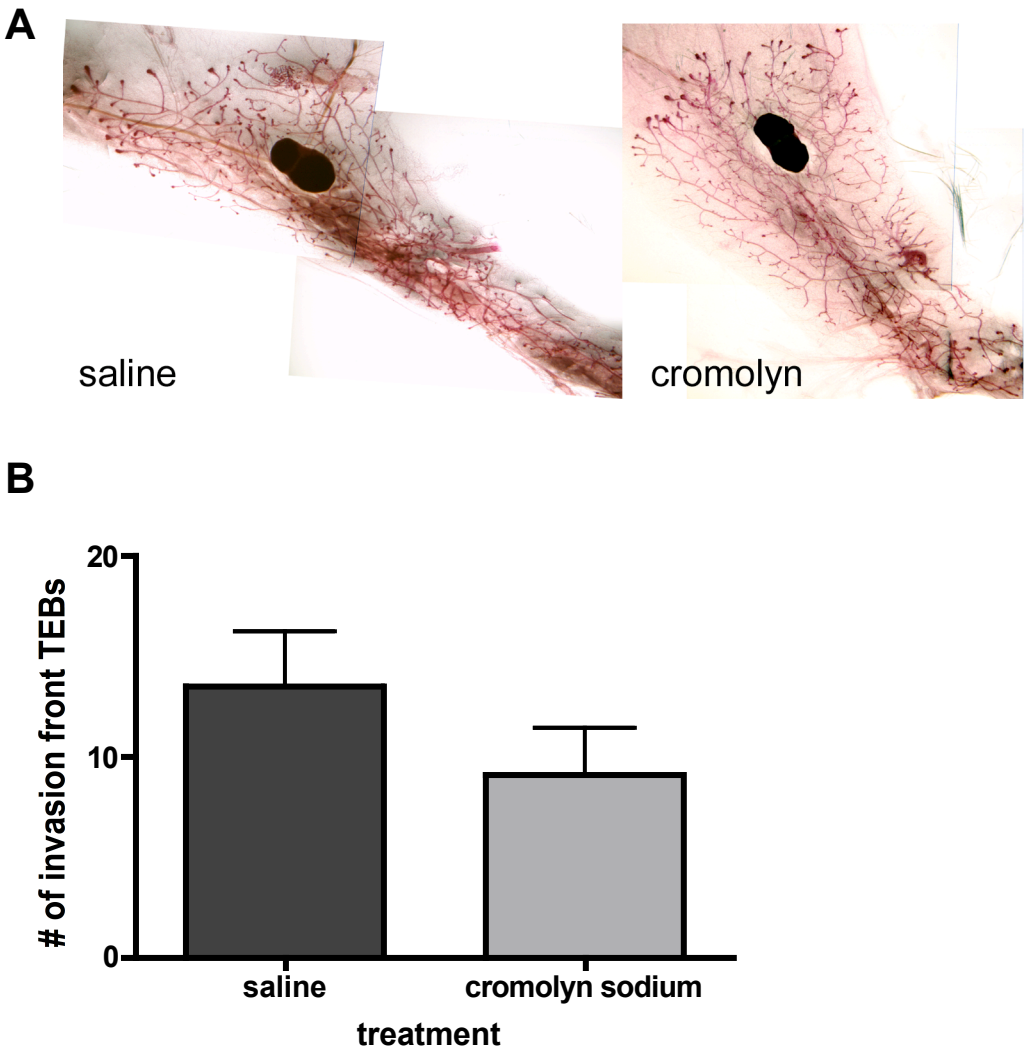

Figure 5, continued

C

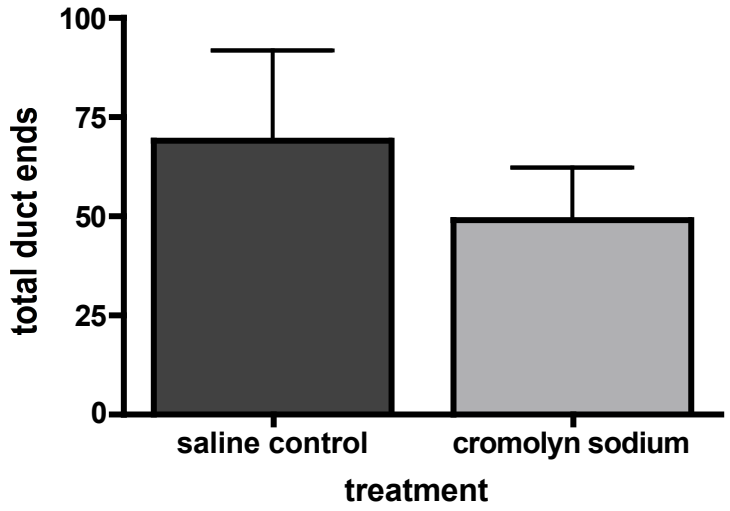

This page contains unpublished data which should be protected.

Figure 6. Mast cell protease activation is necessary for normal mammary gland development. We examined mammary glands of DPPI -/- mice and wild-type controls at 5 and 8 weeks of age. *n*=6 mice/group. A) Carmine-stained whole mounts of wild-type and DPPI -/- mammary glands at 5 and 8 weeks, 10x. B) Mammary glands of DPPI -/- mice have fewer TEBs than wild-type controls at both 5 and 8 weeks of age. Student's t-tests: *5 weeks, P<0.0001; **8 weeks, P=0.0013. Error bars represent standard deviation. C) Mammary glands of DPPI -/- mice have fewer duct ends than wild-type controls as both 5 and 8 weeks of age. Student's t-tests: *5 weeks, P=0.0015; **8 weeks, P=0.0006. Error bars represent standard deviation.

Figure 6

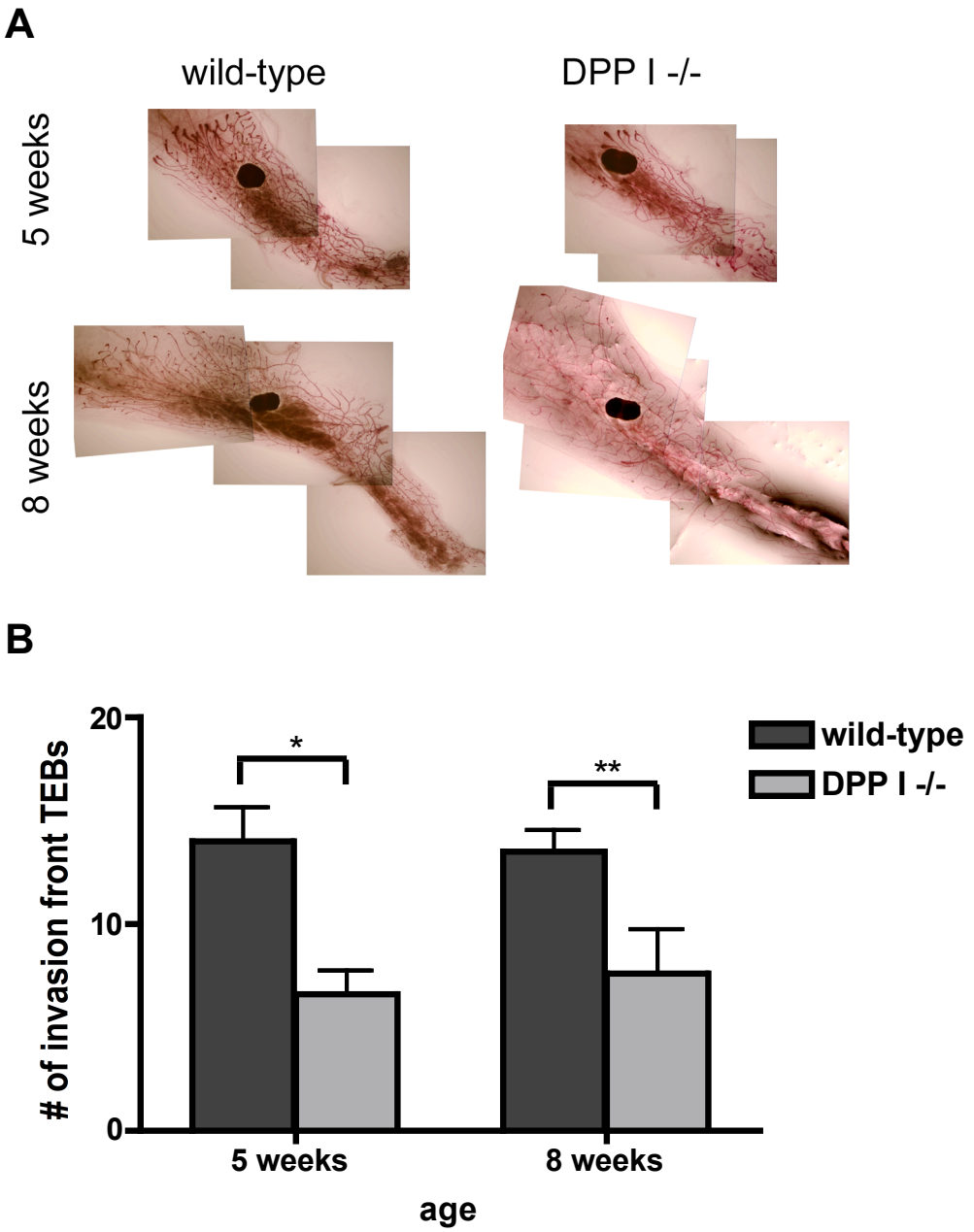

Figure 6, continued

C

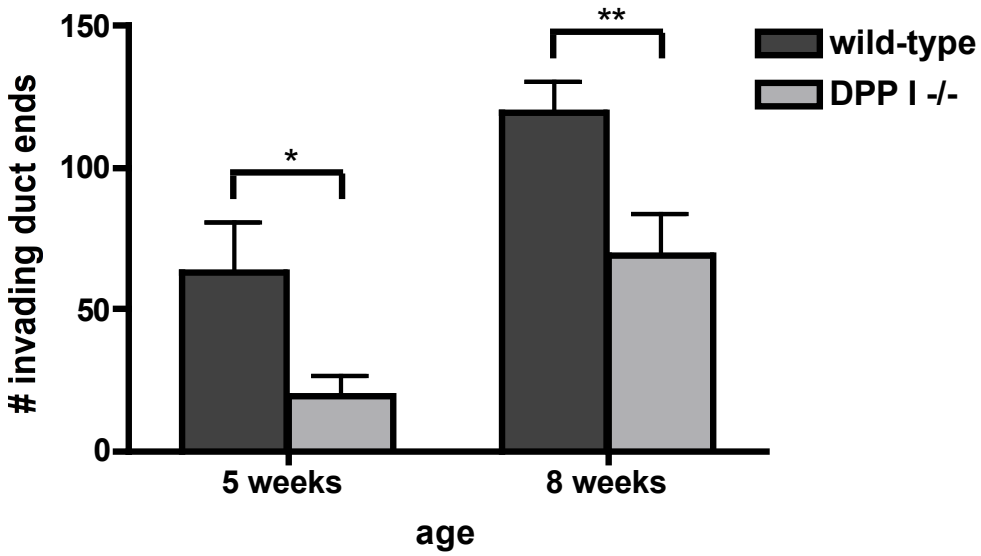

Appendix 4: Abstract for poster presented at the Gordon Research Conference on Plasminogen Activation and Extracellular Proteolysis, February 2008.

Biological Function for Plasma Kallikrein in Mammary Gland Involution

Jennifer N. Lilla[1], A. Allart Stoop[2], Charles S. Craik[2], Zena Werb[1]

[1]Department of Anatomy, Box 0452, University of California, San Francisco
513 Parnassus Avenue, San Francisco, CA 94143

[2]Department of Pharmaceutical Chemistry, Box 2280, University of California, San Francisco
600 16th Street, San Francisco, CA 94143

The plasminogen cascade of serine proteases has been affiliated with both development and tumorigenesis in the mammary gland. The ultimate effector in this cascade, plasminogen (active form: plasmin), is managed by a complicated cascade of plasminogen activators and protease inhibitors. This study focuses on the role of the plasminogen cascade of serine proteases in the last stage of murine mammary development: involution. Plasminogen can be activated to plasmin by urokinase-type plasminogen activator (uPA), tissue-type plasminogen activator (tPA), and plasma kallikrein (PKal). Though tPA and uPA are efficient activators of plasminogen, mice deficient for either or both of these plasminogen activators do not recapitulate the mammary gland involution phenotype of plasminogen null mice. Instead, the dominant plasminogen activator for mammary stromal involution is PKal (zymogen = prekallikrein), a serine protease that participates in the contact activation system of blood coagulation that is present in high concentration (40 μg/ml) in circulating plasma. A variant of ecotin, a macromolecular inhibitor of the trypsin family of serine proteases derived from *E. coli*, was engineered to be highly specific for the active PKal protease. We have shown this ecotin specific for PKal (ecotin PKal) delays alveolar apoptosis, adipocyte replenishment, and stromal remodeling in the involuting mammary gland, resembling the phenotype of plasminogen deficient mice. This effect on involution is mostly relieved five days after the end of ecotin PKal treatment. Furthermore, using a tagged form of ecotin PKal, we have visualized active PKal *in vivo*. As such, PKal has been localized to connective tissue-type mast cells in the stroma and surrounding the blood vessels of the murine mammary gland, and does not appear in tissues devoid of connective tissue-type mast cells or tissues containing mucosal-type mast cells. Additionally, the specific localization of PKal to mast cells is dependent on the activation state of the mast cells. Lastly, we have shown that plasma kallikrein expression is not limited to liver hepatocytes as previously thought; RT-PCR on RNA collected from mammary glands at different developmental stages revealed that PKal is expressed highly during times of stromal remodeling such as during puberty or postlactational involution.

REPORT OF INVENTIONS AND SUBCONTRACTS

(Pursuant to "Patent Rights" Contract Clause) (See Instructions on back)

Form Approved
OMB No. 9000-0095
Expires Jan 31, 2008

PLEASE DO NOT RETURN YOUR COMPLETED FORM TO THE ABOVE ORGANIZATION. RETURN COMPLETED FORM TO THE CONTRACTING OFFICER.

1.a. NAME OF CONTRACTOR/SUBCONTRACTOR	c. CONTRACT NUMBER	2.a. NAME OF GOVERNMENT PRIME CONTRACTOR	c. CONTRACT NUMBER	3. TYPE OF REPORT (X one)
Jennifer N. Lilla	W81XWH-05-1-0272			a. INTERIM [ ] b. FINAL [X]
b. ADDRESS *(Include ZIP Code)*	**d. AWARD DATE** *(YYYYMMDD)*	**b. ADDRESS** *(Include ZIP Code)*	**d. AWARD DATE** *(YYYYMMDD)*	**4. REPORTING PERIOD** *(YYYYMMDD)*
513 Parnassus Ave. San Francisco, CA 94143-0452	20050215			a. FROM 20050215 b. TO 20080214

SECTION I - SUBJECT INVENTIONS

5. "SUBJECT INVENTIONS" REQUIRED TO BE REPORTED BY CONTRACTOR/SUBCONTRACTOR *(If "None," so state)*

NAME(S) OF INVENTOR(S) *(Last, First, Middle Initial)* a.	TITLE OF INVENTION(S) b.	DISCLOSURE NUMBER, PATENT APPLICATION SERIAL NUMBER OR PATENT NUMBER c.	ELECTION TO FILE PATENT APPLICATIONS (X) d.				CONFIRMATORY INSTRUMENT OR ASSIGNMENT FORWARDED TO CONTRACTING OFFICER (X) e.	
			(1) UNITED STATES		(2) FOREIGN			
			(a) YES	(b) NO	(a) YES	(b) NO	(a) YES	(b) NO
N/A	NONE							

f. EMPLOYER OF INVENTOR(S) NOT EMPLOYED BY CONTRACTOR/SUBCONTRACTOR		g. ELECTED FOREIGN COUNTRIES IN WHICH A PATENT APPLICATION WILL BE FILED	
(1) (a) NAME OF INVENTOR *(Last, First, Middle Initial)*	(2) (a) NAME OF INVENTOR *(Last, First, Middle Initial)*	(1) TITLE OF INVENTION	(2) FOREIGN COUNTRIES OF PATENT APPLICATION
(b) NAME OF EMPLOYER	(b) NAME OF EMPLOYER		
(c) ADDRESS OF EMPLOYER *(Include ZIP Code)*	(c) ADDRESS OF EMPLOYER *(Include ZIP Code)*		

SECTION II - SUBCONTRACTS *(Containing a "Patent Rights" clause)*

6. SUBCONTRACTS AWARDED BY CONTRACTOR/SUBCONTRACTOR *(If "None," so state)*

NAME OF SUBCONTRACTOR(S) a.	ADDRESS *(Include ZIP Code)* b.	SUBCONTRACT NUMBER(S) c.	FAR "PATENT RIGHTS" d.		DESCRIPTION OF WORK TO BE PERFORMED UNDER SUBCONTRACT(S) e.	SUBCONTRACT DATES *(YYYYMMDD)* f.	
			(1) CLAUSE NUMBER	(2) DATE *(YYYYMM)*		(1) AWARD	(2) ESTIMATED COMPLETION
NONE							

SECTION III - CERTIFICATION

7. CERTIFICATION OF REPORT BY CONTRACTOR/SUBCONTRACTOR *(Not required if: (X as appropriate))* [ ] **SMALL BUSINESS or** [ ] **NONPROFIT ORGANIZATION**

I certify that the reporting party has procedures for prompt identification and timely disclosure of "Subject Inventions," that such procedures have been followed and that all "Subject Inventions" have been reported.

a. NAME OF AUTHORIZED CONTRACTOR/SUBCONTRACTOR OFFICIAL *(Last, First, Middle Initial)*	b. TITLE	c. SIGNATURE	d. DATE SIGNED
Lilla, Jennifer N	Graduate Student	Jennifer Lilla	20080403

DD FORM 882, JUL 2005 PREVIOUS EDITION IS OBSOLETE. Adobe Professional 7.0